COMPUTATION OF BEARING CAPACITY AND PASSIVE PRESSURE COEFFICIENTS IN SAND USING STRESS-CHARACTERISTICS AND CRITICAL STATE

by

HOVAN Jean-Michel

A thesis
presented to the University of Manitoba
in partial fulfillment of the
requirements for the degree of
MASTER OF SCIENCES
in
CIVIL ENGINEERING

Winnipeg, Manitoba

COMPUTATION OF BEARING CAPACITY AND PASSIVE PRESSURE COEFFICIENTS IN SAND USING STRESS-CHARACTERISTICS AND CRITICAL STATE

BY

JEAN-MICHEL HOVAN

A thesis submitted to the Faculty of Graduate Studies of the University of Manitoba in partial fulfillment of the requirements of the degree of

MASTER OF SCIENCE

I hereby declare that I am the sole author of this thesis.

I authorize the University of Manitoba to lend this thesis to other institutions or individuals for the purpose of scholarly research.

HOVAN Jean-Michel

I further authorize the University of Manitoba to reproduce this thesis by photocopying or by other means, in total or in part, at the request of other institutions or individuals for the purpose of scholarly research.

HOVAN Jean-Michel

The University of Manitoba requires the signatures of all persons using or photocopying this thesis. Please sign below, and give address and date.

ABSTRACT

Bearing capacity coefficients for footings and passive pressure coefficients for walls in sand are computed using stress-characteristic solutions with the Cambridge 'Critical State' strength model. The basic equilibrium equations are combined with the Coulomb criterion to produce a set of so-called 'basic differential equations'. These equations are solved using a finite differences method and stress-characteristics are computer-drawn. The solution is rigid-plastic and does not take into account volume strains prior to failure. In the Critical State model, and hence in the analysis, the angle of shearing resistance is not considered to be constant in the sand, and is allowed to vary in the domain under stress. This takes account of the well-known curvature Coulomb-Mohr envelope, in contrast with most solutions which assume it is straight.

Bearing capacity coefficients for footings and passive pressure coefficients for walls are plotted as functions of the size of the structure (breadth of the footing, or height of the wall) and of the compressibility of the sand. These theoretical results agree well with experimental data and with previous analysis.

ACKNOWLEDGEMENTS

I wish to thank Dr J.Graham for his invaluable guidance throughout the development of this thesis project.

I am grateful for the fact that this work has enabled me to approach the new technology of computers in a problem of foundations involving one of the oldest crafts of mankind.

I also wish to thank the Governments of Canada and of Manitoba without which my stay in Canada would have never been feasible.

CONTENTS

LIST OF SYMBOLS

a - $\sin(\psi+\mu)/((2\sigma\sin\phi\ \cos(\psi-\mu))$

b - $-\sin(\psi-\mu)/((2\sigma\sin\phi\ \cos(\psi+\mu))$

B - footing breadth

c - soil cohesion

Cc - compression index

CSL - critical state line

CVR - critical void ratio

e - void ratio

G_s - specific gravity

H - wall height

I_D - relative density

k - real variable

K_p - passive pressure coefficient

l - scale parameter

m - number of radial lines

M - slope of the critical state line when it is projected on to a constant volume plane

n - number of spiral lines

$N\gamma$ - bearing capacity coefficient

p - pressure (mean principal stress)

q - deviator stress

Q - ultimate bearing capacity

S - $S = \sigma_n$

T - $T = \tau_f$

V - specific volume

V_λ - specific volume on reference section

X - coordinates axis

Y - idem

Z - idem

ξ - $\chi + \psi$

δ - contact friction angle mobilized between sand and footing base or wall surface

ϵ - strain

ϕ - angle of shearing resistance

γ - bulk density of soil

η - $\chi - \psi$

λ - slope of the critical state line

μ - $\pi/4-\phi/2$, the angle between the slip lines and the major principal stress direction

σ - normal stress

τ - shear stress

ω - $\pi/2-\mu$

χ - $(\ln\sigma)/2\tan\phi$

ψ - inclination of major principal stress to the vertical axis (counterclokwise +ve)

Subscripts

ave - average

f - at failure

H - horizontal

i - initial

max - maximum

min - minimum

n - normal (to the plane of application)

ps - plane strain

tx - triaxial

v - vertical

1,2,3 - principal (stresses)

LIST OF TABLES

LIST OF FIGURES

FIGURE

Chapter I

INTRODUCTION

Bearing capacity factors for footings and passive pressure coefficients for walls are invariably reported in the literature as functions of the angle of shearing resistance of the soil. However, it is well acknowledged that identifying the angle of shearing resistance in a given problem is difficult. This thesis starts from the understanding that sand behaviour cannot be adequately described by a straight Coulomb-Mohr-Strength envelope as is done in traditional analysis

To get better correlation between theoretical results and experimental tests, it appears necessary to improve the methodology with respect to the sand parameters involved. One such parameter is the angle of shearing resistance that is commonly considered to be constant for reasons of simplicity. However, experimental evidence (Schofield and Wroth,1968) shows that the Coulomb envelope flattens with increasing stress. An understanding of this evidence is mainly based on the reasonable assumption that while the intergranular friction component of the angle of shearing resistance may be essentially independent of stress level, the dilatancy component is not. That is, the angle of shearing

resistance is not a soil constant but more a variable indicating the response of the soil structure under stress.

One attempt was made by Graham and Pollock (1972) to develop a non-constant-ϕ solution for the failure of walls and footings. To compute the ultimate stresses under a footing base or behind a retaining wall, Graham (1974) used the so-called 'slip-line' or 'stress-characteristic' method and introduced some developments of the Sokolovski[1] (1960) solutions. The varying-ϕ relationship was composed of three distinct linear parts as a function of stress level, and had been proposed earlier by De Beer (1963). It is important to note that the work required the use of computers that fortunately became available at that time (late 1960's and early 1970's). Although the consideration of a non-constant ϕ represented a more realistic approach to computer modelling of sand behaviour, some limitations could be put forward due the simplicity of the De Beer model.

With the appearance of a more reliable soil model, namely the critical state model (Roscoe,Schofield,Wroth,1958) in conjunction with great improvement of the computer software,it was felt that the time had come to address the variable ϕ question in a new 'critical state' framework. In view of these developments and in order to arrive at an adequate assement of the influence of the angle of shearing resistance, it was thus necessary to reprogram the stress charac-

[1] Also written "Sokolovskii"

teristic solution for a varying angle of shearing resistance based on the critical state model. This is the main objective of this thesis.

Firstly, in chapter 2, in order to comprehend and predict the behaviour of a sand, a conceptual framework is established : this is the critical state model. In chapter 3, a numerical procedure adapted by the author to include a new form of ϕ-variation is developed and used to address the two different cases of a rough footing and of a rough passive wall. Chapter 4 describes the parametric study that has been conducted by means of a revised computer program and also the choice of the required input parameters. Results and their discussion follow in Chapter 5 and 6. Topics for further research and conclusions are listed in Chapter 7. Appendix A deals with the question of how the theoretical and parametric results could be applied in construction problems of engineering interest. Appendix B contains the computer listing and a typical output. Finally, A sample of a computer plotting program is presented in Appendix C.

Chapter II

SAND MODELLING

2.1 INTRODUCTION

Since Coulomb introduced the simple equation $\tau = c + \sigma\tan(\phi)$ (τ shear stress at failure, σ normal stress at failure) to describe how the normal stress and the shear stress relate in a soil failure, soil mechanics has had to be developed in order to cope with the increasing complexity of industrialized society. In this process, researchers have had to approach various difficult situations such as the liquefaction of sands, slope stability problems, earthquakes, etc . These studies led them to acknowledge the complexity of the soil's response and induced them to conceive a 'unified' theory capable of handling various possible states of soil media.

2.2 THE CRITICAL STATE MODEL

Roscoe, Schofield and Wroth (1958) following ideas suggested earlier by Taylor(1948) proposed that the basic parameters 'τ,σ,e' were necessary and sufficient to describe the behaviour of a soil element. They conducted a series of drained and undrained tests on sand to obtain a unique yield surface composed of two major subsurfaces (Fig 2.1):

1. The Hvorslev surface
2. The Roscoe surface

The link between the two subsurfaces is called the critical void ratio line (CVR) or critical state line (CSL) and represents the ultimate state of a soil sample. Once at this 'critical state', the soil can be sheared without any further change of the three basic parameters.

Technically in material science we are dealing with yield surfaces because plastic-hardening is involved. However, in most soil mechanics work using the Coulomb-Mohr criterion, this should be called a 'rupture' or 'failure' envelope.

Fig 2.1 represents a schematic diagram of the model. This three dimensional plot can be expressed in two ways :

1. a (τ,σ,e) diagram
2. a (q,p',V) diagram
   a) with $p' = (\sigma_1' + \sigma_2' + \sigma_3')/3$, the mean principal stress.
   b) $q = \sigma_1' - \sigma_3'$, the deviator stress
   c) $V = 1 + e$, the specific volume

Although plot(1) is easier to visualize, plot(2) has the merit of taking into account the intermediate principal stress. As acknowledged by the position and the shape of the yield surface the shearing resistance of a soil depends not only on the normal stress but also on the value of the

initial void ratio. However, it important to note that the ultimate state represented by the CVR line is associated with independence from stress history effects.

In a ln(p'):V space, the normal consolidation line (NCL) and the critical state line (CSL) are experimentally found to be parallel (Wroth and Basset,1965,Fig 2.2). For various reasons associated with the low compressibility λ of sands[2] it has proved helpful to modify the original presentation of the critical state model by projecting all the points onto a reference section set arbitrarily as p'=1. This has permitted the three dimensional model to be represented in a two dimensional space,namely q/p' : V_λ (Atkinson and Bransby,1978,Fig 2.3), where

1. $V_\lambda = V + \lambda \, Log(p')$, and
2. λ is the slope of the CSL.

The present study has used these normalized plots as a representation of the critical state model for sand. This has enabled the author to develop a simple iteration process which can be used in calculating failure loads of structures in sand (section 3.6)

---

[2] The term 'compressibility' is retained for λ (λ=Cc/2.3)

2.3 MODELLING

In 1937, Casagrande stated simply that a dense sand exibits a high friction angle whereas a loose sand tends to exibit a lower friction angle (Rowe,1967). In the context of the sophistication and the simplicity of the critical state model and since the angle of shearing resistance is the characteristic that determines the response of the soil structure to external stresses, it has become necessary to understand the dependency of the angle of shearing resistance with respect to the ' basic parameters' e and p' (or e and σ).

Rowe (1967) separated the angle of shearing resistance ϕ into three components :

1. strength developed by frictional resistance and depending on the mineralogical content of the sand.
2. strength developed by the energy required to cause expansion or dilation of the material.
3. strength developed by energy required to rearrange and reorient soils particles.

Fig 2.4 shows the distribution of each component as a function of the relative density I_D . As might be expected, the dilatancy effect plays an increasing role as the relative density increases. This explains the higher friction angle of denser sands.

Although Rowe's diagram (Fig 2.2) is of considerable interest in understanding the behaviour of ϕ as a function of

the void ratio (represented by I_D) it does not address the influence of the confining pressure, that is, the second basic parameter of the critical state model.

Studying the behaviour of sands at extremely low pressures, Ponce and Bell (1971) found themselves in the position where they had to take into account the influence of the confining pressure and proposed a three-dimensional diagram $\phi = f(e,P)$; (Fig 2.5).

With regards to this representation, it is important to note that at extremely low pressures, shear produces almost no rearranging of particles since most of the energy is dissipated in expansion and true sliding; in other terms, it can be stated that low confining pressures cannot sufficiently restrain the sand to permit an internal reorganisation. Another consideration is the rapid decrease of ϕ with increasing pressure and the greater influence of the rearranging component over the dilatancy one for loose sands.

Even if the detailed study of each component of the angle of shearing resistance does not come directly into use in geotechnical calculations, that is, only the overall knowledge of ϕ is used, the parallel between the critical state model (e, σ, τ) in Fig 2.1a, and the three-dimensional ϕ diagram (e,σ,ϕ) in Fig 2.5 permits the establishement of a sound 'foundation' to explain the systematic variation of the angle of shearing resistance. More particularly should

be noticed the conceptual parallels between the τ-axis which represents the real physical shearing resistance of soil in engineering applications (macro-behaviour) and the ϕ-axis representing a measure of strength arising from engineering analysis (micro-behaviour).

2.4 CHOICE OF A $\phi_{ps} = f(\phi_{tx})$ RELATIONSHIP

This thesis addresses the computation of bearing capacity coefficients for strip footings and passive pressure coefficients for retaining walls. Both cases are two-dimensional and require the knowledge of a plane strain friction angle. Since triaxial tests are easiest to perform in the laboratory, they are used to establish the critical state model and they lead to angles of shearing resistance for three dimensional (axisymetric) stress states. It was therefore necessary to find a relationship that would transform triaxial ϕ-values (ϕ_{tx}) to ϕ-plane strain values (ϕ_{ps}).

Various researchers have proposed such relationships:

1. Wroth (1984,pers. comm.) $\phi_{ps} = 9/8\ \phi_{tx}$
2. Lade (1976)
   a) $\phi_{ps} = 1.5\ \phi_{tx} - 17^{o}$ for $\phi \geq 34^{o}$.
   b) $\phi_{ps} = \phi_{tx}$ $\phi_{tx} \leq 34^{o}$
3. Bishop (1966) : Fig 2.6 in the Sixth Rankine Lecture,1966 (after Cornforth,1964).

These various proposals are presented in Fig 2.7.

In this thesis, relationship (3) by Bishop has been used in the revised form shown in Fig 2.8. For use in the computer, the relationship was plotted in logarithmic terms and was subdivided into three linear parts (Fig 2.8) :

1. $\phi_{tx} < 33^{o}$ $\quad \phi_{ps} = \phi_{tx}$
2. $33^{o} \leq \phi_{tx} < 36^{o}$ $\quad \ln\phi_{ps} = 1.666\ln\phi_{tx} - 2.336$
3. $\phi_{tx} \geq 36^{o}$ $\quad \ln\phi_{ps} = 1.293\ln\phi_{tx} - 1.002$

Chapter III

STRESS-CHARACTERISTIC METHOD AND METHODOLOGY

3.1 INTRODUCTION

At the state of plastic limit equilibrium, the soil benea a footing or behind a passive retaining wall is stressed its limiting or yield condition. In loose and medium den sands, failure is close to the critical state, with : $\frac{\partial p}{\partial \varepsilon} = \frac{\partial q}{\partial \varepsilon} = \frac{\partial v}{\partial \varepsilon} = 0$. In dense sands, further straining is req red after failure before critical state is reached. Sokolov (1960) developed the stress-characteristic method to compu the stresses at failure. Graham (1968) pursued this idea an improved the numerical accuracy of the solution.

3.2 CHOICE OF A YIELD CRITERION

Coulomb (1776) suggested the equation :

$$\tau_f = c + \sigma_n \tan(\phi)$$

This equation states that plastic flow will occur (plasti failure) when the shear stress τ reaches a value that de pends on two material parameters and on the stress level These are the cohesion of the soil c , the angle of shearin resistance ϕ and the normal stress to the plane of applica tion σ_n .

Although this equation does not take into account the influence of the intermediate stress, Fig 3.1 provides some experimental evidence that the use of the Coulomb criterion is more accurate than the corresponding Tresca or the Von Mises criteria. The Coulomb criterion has been adopted in this thesis to define a 'yield' criterion.

3.3 SOKOLOVSKI METHOD

The Coulomb criterion is combined with the static equilibrium equations to provide a set of so-called 'basic equations' (Sokolovski,1960). One method of solving these equations consists of using logarithmic transformations to generate curvilinear coordinates whose directions coincide with the direction of the failure planes. This is commonly known as the method of stress characteristics. In turn, the solved system in logarithmic stress space provides a set of slip lines or a slip-line field whose positions are known in the physical (x,z) plane.

Assuming that the soil could be modelled by a constant value of the angle of shearing resistance, Sokolovski (1960) developed a numerical procedure based on approximations of the hyperbolic differential equations to obtain the slip-line field for cohesionless as well as cohesive soils. Since this thesis aims at analysing localized ϕ-variations in a granular (cohesionless) material, a more general application of Sokolovski's procedure has had to be developed in this thesis project.

3.4 LOCAL ϕ -VARIATION ASSOCIATED WITH SOKOLOVSKI'S METHOD

3.4.1 Local system of references

The proposed model is based on the representation of Fig 3.2. Locally, the curvature of the Coulomb-Mohr envelope can be treated as presenting a 'cohesive' component in a general system of references. This entails using the general differential equations developed for a (c,ϕ) medium (Sokolovski,1960). This is justified by the more general aspect of a cohesive frictional medium over a non-cohesive one. That is, a cohesionless soil is a more restricted case where the envelope has no intercept with the τ-axis.

3.4.2 General system of references

a) In a two-dimensional representation (Fig 3.2), the equilibrium equations are :

$$1. \quad \frac{\partial \sigma_{xx}}{\partial x} + \frac{\partial \tau_{xy}}{\partial y} = X$$

$$2. \quad \frac{\partial \tau_{xy}}{\partial x} \quad \frac{\partial \sigma_{yy}}{\partial y} = Y \qquad \text{Eqs. 3.1}$$

b) The Coulomb-Mohr criterion as a yield condition is described by (Fig 3.3) :

$$1. \quad \max(|\tau_n| - f(\sigma_n)) = 0$$

2. or $T = f(S)$ where

   a) $T=\tau_n$

   b) $S=\sigma_n$

This yield condition can be written as (Fig 3.3) :

$$\frac{d}{d\omega}(|\tau_n| - f(\sigma_n)) = 0 \qquad \text{Eq. 3.2}$$

where

1. $\sigma_n = 1/2(\sigma_1+\sigma_3) + 1/2(\sigma_1-\sigma_3)\cos2\omega$
2. $\tau_n = 1/2(\sigma_1-\sigma_3)\sin2\omega$

Substituting σ_n and τ_n into Eq. 3.2 :

$$\frac{d}{d\omega}(|\tau_n| - f(\sigma_n)) = (\sigma_1-\sigma_3)\sin2\omega(\cos2\omega + f'(\sigma_n))$$

and therefore $\frac{d}{d\omega}(|\tau_n| - f(\sigma_n)) = 0$ provides the general condition $\cot2\mu = f'(\sigma_n)$ where $2\mu = \pi - 2\omega$ (Fig 3.4). This angle determines the position of the slip lines inclined to the principal axis at the angle $\pm\mu$. At failure the stress conditions are :

1. $\sigma_n = 1/2(\sigma_1 + \sigma_3) - 1/2(\sigma_1 - \sigma_3)\cos2\mu$
2. $\tau_n = 1/2(\sigma_1 - \sigma_3)\sin2\mu$

In a chosen system of references (Fig 3.5), for any point A

1. $\begin{matrix}\sigma_x \\ \sigma_y\end{matrix} = 1/2(\sigma_1+ \sigma_3) \pm 1/2(\sigma_1- \sigma_3)\cos2\mu$

2. $\tau_{xy} = 1/2(\sigma_1 -\sigma_3)\sin2\psi$

Substituting σ_n and τ_n into $\sigma_x, \sigma_y, \tau_{xy}$ we get :

1. $\begin{matrix}\sigma_x \\ \sigma_y\end{matrix} = \sigma_n + \tau_n \frac{\cos 2\mu \pm \cos 2\psi}{\sin 2\mu}$

2. $\tau_{xy} = \tau \sin 2\psi / \sin 2\mu$

Substituting σ_x , σ_y , τ_{xy} into the equilibrium equations 3.1 produces a new set of equilibrium equations 3.3 :

1. $(1+\cos 2\mu\cos 2\psi)\frac{\partial \chi}{\partial x} + \cos 2\mu \sin 2\psi \frac{\partial \chi}{\partial y} - \sin 2\mu (\sin 2\psi \frac{\partial \psi}{\partial x} - \cos 2\psi \frac{\partial \psi}{\partial x})$

$$= \frac{\sin^2 2\psi}{2\tau_n}$$

2. $\cos 2\mu \sin 2\psi \frac{\partial \chi}{\partial x} + (1-\cos 2\mu\cos 2\psi)\frac{\partial \chi}{\partial x} + \sin 2\mu (\cos 2\psi \frac{\partial \psi}{\partial x} + \sin 2\psi \frac{\partial \psi}{\partial x}$

$$= \frac{\sin^2 2\mu}{2\tau_n}$$

where the Mandel function χ is defined by :

$$2\chi = \frac{d\sigma_n}{\tau_n} - 2d\chi$$

It is now convenient to introduce new variables defined by :

1. $\eta = \chi(\mu) - \psi$
2. $\xi = \chi(\mu) + \psi$

Using these variables, Eqs. 3.3 become :

1. $$\frac{\partial \eta}{\partial x} + \tan(\psi-\mu)\frac{\partial \eta}{\partial y} = a$$

2. $$\frac{\partial \xi}{\partial x} + \tan(\psi+\mu)\frac{\partial \xi}{\partial y} = b$$ Eqs. 3.4

where

$$\frac{a}{b} = \pm \frac{\sin 2\mu (X\sin(\psi \pm \mu) - Y\cos(\psi \pm \mu))}{2\tau_n \cos(\psi \mu)}$$

If the present problem is redefined in dimensionless terms with gravitational acceleration in the X-direction, the body forces are (Fig 3.5) :

$$x = 1 \quad \text{and} \quad y = 0$$

The right-hand part of Eqs. 3.4 becomes :

$$\frac{a}{b} = \pm \frac{\sin 2\mu \sin(\psi \pm \mu)}{2\tau_n \cos(\psi \pm \mu)}$$

Since at failure $\tau_n = 1/2(\sigma_1 - \sigma_3)\sin 2\mu$ (Fig 3.4), we obtain :

$$\frac{a}{b} = \pm \frac{\sin(\psi \pm \mu)}{(\sigma_1 - \sigma_3)\cos(\psi \pm \mu)}$$

For cohesionless materials, the angle of shearing resistance ϕ is defined as the angle between the tangent to the Coulomb-Mohr circle passing through the origin and the σ-axis. In principle, in the general case, the locus of the intersection of the tangent and of the Coulomb-Mohr stress circle could describe any curve (Fig 3.6). In order to match the definition of ϕ with the theoretical general case, an assumption is made in the context of the finite differences method :

Locally , ϕ can be determined as : $\sin\phi = (\sigma_1 - \sigma_2)/2\sigma$

where $\sigma = (\sigma_1+\sigma_3)/2$

In view of this assumption, a and b in Eqs.3.4 can be rewritten as :

$$\frac{a}{b} = \pm \frac{\sin(\psi \pm \mu)}{2\sigma \sin\phi \cos(\psi \pm \mu)}$$

The system of equations to be solved becomes, in the adopted system of coordinates (Fig 3.7) where now the z-axis is in the gravity direction, and the x-axis is horizontal :

1. $$\frac{\partial \xi}{\partial Z} + \tan(\psi + \mu)\frac{\partial \eta}{\partial X} = b = \frac{-\sin(\psi - \mu)}{2\sigma \sin\phi \cos(\psi + \mu)}$$

2. $$\frac{\partial \eta}{\partial Z} + \tan(\psi - \mu)\frac{\partial \eta}{\partial X} = a = \frac{\sin(\psi + \mu)}{2 \sin \cos(\psi - \mu)}$$ Eqs. 3.5

, as before $\eta = \chi - \psi$ $\xi = \chi + \psi$

and $2d\chi = d\sigma_n/\tau_n - 2d\mu$

Now $d\psi$ can be integrated after substitution of σ_n and τ_n, bearing in mind that $\sigma_n = \sigma - \tau_n$

$$2d\chi = \frac{2\sin^2 2\mu + 2\tau_n d\mu}{\tau_n} - 2d\mu$$

τ can be found from : $\sin\phi = \tau/\sigma \sin 2\mu$.

Since $2\mu = \pi/2 - \phi$,

we have $\sin\phi = \tau/\sigma\cos\phi$,

and thus $\tau = \sigma\sin\phi\cos\phi$.

Finally, $2d\chi = d\sigma/\sigma\tan\phi$

With the assumption that ϕ is non-variable within a limited finite range of stresses, the last equation can be integrated to give :

$$\chi = \log\sigma/2\tan\phi$$

The set of differential equations 3.5 can now be easily solved by the method of the characteristics. Use the differential relations :

$$d\xi = \frac{\partial\xi}{\partial Z}dZ + \frac{\partial\xi}{\partial X}dX \quad ; \quad d\eta = \frac{\partial\eta}{\partial Z}dZ + \frac{\partial\eta}{\partial X}dX$$

Solving Eq. 3.5 with these relations we obtain :

1. $$\frac{\partial\xi}{\partial Z} = \frac{b\,dX - \tan(\psi + \mu)\,d\xi}{dX - \tan(\psi + \xi)\,dZ}$$

2. $$\frac{\partial\eta}{\partial Z} = \frac{a\,dX - \tan(\psi - \mu)\,d\eta}{dX - \tan(\psi - \mu)\,dZ}$$

Eqs. 3.6

The stress characteristics correspond to cases where the numerator and the denominator are simultaneously equal to zero. This determines two real separate families of stress characteristics :

1. $$\frac{d\eta}{dZ} = a \quad \text{along} \quad \frac{dX}{dZ} = \tan(\psi - \mu)$$

2. $$\frac{d\xi}{dZ} = b \quad \text{along} \quad \frac{dX}{dZ} = \tan(\psi + \mu)$$

Eqs. 3.7

Note that the slopes $(\psi \pm \mu)$ of the characteristics are in the direction of limiting shear stress, and are therefore the local inclinations of failure planes.

Rewriting the above set in finite-difference terms

$$1.\ (X-X_1) = (Z-Z_1)\tan(\psi_1 - \mu) \quad ; \quad \eta - \eta_1 = (Z-Z_1)a_1$$

$$2.\ (X-X_2) = (Z-Z_2)\tan(\psi_2 + \mu) \quad ; \quad \xi - \xi_2 = (Z-Z_2)b_2$$

Eqs. 3.8

The unknowns are the variables X, Z, η, ξ which can be evaluated from the previously known variables $X_1, X_2, Z_1, Z_2, \eta_1, \xi_2$. The solution will then proceed from two previously determined points say P_1, P_2 to a new point P (Fig 3.8).

Solving Eqs. 3.8 directly for X, Z, η, ξ .

$$Z = \frac{Z_1\tan(\psi_1 - \mu) - X_1 - Z_2\tan(\psi_2 + \mu) + X_2}{\tan(\psi_1 - \mu) - \tan(\psi_2 + \mu)}$$

$$X = X_1 + (Z-Z_1)\tan(\psi_1 - \mu) = X_2 + (Z-Z_2)\tan(\psi_2 + \mu)$$

$$\eta = \eta_1 + (Z-Z_1)a_1 \ ; \ \xi = \xi_2 + (Z-Z_2)b_2$$

On . reversing the logarithmic transformation :

$$\sigma = \exp((\xi + \eta)\tan\phi) \qquad \psi = 1/2(\xi - \eta)$$

This simple finite-difference method yields only approximate results since no account of the curvature of the slip lines is considered in the use of ψ_1 and ψ_2 . Previous researchers have used iteration pro-

cesses on ψ (De Jong,1959, Sokolovski,1960), and on both σ and ψ (Graham,1968) to take account of the curvature of generalized slip-line fields.

The computer program used in this thesis added one additional iteration process.

1. iteration on σ (Sokolovski,1960; De Jong,1959)
2. iteration on ψ (Graham,1968)
3. iteration on ϕ (Author)

This is a new development of earlier procedures suggested by Graham and Pollock (1972). The additional iteration is used to model the dependency of ϕ on pressure, that is, the curvature of the Coulomb-Mohr envelope.

3.5 THE ϕ -ITERATION PROCESS

The process has been developed specifically to improve computational accuracy in a domain where ϕ varies with stress level. That is, the ϕ-value used in any small section of the solution arises from the solution itself, and is not predetermined by the analyst. It is based on the normalized plot of the critical state model outlined in chapter 2. Fig 2.2 represented this model on a plot of q/p' vs $V+\lambda\ln(p')$. For every state of stress and every specific volume there corresponds a value q/p' on the overconsolidated Hvorslev surface represented by the straight line in the normalized plot.

Since $q/p' = 6 \sin\phi / (3 - \sin\phi)$,

$\phi_{tx} = \text{Arcsin}(3M/(6 + M))$ where $M = q/p'$

In the ϕ-iteration procedure, this value of ϕ_{tx} is compared with the initial value of ϕ previously used to calculate p'. If $|\phi_{tx} - \phi_i| / \phi_i > 10^{-3}$, the initial value of ϕ is reset as $\phi_i = \phi_{tx}$. The process is repeated until the convergency criterion set as 10^{-3} in the program is satisfied.

3.6 DETERMINATION OF THE SLIP-LINE FIELD

Proceeding from a known boundary, that in this work is commonly taken as the edge of a passive zone beneath the free surface where $\psi = \pi/2$, the program computes point by point the slip-line field towards an end boundary where failure stresses are to be evaluated.The type of problem being examined (that is wall or footing, for K_p or $N\gamma$ values respectively) determines the data input to the program.

If point O is taken as the point of origin of the adopted system of physical coordinates, set as either the bottom corner of a footing or the top of a passive wall, the slip-line field consists of two families of characteristics :

1. a set of curved radial lines originating from point O.
2. a set of spiral lines intersecting the radial lines in turn at an angle of $2\mu = \pi/2 - \phi$

Since point O is a singular point of the slip-line field, it represents a point of discontinuity in the mathematical solution of the basic equations. At stress equals zero, the logarithmic transformations that are involved in the solutions tend to infinity. In order to handle this problem, Graham (1968) introduced a surcharge term in the computation of the slip-line field that allows the logarithmic stress range to remain finite. The effect of the surcharge term is then reduced by 'shrinking' the field by a factor of 10^{n}, n being a number of scale reductions necessary to almost eliminate the effect of the surcharge. Graham (1968) showed that the surcharge component is negligible after four or five scale reductions depending on the required accuracy. It is important to note that this scale reduction process does not introduce any scale effects itself since all computations are carried out in dimensionless terms. The influence of footing size on the results is handled separately in chapter 6 (Discussion of Results).

The present study has retained this procedure for handling the singularity at point O.

3.7 EDGE OF THE PASSIVE ZONE :THE INITIAL BOUNDARY CONDITION

This boundary is determined prior to any computation of the characteristic field and is defined as :

x : horizontal distance from O

$z = x \tan (\pi/4 - \phi/2)$ depth of the soil.

σ = (1.0 + Z) / (1 - sinϕ) where 1.0 is the surcharge term

ψ = $\pi/2$ direction of the major principal stress

Since the solution addresses a non-constant ϕ problem, the edge of the passive zone has to be developed as a boundary using the ϕ iteration process to compute a coupled set of compatible ϕ- and σ- values. As a result, the shape of this boundary is not a straight line but exhibits a slight convex curvature with increasing depth because stress levels (and therefore ϕ-values) change with depth.

3.8 THE END BOUNDARY : SURFACE WHERE LOADINGS ARE NEEDED

Two distinct cases can be identified.

3.8.1 Passive wall

The solution addresses the case of a fully rough wall where the angle of wall friction which is mobilized corresponds to the local angle of shearing resistance of the sand (Graham,1971; Shields and Tolunay,1972)). Since no discontinuities exist at the interaction between the sand and the wall, the wall is in this case a slip surface where normal stresses computed by the solution can be integrated as a force boundary. The computer program includes a subroutine that performs this operation and integrates the pressures into the dimensionless coefficient $K = \left(\int_0^H \sigma_H dX \right) / 0.5\gamma H^2$ where H is the wall height, and σ_H is horizontal pressure.

In this case, K_p is a function of the height of the wall, even though it it a dimensionless coefficient. That is, the program permits the examination of scale effect.

3.8.2 Bearing capacity for footings

Differing from the passive wall failure, a foundation failure presents two symmetrical zones of failure where the soil flows outward from the centre-line.

Graham (1971) showed that a solution that involves the extension of the slip lines up to the base of the footing should also address the problem of the discontinuity of the base friction angle δ at the centre-line of the footing base. He proposed a linear-δ variation to handle this situation where the footing base is considered to be a slip surface.

An alternative considers that an elastic wedge is trapped below the footing preventing the extension of the slip lines. This concept seems now acknowleged by various reseachers. Vesic (1973) concluded that the stress and the deformation patterns under a compressed area in an actual footing is such that it always leads to the formation of a wedge.

The present solution is based on the assumption of an elastic trapped wedge. In this case, the end boundary in the stress field computation is the lower edge of the elas-

tic wedge and is also a slip-line. This boundary is inclined to an angle ϕ with the footing base. Since the angle of shearing resistance has been allowed to vary in this thesis, the edge of the elastic zone must be determined using the ϕ iteration procedure. This leads to a slightly curved edge which is concave upwards.

Vertical stresses on the two symmetrical lower boundaries of the wedge are calculated for different-sized footings and then expressed as the dimensionless (but scale dependent) parameter $N\gamma$, where for surface footings :

$$Q = 0.5\ \gamma B^2 N\gamma$$

3.9 THE RIGID-PLASTIC ASSUMPTION

The solution which has been developed above is based on :

1. a yield criterion : the Coulomb-Mohr criterion incorporated into a critical state model,
2. static equilibrium equations, expressing rigid-plastic behaviour (Fig 3.9).

The solution does not take into account any strain-stress relationship in the sand and assumes negligible volume strains prior to failure. Clearly, the validity of such an assumption must be associated with the mode of failure observed. Even if the soil density alone does not determine the mode of failure patterns, Fig 3.10 shows that a loose sand (compressible) tends to fail in a 'punching shear fail-

ure' mode whereas a dense sand (incompressible) tends to fail in a 'local' or 'general shear failure' mode. These various failure modes were reported by Vesic (1963) and De Beer (1970).

It therefore seems that the idea of associating a relatively incompressible material such as a medium dense sand with a rigid-plastic behaviour does not alter the basic validity of the theoretical stress-characteristic solution. In the absence of an exact solution, this assumption is retained, especially for the range of densities considered (medium dense sand). By careful consideration of boundary conditions that changed with displacement of the stucture, Graham (1974) was able to compute approximate load-displacement interactions.

Chapter IV

PARAMETRIC STUDY

4.1 INTRODUCTION

In order to address a great number of possible variables , a broad range of input parameters has been tested.

4.2 DEFINITION OF THE CRITICAL STATE MODEL

The use of normalized plots of the sand behaviour (Fig 4.1) requires the input of a series of parameters necessary to define the q/p' and the V_λ axes.

4.2.1 V_λ axis

V_λ is defined by $V_\lambda = V+\lambda \ln(p')$ where V is the specific volume (V=1+e) and λ is the slope of the critical state line. V_λ has been allowed to vary within a range of values referred to as $(V_\lambda)_{min}$ and $(V_\lambda)_{max}$ where :

$$(V_\lambda)_{min} = (1+e_{min}) + \lambda \ln(p'_{min})$$

$$(V_\lambda)_{max} = (1+e_{max}) + \lambda \ln(p'_{max})$$

Two ranges of values were tested. They are hereafter referred to the 'limited' range case, and the 'broad' range case. For the limited range , the necessary values were fixed to be :

$e_{min} = 0.5, \quad p'_{min} = 10$ kPa

$e_{max} = 0.7, \quad p'_{max} = 10^4$ kPa

For the broad range case, these values were :

$e_{min} = 0.4, \quad p'_{min} = 10$ kPa

$e_{max} = 0.8, \quad p'_{max} = 10^4$ kPa

It is important to note that the values of the void ratio and pressure were chosen to be representative of extreme values that might be encountered in real sands, and to permit a parametric study. Bearing in mind that this study is directed particularly at medium dense sands (section 3.9), values of the void ratio should be associated with a 'medium' range. This question is addressed in Appendix A. The literature records few cases where the compressibility λ (or Cc) has been measured. Mostly, the behaviour of sands is related to its placement void ratio and unit weight. Values which have been found include :

Ref.	Sand type	λ
Lee and Farhoomand,1967	subrounded	0.150
Lee and Farfoomand,1967	angular	0.250
Atkinson and Bransby,1978	"typical"	0.100
Vesic and Clough,1968	Chatahoochee river	0.175

The work in this thesis has been performed on the basis of λ-values chosen to cover the range described by this limited number of references. In order to study the influence of the compressibility λ, a range of values of λ was tested for both the limited and the broad range cases. These values are :

$\lambda = 0.05,\ 0.10,\ 0.175,\ 0.250$

4.2.2 q/p'-axis

The limits of the chosen range were fixed as $(q/p')_{min}$ and $(q/p')_{max}$ corresponding respectively to $(V_\lambda)_{max}$ and $(V_\lambda)_{mi}$ A minimum and a maximum angle of shearing resistance were given as input parameters and the use of the relationship $q/p' = 6\sin(\phi)/(3-\sin\phi)$ provided the two limits $(q/p')_{mi}$ and $(q/p')_{max}$. For the limited range case, the values of the limits of the angle of shearing resistance were chosen as :

$\phi'_{min} = 32^0$

$\phi'_{max} = 40^0$

For the broad range case, these values were :

$\phi'_{min} = 28^0$

$\phi'_{max} = 45^0$

4.3 OTHER INPUT PARAMETERS

4.3.1 Density γ

An average dry density was considered for each case and was defined by :

$$\gamma_{ave} = \frac{G_s}{1 + e_{ave}} \gamma_w$$

where e_{ave} =

G_s = 2.65 specific gravity

γ_w = 9.81 kN/m^3 water unit density

4.3.2 Scale parameter : l

All the variables throughout the computation of the stress-characteristics were expressed in dimensionless terms. That is $\sigma=\sigma_r/\gamma l$, $X=X_r/l$, $Z=Z_r/l$ where l is a scale parameter used to convert real physical plane dimensional parameters σ ,X, Z into dimensionless ones, and vice-versa.The scale parameter l was chosen as the horizontal length of the edge of the passive zone (Fig 4.1 and 4.2).

4.3.3 Number of spiral and radial lines

In order to compare results from each case studied, the numbers of spiral and of radial lines used in the computation were kept identical throughout the parametric study. Ten spiral lines and twenty radial lines were considered. It is important to note that the radial lines are not straight lines but curved under gravity forces. This in effect re-

quires the computation of extra radial lines after each scale reduction of the domain (section 3.5). To input a higher number of spiral lines and of radial lines would slightly improve the accuracy of the solution. However, it would also lengthen the computation time. It was felt that a compromise has been reached with the chosen figures (10 spirals, 20 radials). This question was explored by Graham (1968).

4.3.4 Edge of the passive zone

The number of spirals having being chosen, the abscissas of the intersection of the spirals and of the edge the passive zone are input in dimensionless terms. Corresponding z, σ, ψ-values are then computed by the computer program (section 3.7)

4.3.5 Summary of all input parameters

For each case computed , the input parameters are:

1. e_{min}, e_{max} : minimum, maximum void ratio
2. p'_{min}, p'_{max} : minimum, maximum pressure
3. ϕ'_{min}, ϕ'_{max} : minimum, maximum angle of shearing resistance
4. λ : compressibility ($\lambda = Cc/2.3$)
5. l : scale parameter
6. n : number of spiral lines
7. m : number of radial lines

8. x(n) : abcissa of the intersections of the spirals and of the edge of the passive zone

Further discussion of factors influencing the choice of input parameters in a given problem is given is Appendix A.

4.4 VALIDITY OF THE COMPUTER PROGRAM

The validity of the numerical results produced by the computer has been established by testing the program with a constant-ϕ solution. That is, the ϕ-angle was not allowed to vary throughout the computation but was fixed at a constant value. Various values of the ϕ-angle were tested and results are summarized in Table 4.1 together with results previously obtained by Graham and Stuart (1971). Both sets of numerical results agree within 1% representing slight differences in computer rounding. This confirms the basic validity of the computer program for constant-ϕ modelling. This step is needed because the original program was in ALGOL, and had to be translated into WATFIV for use at the University of Manitoba. This comparison does not however confirm the validity of the variable-ϕ subroutine calculations which form the new contribution by the author.

Chapter V

RESULTS

5.1 BEARING CAPACITY COEFFICIENT FOR FOOTINGS

Since the determination of the slip-line field proceeds from an assumed "known" boundary (edge of the passive zone) towards the initially unknown boundary (edge of the elastic wedge), the coordinates of this end boundary are determined at the very end of the computation and depend on the input parameters. Fig 4.1 showed the position of the end boundary (E), the edge of the passive zone (P) and the direction of the computational process. Point A which is the intersection of the extreme characteristic and of the elastic wedge lies also on the centre-line of the considered footing. Therefore, the actual breadth of the footing is not predetermined but computed after the development of the stress-characteristics from the known passive zone boundary. Due to the symmetry of the problem, the actual breadth of the footing is twice the abcissa of point A. For every set of input parameters e_{min}, e_{max}, γ, λ, p'_{min}, p'_{max}, ϕ_{min}, ϕ_{max} and l, the computer program calculates a set of coupled results :

1. dimensionless bearing capacity coefficient $N\gamma$, where
   a) $N\gamma = 2\int_{o}^{B/2} \sigma_v \, dx / 0.5\gamma B^2$, and

b) where the vertical stress $\sigma_v = \sigma(1 + \sin\phi\cos^2\psi)$

2. breadth of the footing B (metres)

5.2 PASSIVE PRESSURE COEFFICIENT FOR WALLS

Similar to the computation of the bearing capacity coefficients for footings, the determination of the slip-line field behind a retaining passive wall proceeds from the edge of a passive zone towards the end boundary. In this case, the end boundary represents the fully rough back-surface of the wall. Fig 4.2 showed the position of the intersection of the extreme characteristic with the wall. As in the footing case where the breadth is determined a postiori, the actual height of the wall is determined at the end of the computation process and is represented by point A. Therefore, the ordinate z(A) of point A is the computed actual height of the wall. As a result of the parametric study outlined in the preceding chapter, every set of input parameters produces :

1. the passive pressure coefficient for a retaining wall K_p (dimensionless).
   a) $K_p = \int_o^H \sigma_H dz/0.5\gamma H^2$
   b) where $\sigma_H = \sigma(1-\sin\phi\cos^2\psi)$
2. the height of the wall H (metres).

5.3 SLIP-LINE FIELDS

Due to the number of characteristics, plots of the resulting slip-line fields are unacceptably "dense". For clarity, all the spirals but only half of the radial lines have been computer-drawn. Fig 5.1 shows the slip-line field for the footing case, only half of the total field is drawn, the other part being symmetric about the centre-line of the base of the footing. Fig 5.2 shows the slip-line field behind a failing passive wall.

5.4 RESULTS

5.4.1 Bearing capacity coefficient for footings

Chapter 4 described the parametric study that was conducted. Results of the computations are plotted in :

1. semi-log scale[3] : Figs 5.3a,b
2. log-log scale : Figs 5.4a,b where the abcissa ranges from 0.1 m to 10 m.
3. Compressed log-log scale : Figs 5.5a,b where the abcissa ranges from 0.01 m to 10 m.

Figs 5.6a,b present the plot of $N\gamma$ versus the compressibility λ.

---

[3] a and b refer to the "limited" and to the "broad" range case respectively.

5.4.2 Passive pressure coefficient for walls

Results are plotted in :

1. semi-log scale : Figs 5.7a,b
2. log-log scale : Figs 5.8a,b
3. compressed log-log scale : Figs 5.9a,b

Figs 5.10a,b represent the plots of the passive coefficients for wall as function of the compressibility λ of the sand.

These results are discussed in more detail in Chapter 6.

Chapter VI

DISCUSSION OF RESULTS

6.1 BEARING CAPACITY COEFFICIENTS FOR FOOTINGS

6.1.1 Influence of the breadth of the footing

Figs 5.3a,b showed semi-logarithmic plots of the bearing capacity coefficients versus breadth of footing. The bearing capacity coefficients increase rapidly as breadth decreases and flatten almost asymptotically as the breadth increases. This behaviour is observed for both the broad range case and the limited range case. However, it is important to note that the broad range case produces higher values at small sizes ($N\gamma$ = 303 for B=0.08 m ,λ = 0.250) than the limited range case ($N\gamma$ = 170 for B=0.10 m ,λ = 0.250). At large footing sizes, a reversed behaviour is observed : the broad range case gives lower values ($N\gamma$ = 44 for B=8 m ,λ = 0.250) than the limited range case ($N\gamma$ = 55 forB= 7.8 m ,λ = 0.250). An explanation of this phenomenon is due to the curvature of the Coulomb-Mohr envelope. In a given range of stresses, the broad range model is associated with higher and lower angles of shearing resistance than the limited range model. Therefore, the stresses at which the soil reaches its minimum ϕ-value under large footings on sands permitting angles of shearing resistance as low as 28° (the

broad range case) are greater than the equivalent stresses under similar footings resting on sands that exibit angles of shearing resistance as low as 32^0 (the limited range case). This in turn leads to lower values of the bearing capacity coefficients for the broad range case for large sizes as compared with those obtained for the limited range case.

A similar phenomenon occurs for small-size footings where stresses at which the soil first reaches its maximum value in the broad range case ($\phi'_{max} = 45^0$) are lower than those in the limited range case ($\phi'_{max} = 40^0$). In turn, higher $N\gamma$ values are observed for the broader range case.

Another factor attracts attention for both ranges, although it is more acute for the broad range case. Lines representing the behaviour of the sand in Figs 5.4a,b and Figs 5.8a,b for various compressibilities intersect at a breadth around 0.8 m. Thus, for a large footing, say breadth over 0.8 m, the $N\gamma$ value associated with a more compressible sand (for instance $\lambda = 0.250$) is lower than the $N\gamma$ values associated with a less compressible sand (for instance $\lambda = 0.050$). The reverse behaviour is observed for small footings with breadth say, less than 0.8 m. That is, the $N\gamma$ values associated with a more compressible sand ($\lambda = 0.250$ for instance) are greater than those associated with a less compressible sand ($\lambda = 0.050$ for instance).

It appears necessary to set upper and lower limits for the values of the $N\gamma$ coefficients since the mode of failure changes with the size of the footing. It was remarked earlier that large footings fail by 'punching' and small footings along localized shear surfaces (Vesic,1963). The notion of punching failure is understandable when thinking of the amount of energy required to develop a general shear failure mode in compressible soils, that is to move the soil outside the footing in an upward direction. The upper and lower limits of $N\gamma$ correspond to cases where only part of the foudation soil has reached limiting equilibrium. In narrow foundations, this part is restricted to the narrow zones in which continuous shear failure has developed. In very large foundations, or on compressible soil, the plastic region is bounded to the side of the footing by soil whose straining has not taken it into plastic behaviour. Controversy may arise in determining the criterion to fix the boundaries between these different failure mechanisms. It has not been possible in the past to approach this question quantitatively. As the changes of behaviours are probably subtle and progressive, experimental evidence is needed. This remains outside the scope of this thesis.

6.1.2 Influence of the compressibility λ

Both the limited and the broad range cases show similar patterns of behaviour (Fig 5.6). At small sizes $N\gamma$ increases with compressibility λ. However, for large footings, the

trend is reversed, and $N\gamma$ decreases slightly with increasing compressibility. The value is found to remain constant (non-varying with λ) for a size of 1.3 m in the case of a limited range and for a size of 1.21 m in the broad range case.

The explanation of this behaviour resides in the counteracting influences of the size of the footing and that of the compressiblity λ of the sand. For small footings, say B=0.5 m, the likelihood of failing in a rigid-plastic mode diminishes as the soil becomes more compressible. The sand compresses but does not fail and postpones failure at higher stresses. This explains the increases of the $N\gamma$ values. However, the same pattern of change is not observed in the case of large footings, say B=8 m. Here, the influence of the compressibility still does exist (leading to a higher $N\gamma$) but this influence is overriden by the influence of the scale effect and failure envelope curvature. As shown in the preceeding paragraph, for constant λ, the $N\gamma$ value decreases as the footing size increases. The combined effect of the influences of both the scale effect and compressibility leads to the observed behaviour, that is an overall decrease of bearing capacity coefficients for large footings. This behaviour is readily apparent in footings at large field scale. It contributes to an understanding of the common perception that small laboratory footings behave differently from field-scale footings.

It is important to note that the behaviour described above in Fig 5.6 is compatible with that observed in the preceding paragraph (Fig 5.4). As mentioned previously in section 6.1, the $N\gamma$ values for large footings decrease as the compressibility of the sand increases while the $N\gamma$ values of small footings increase with compressibility (lines 1,2,3,4 of Figs 5.4a,b).

Although it is difficult to separate the influence of the compressibility from that of pressure-dependent scale effects, this study shows that the two separate influences should not be neglected when an accurate evaluation of the $N\gamma$ coefficients is required.

6.2 COEFFICIENTS OF PASSIVE PRESSURE FOR WALLS

Computation of the coefficients of passive pressure for walls are very similar to those carried out for the estimation of the bearing capacity coefficients for footings . The patterns of the results are also similar. Consequently, a detailed discussion of these results and an explanation of the observed behaviour will not be repeated. The main points will be highlighted here and reference made to the previous detailed discussion of the bearing capacity coefficients.

6.2.1 Influence of the height of the wall

Both the limited range and the broad range exhibit the same general characteristics:

1. For a given λ, the coefficient of passive pressure for walls K_p decreases with the height of the wall (Figs 5.7a,b).
2. Curves correponding to various compressibilities intersect for a wall height of 1.8 m . This is apparent on Figs 5.8a,b.
3. For large wall heights, say over 1.8 m, the K_p coefficients associated with more compressible sand are smaller than those associated with less compressible sands (lines 1,2,3,4 on Figs 5.7;5,8).
4. For small wall heights, say less than 1.8 m, the K_p coefficients associated with more compressible sand are larger than those associated with less compressible sands (lines 4,3,2,1 on Figs 5.6;5.8).

Similar to the case of the bearing capacity problem, the general tendency is for the K_p coefficient to decrease with increasing wall size. This decrease is affected by the compressibility of the sand. Differences between the various lines representing the compressibility of the sand are also more marked for the broad range case.

6.2.2 Influence of the compressibility

The general characteristics for both the limited range and the broad range case (although more marked for the broad one) are:

1. For small heights, less than 1.8 m, the K_p coefficient increases with increasing compressibility. This is due to a lower likelihood of the sand of failing in a rigid-plastic mode . The sand compresses and postpones failure to higher stresses.
2. For large wall heights, over 1.8 m, the K_p coefficient decreases with increasing compressibility. This is due to the counteracting influences of pressure dependent size increases leading to lower values and of increased compressibilities leading to larger values. The overall observed behaviour is a decrease of the K_p coefficient with increasing compressibility.

6.3 CONTOURS OF THE ANGLE OF SHEARING RESISTANCE

6.3.1 Distribution of the ϕ-angle under a footing

Figs 6.1a,b show the contours of the angle of shearing resistance under 0.1 m wide and 2 m wide footings. In both cases, λ=0.250 and the broad range values are considered. The contours are represented by the dash lines. For both footing sizes, a decrease of roughly 10^0 is observed between the edge of the passive zone and the centre line. As expected, values of the ϕ-angle are greater for a small footing

(38^0-48^0) than those for a large footing (32^0-42^0 for the 2 m footing); this is due to the larger pressures under the large footing.

It is interesting to compare the $N\gamma$ values obtained from a constant ϕ-solution (Table 6.1) where ϕ is now taken as the average mobilized shearing resistance throughout the domain under stress, and corresponding $N\gamma$ values obtained from the present analysis based on the size of the footing and on the compressibility of the sand. The importance of this step in selecting appropriate ϕ-values was intoduced earlier by Graham and Stuart (1971).

For small footings, the $N\gamma$ value corresponding to a constant-ϕ analysis is 224 for $\phi=44^0$ and 330 for $\phi=46^0$. The $N\gamma$ value obtained from Fig 5.6b (broad range case, $\lambda=0.250$, $B=0.1$ m) is 300. For the large footing, the respective figures are 78 for the constant-ϕ solution with $\phi=38^0$ and 75 from Fig 5.6b Depending on the average value of ϕ which is taken to model the failure domain, the $N\gamma$ values from the two methods are clearly similar. It therefore appears that a conventional constant-ϕ analysis may produce accurate results as long as the 'correct' ϕ is chosen for the analysis. Since in practice it is extremely difficult to estimate a 'correct' angle of shearing resistance for a domain under stress, the present analysis based on the size of the footing and on the compressibility of the sand is inherently sound.

6.3.2 Distribution of ϕ behind a passive wall

Figs 6.2a,b show the contours of the angle of shearing resistance behind passive walls for heights of 0.1 m and 2.0 m. In both cases, the variation of ϕ in the failure zone is of the order of 8^0 . However, the mobilized ϕ angles for a 2 m wall are much smaller (36^0- 44^0) than those obtained for the 0.1 m wall (41^0-49^0). This is due to the larger pressures involved in the case of the larger wall.

As was shown for the bearing capacity problem, it is interesting to compare the K_p values that arise from the present analysis[4] with those obtained for a constant ϕ-solution where ϕ is taken as the average value of the angle of shearing resistance throughout the failing domain. Table 6.2 summarizes these values. The results of the two analyses are reasonably close but depend strongly on the average value of the ϕ-angle which is taken. Like the bearing capacity problem, it is apparent that estimation of the average ϕ-angle of the failing domain remains difficult. The critical state analysis presents a potentially easier alternative.

---

[4] referred as a 'critical state' analysis.

6.4 COMPARISON WITH OTHER THEORETICAL RESULTS

Fig 6.3 and 6.4 show the comparisons for walls and for footings with results obtained by Graham and Stuart (1971) who used the De Beer (1963) ϕ-pressure relationship. Only the broader- and the narrower-range results of the present analysis are plotted. Line (3) represents the results obtained for the broader range case with λ=0.250. Line (2) corresponds to the results obtained for the limited range case with λ=0.050. Lines (1) and (4) represent results provided by the Graham and Stuart study for a loose sand and for a dense sand respectively.

It is important to notice that for both the wall problem and the footing one, the curves corresponding to the narrower range (line 2) remain in the Graham and Stuart range and almost parallel to the loose sand. Ideally, if the variation of the ϕ-angle did not have any influence, curves corresponding to a medium sand (lines 2) should approximatively be situated in the middle of the Graham and Stuart range. Therefore, the fact that lines (2) are offset towards the loose sand brings some evidence that the variation of the ϕ-angle does alter the computation of the ultimate stability of the domain under stress.

Lines (3) representing the broader range where the ϕ-angle is allowed to vary from 28^0 to 45^0 must be understood as an accentuation of what lines (2) represent (narrow range, $\phi = 32^0 - 40^0$). In view of this fact, it is therefore expected

that lines (3) be closer to the Graham and Stuart dense state for small sizes and closer to the Graham loose state for large sizes. This is what Figs 6.3 and 6.4 reveal. However, since the minimum ϕ-angle in the broader range in the present study is as low as 28^{0}, compared with the Graham and Stuart minimum of 32^{0}, the range of behaviour of the sand represented by lines (3) is broader than the Graham and Stuart range. Consequently, bearing capacity coefficients for large footings and passive pressure coefficients for large walls are lower than those obtained by Graham and Stuart.

6.5 COMPARISON WITH EXPERIMENTAL RESULTS

6.5.1 Footing case

Experimental results provided by Vesic (1973), Graham and Stuart (1971) and Meyerhof (1951) have been plotted in Fig 6.5. In order to compare these results with the range of values produced by the critical state analysis, the upper limit of the set of $N\gamma$ values produced (broad range, λ=0.05) as well as the equivalent lower limit (limited range, λ=0.250) have also been plotted in Fig 6.5. Clearly, the general trend of experimental values correlate reasonably well with the form of the solution arising from the critical state analysis. In particular, the range of the theoretical solutions which have been primarily carried out for medium dense sands covers closely the range of experimental values obtained for medium relative density sands.

However, it is clear that it is still not possible without extensive additional testing to predict from this work, the bearing capacity of a footing on a particular sand. Since this thesis was prepared, the author has been made aware of a recent literature review in the paper: Amar,S., Baguelin,F., and Canepa,Y., 1984 : "Etude experimentale du comportement des fondations superficielles",Anales de l'institut technique du batiment et des travaux publics, sols et fondations 189 # 427,Paris,France.

6.5.2 Wall case

Similar to the footing problem, the broadest range of K_p values obtained from the critical state analysis have been plotted against experimental data (Fig 6.6). The upper limit of the range is described as the set of values yielded by the broad range case analysis (λ=0.05), whereas the lower limit correspond to the limited range (λ=0.250). As for the experimental data, results obtained by Kerisel (1972), Horn (1967) and Graham (1971) have been considered. Even if the experimental values seem quite dispersed, a general trend still appears, that is, a decrease of the K_p values with increasing wall height. Like the bearing capacity problem, the range of theoretical values which is primarly valid for medium dense sands broadly covers the range of experimental data.

In both cases ($N\gamma$ and K_p values), the theoretical solutions and field data encompass scale effect influences whereas small scale laboratory tests do not in general. It therefore appears that the scattering of the experimental values outside the theoretical range is not an abnormality of the sand behaviour but represents tests on sands which may be very angular, rounded, or well-graded, and which lie outside the ranges of behaviour shown in Figs. 4.3a,b.

6.6 SINGULARITY OF SIZE 1m

Figs 5.5a,b and Fig 5.9a,b showed respectively the plots of the bearing capacity coefficients against the breadth of the footing, and the passive pressure coefficients against the height of the wall . These are plots where abscissas represent a broader range (0.01,0.1,1.0,10 m) compared with the preceding plots (Figs 5.4 and 5.8) where the the range was (0.1,1.0,10.0 m). This has the effect of compressing the diagrams in the X-direction and thus accentuating all the possible singularities in the curves. Such a singularity is situated for a size of 1 m (height of the wall or breadth of the footing). As is apparent in Figs 5.5 and 5.9, the $N\gamma$ values and the K_p values exhibit localized slope discontinuities at size 1 m. These discontinuities can be explained by the way the $N\gamma$ values and the K_p values are calculated.

For a passive wall, K_p is evaluated from the equation :

$$P_p = 0.5\ \gamma H^2 K_p$$

For a footing, $N\gamma$ is calculated from :

$$Q = 0.5\ \gamma B^2 N\gamma$$

Both equations have the same form :

$$y = 0.5\ k\gamma x^2$$

The function x^2 shows a singularity when the variable x=1, that is $x^2 = x$ ($1^2 = 1$). Therefore it is important to consider the singularity which is introduced by squaring the variable x which as explained above represents the breadth of the footing or the height of the wall.

Consider : $x^2-x = x(x-1)$ and notice that K_p and $N\gamma$ are evaluated as a function of the form : $k / |x(x-1)|$.
The function $y=1 / x(x-1)$ is plotted in Fig 6.7. Three intervals can be distinguished:

1. $0 < x < 0.5$ asymptote at x=0 with y decreasing.
2. $0.5 < x < 1$ asymptote at x=1 with y increasing.
3. $1 < x$ asymptote at y=0 with y decreasing

These patterns of slope changes are similar in some respects to those observed in Figs 5.5 and 5.9 :

1. 0 < size < 0.5 m $N\gamma$ and K_p decrease rapidly
2. 0.5 < size < 1m $N\gamma$ and K_p decrease slowly and a local slope discontinuity obtained at size 1 m.
3. 1 < size $N\gamma$ and K_p decrease first rapidly and seem to tend to an asymptotic value.

The mathematical function $y=1/|x(x-1)|$ explains the behaviour observed for K_p and $N\gamma$. The local slope discontinuity at size 1 m is therefore not due to some particular feature of the sand response but is introduced artificially by the normalizing equations which serve the purpose of defining the bearing capacity and passive pressure coefficients in dimensionless terms.

These results have shown that an estimation of bearing capacity and passive pressure coefficients based solely on a constant angle of shearing resistance seriously underestimate the complexity of the problem. The scale effect factor plays notably such an important role that practicing engineers use some empirical rules to take it into account. Alternatively, they neglect the usefulness of calculating failure loads in sands for full size structures. Bjerrum (1973) mentions such an empirical rule by stating that calculation of large footings for gravity stuctures in the North Sea is done by applying a reduction of ϕ of the order $n.1^0$ to $n.4^0$ for each 10^n reductions of the footing size (n is an integer). This rule arises from the qualitative work presented by Graham and Pollock (1972). It thus appears that current practice acknowledges the importance of known but poorly determined factors such as those described in this thesis.

Chapter VII

CONCLUSIONS AND FURTHER RESEARCH

7.1 CONCLUSIONS

Conclusions drawn from this study are :

1. The advent of more powerful and more convenient computers and peripherals makes it possible to investigate the development of the static equilibrium equations combined with a new sand model (Critical State model).
2. The angle of shearing resistance is only one component among others that are necessary to get accurate computations of bearing capacity coefficients for footings and passive pressure coefficients for walls.
3. The two most important additional parameters that are taken into account in this study are :
   a) the footing breadth or the wall height.
   b) the compressibility of the sand (λ or Cc).
4. Bearing capacity coefficients for footings and passive pressure coefficients for walls have been expressed in dimensionless terms. For a given sand, they decrease with increasing size (breadth of the footing or height of the wall). This is due to the effect of higher pressures associated with larger

walls or footings which decrease the mobilized angle of shearing resistance.

5. The variation of the angle of shearing resistance has been found to be approximatively 10^0 in the rigid-plastic domain beneath a footing (Fig. 6.1). The equivalent variation of the ϕ-angle behind a passive wall is 8^0 (Fig. 6.2).
6. The produced solutions correlate well with other theoretical and experimental results (Figs. 6.3 to 6.6).

7.2 SUGGESTIONS FOR FURTHER RESEARCH

1. The behaviour of rigid-plastic zones has been described using stress-characteristics. It would be of considerable interest to model with a Finite Element mesh the trapped elastic zone beneath a footing and connect it to the stress-characteristic solution. Similarly, a major further development would be to connect a stress-characteristic solution to the compressed non-failing field to the side of a footing on strain-hardening soil when "punching" is occurring.
2. Contours of the mobilized angle of shearing resistance have been drawn. The critical state analysis could also permit the computation of the variation of the void ratio. This could be investigated to draw the contours of the void ratio or volume strain be-

neath a footing or behind a passive wall. In turn, the variation of the density could be addressed.

3. The rigid-plastic assumption does not take into account volume strains prior to failure. Experimental tests could determine some index of "compressibility" that could be used to factor the $N\gamma$ and K_p values for compressible sands. Alternatively, approximate load-displacement relationships can be derived by close attention to boundary conditions.

4. Further laboratory tests should be performed to further confirm the validity of the critical state model. This, in turn, will reinforce confidence in the critical state analysis.

BIBLIOGRAPHY

Amar, S., Baguelin, F.,Canepa, Y., 1984 : "Etude experimentale du comportement des fondations superficielles", Annales de l'Institut du batiment et des travaux publics, Serie Sols et Fondations 189,# 427, Paris, France.

Atkinson, J.H., and Bransby, P.L., 1978 : "The Mechanics of Soils, an introduction to Critical State soil Mechanics". Mc Graw-Hill, London, England.

Bishop, A.W., 1966 : "The strength of soils as engineering material", Geotechnique, 16, pp. 91-128.

Bjerrum, L., 1973 : "Geotechnical problems involved in foundations of structures in the North Sea", Geotechnique, 23, num. 3, pp. 319-358.

Caquot, A., and Kerisel, J., 1956 : "Traite de Mecanique des sols", 3rd. ed., Gauthier-Villars, PARIS, FRANCE.

Cornforth, D.H., 1961 : "Plane strain failure characteristics of a saturated sand", Phd Thesis, Imperial College of Science and Technology, London, England.

Coulomb, C.A., 1776 : "Essai sur une application des regles de maximis et minimis a quelques problemes de statique, relatif a l'architecture", Memoires de Mathematique de l'Academie Royale des Sciences, PARIS, 7, pp. 343-382.

De Beer, E.E., 1963 : "The scale effect in the transposition of the results of deep sounding tests on the ultimate bearing capacity of piles and caisson foundations", Geotechnique, 13, pp. 39-75.

De Beer, E.E., 1970 : "Experimental determination of the shape factors and the bearing capacity factors of sand", Geotechnique, 20, Num. 4, pp. 387-411.

De Jong, G. de J., 1959 : "Statics and Kinematics in the failable zone of a granular material", Delft : Uitgeverij-Waltman.

Graham, J., 1968 : "Plane plastic failure in cohesionless soils", Geotechnique, 18, Num. 3, pp. 301-316.

Graham, J., 1971 : "Calculation of passive pressure in sand", Canadian Geotechnical Journal, 8, Num. 4, pp. 566-578.

Graham, J., 1974 : "Plasticity solutions to stability problems in sand", Canadian Geotechnical Journal, 11, num 2, pp. 238-247.

Graham, J., and Pollock, D.J., 1972 : "Scale-dependent plasticity analysis for sand", Civil Engineering and Public Works Review, 67, pp.245-251.

Graham, J., and Stuart, J.G., 1971 : "Scale and boundary effects in foundation analysis", Proc. ASCE, 97, SM 11.

Green, G.E.,Bishop, A.W., 1969 : "Note on the drained strength of sand under generalized strain conditions", Geotechnique 19.

Kerisel, J., 1972 : "Le langage des modeles en Mecanique des sols", Proc. 5th Eur. Conf. Soil Mech. Found., Eng., Madrid, Spain, Vol 2, pp. 9-30.

Lade, P.V, and Lee, K.L., 1976 : "Engineering properties of soils", Report UCLA-ENG-7652.

Lambe, A.W., and Whitman, R.V., 1969 : "Soil Mechanics, S.I Version", John Wiley, New York.

Lee, K.L., and Farhoomand, I., 1967 : "Compressibility and crushing of granular soil in anisotropic compression", Canadian Geotechnical Journal, 4, Num 1, pp.68-86.

Meyerhof, G.G., 1951 : "The ultimate bearing capacity of foundations", Geotechnique, 2, pp.301-332.

Ponce, M., and Bell, J.M., 1971 : "Shear strength of sand at extremely low pressures", ASCE, 97, SM 4.

Roscoe, K.H.,Schofield, A.N., and Wroth, C.P., 1958 : "On the yielding of soils", Geotechnique, 8, .pp 22.

Rowe, P.W., 1967 : "Three components of the strength of a granular material", ASCE, 93, SM 6.

Schofield, A.N., and Wroth, C.P., 1968 : "Critical State Soil Mechanics", Mc Graw-Hill, London, England.

Shields, D.H., and Tolunay, Z.A., 1972 : "Passive pressure coefficients for sand", Canadian Geotechnical Journal, 9, pp. 501-503.

Sokolovski, V.V., 1960 : "Statics of Soil Media", Butterworths Scientific Publications, London, England.

Taylor, D.W., 1948 : "Fundamentals of soil mechanics", John Wiley, New York.

Vesic, A., 1963 : "Theoretical studies of cratering mechanisms affecting the stability of cratered slopes", Final report, Project # A-655, Engineering Experimental Station, Georgia Institute of Technology, Atlanta, Georgia, pp. 1-67.

Vesic, A., 1973 : "Analysis of ultimate loads of shallow foundations", Proc. ASCE, 99, SM 1, pp. 45-73.

Vesic, A.S., and Clough, G.W., 1968 : "Behaviour of granular material under high stresses", Proc. ASCE, 94, SM 3, pp. 661-688.

Winterkorn, H.F., and Fang, H.Y., 1975 : "Foundation Engineering Handbook", Van Nostrand Reinhold Company, New York.

ϕ-angle	N_γ-value from Graham and Stuart	N_γ-value from the computer program
30^o	23	23.17
32^o	31	31.25
34^o	45	45.60
36^o	68	69.20
38^o	98	98.90
40^o	146	147.90
42^o	240	242.97

ϕ-angle	K_p-value from Graham and Stuart	K_p-value from the computer program
30^o	5.6	5.65
34^o	7.8	7.85
38^o	11.3	11.60

TABLE 4 .1 - CHECK OF NUMERICAL ACCURACY OF THE PROGRAM, COMPARISON OF CONSTANT- ϕ SPECIFICATION WITH EARLIER RESULTS FROM GRAHAM AND STUART (1971).

	Average-ϕ in the domain under stress	N_γ value from Fig 5.4 b	N_γ value for a constant-ϕ
0.10 m footing	44^0 46^0	300	224 330
2.0 m footing	38^0	75	78

FIG 6.1 - COMPARISON OF N_γ-VALUES FROM THE CRITICAL STATE MODEL (VARIABLE -ϕ) WITH EQUIVALENT VALUES USING A CONSTANT AVERAGE MOBILIZED ϕ IN FAILURE DOMAIN.

	Average-ϕ in the domain under stress	Critical state analysis Fig 5.8 b	K_p value for a constant-ϕ Caquot, Kerisel (1956)
0.10 m wall	45^0	25.5	25
2.0 m wall	40^0	12.5	14

FIG 6.2 - COMPARISON OF K_p-VALUES FROM THE CRITICAL STATE MODEL (VARIABLE-ϕ) WITH EQUIVALENT VALUES USING A CONSTANT AVERAGE MOBILIZED ϕ IN FAILURE DOMAIN.

Classification	γ_{min}	γ_{max}	e_{min}	e_{max}	Max. size	D_{10}	C_u	C_c	F
SP-SM	90	108	0.54	0.84	#16	.058	6.0	2.2	.555
SM	75	97	0.83	1.36	3/4"	.0065	31	5.5	.638
SP	92	112	0.48	0.80	#4	.15	3.0	.93	.667
SP	93	113	0.46	0.77	1 1/2"	.16	2.4	.92	.674
SP	95	116	0.43	0.74	#4	.30	3.7	1.0	.721
SP-SM	92	113	0.46	0.80	3/4"	.08	3.0	.88	.739
SP	85	107	0.54	0.94	#30	.10	2.3	1.3	.740
SP	97	118	0.40	0.70	1 1/2"	.11	3.2	1.2	.750
SP	99	120	0.38	0.67	1 1/2"	1.8	4.4	.76	.763
SM-ML	83	108	0.62	1.11	#4	.012	8.3	1.5	.790
SP-SM	79	103	0.60	1.08	#30	.09	2.4	1.5	.800
SP	103	124	0.33	0.60	3/8"	.17	5.0	.75	.818
SM	105	126	0.31	0.57	5"	.02	350	.30	.838
SP-SM	87	112	0.48	0.90	#4	.08	3.0	1.3	.875
SM	82	108	0.54	1.02	#16	.023	6.5	1.4	.889
SW-SM	95	119	0.39	0.74	3"	.05	10	1.4	.897
SP	98	122	0.36	0.69	#4	.37	5.1	1.2	.917
SW-SM	98	125	0.34	0.71	3"	.07	6.8	1.0	1.088
SP-SM	97	124	0.33	0.70	3/4"	.10	5.0	1.4	1.121
SP-SM	84	115	0.44	0.97	1 1/2"	.065	4.7	1.4	1.205
SP-SM	94	123	0.34	0.76	1 1/2"	.12	4.4	1.3	1.235
SM	99	128	0.31	0.70	3"	.02	240	1.8	1.258
SP-SM	80	114	0.44	1.06	#16	.07	3.7	1.6	1.409
SW-SM	80	116	0.42	1.07	1 1/2"	.074	6.6	2.4	1.547
SM	83	120	0.38	0.99	#4	.015	26	6.1	1.605
SM	102	134	0.23	0.62	3/4"	.01	120	1.9	1.695
GN-GM	113	127	0.31	0.47	3"	.14	86	1.2	.517
GP-GM	112	129	0.32	0.52	3"	.03	200	.50	.625
GW-GM	116	133	0.26	0.44	5"	.17	171	2.2	.692
GP-GM	110	128	0.30	0.51	3"	.11	191	15	.700
GP-GM	117	133	0.24	0.41	5"	.125	160	4.0	.708
GW-GP	111	130	0.27	0.49	3"	.20	105	7.5	.815
GP	116	134	0.23	0.43	5"	.27	111	6.2	.870
GW	119	139	0.24	0.45	3"	.51	45	2.2	.875
GW	120	139	0.20	0.39	3"	.45	51	1.6	.950
GW	119	139	0.21	0.41	3"	.18	94	1.1	.952
GW	111	132	0.25	0.49	3"	2.9	9.7	1.8	.960
GP	115	136	0.22	0.44	5"	.38	29	.61	1.000
GP	114	135	0.22	0.45	3"	2.0	11	.77	1.045
GW-GM	121	141	0.19	0.39	3"	.30	77	2.3	1.052
GM	122	141	0.17	0.36	1 1/2"	.025	381	3.0	1.118
GW-GM	114	137	0.21	0.45	3"	.60	16	1.2	1.143
GW	112	138	0.20	0.48	3"	2.0	12	1.3	1.400
GW	109	137	0.21	0.52	3"	2.0	14	2.6	1.476
GP	114	140	0.18	0.45	3"	1.7	10	.76	1.500
GM	101	132	0.25	0.64	1 1/2"	.03	260	12	1.560
GW-GM	111	139	0.19	0.49	3"	1.8	13	2.3	1.578
GP	115	142	0.17	0.44	3"	.31	87	8.2	1.588
GW	123	146	0.13	0.34	3"	.21	124	1.1	1.615
GW-GM	110	139	0.19	0.50	5"	.42	43	2.1	1.631
GW-GM	115	142	0.17	0.45	3"	.15	133	1.1	1.647
GP-GM	112	140	0.18	0.48	3"	.42	26	4.2	1.667
GW-GM	112	140	0.18	0.48	5"	.25	56	1.0	1.667
GW-GM	114	142	0.16	0.45	3"	1.2	15	1.7	1.812
GP	112	141	0.17	0.48	3"	1.4	7.1	.73	1.823
GW-GM	118	147	0.12	0.40	3"	1.3	19	1.1	2.333

TABLE A.1 - COMPACTIBILITY(F) OF COHESIONLESS SOILS (WHERE $F=(e_{max} - e_{min})/e_{min}$), AFTER WINTERKORN AND FANG (1975).

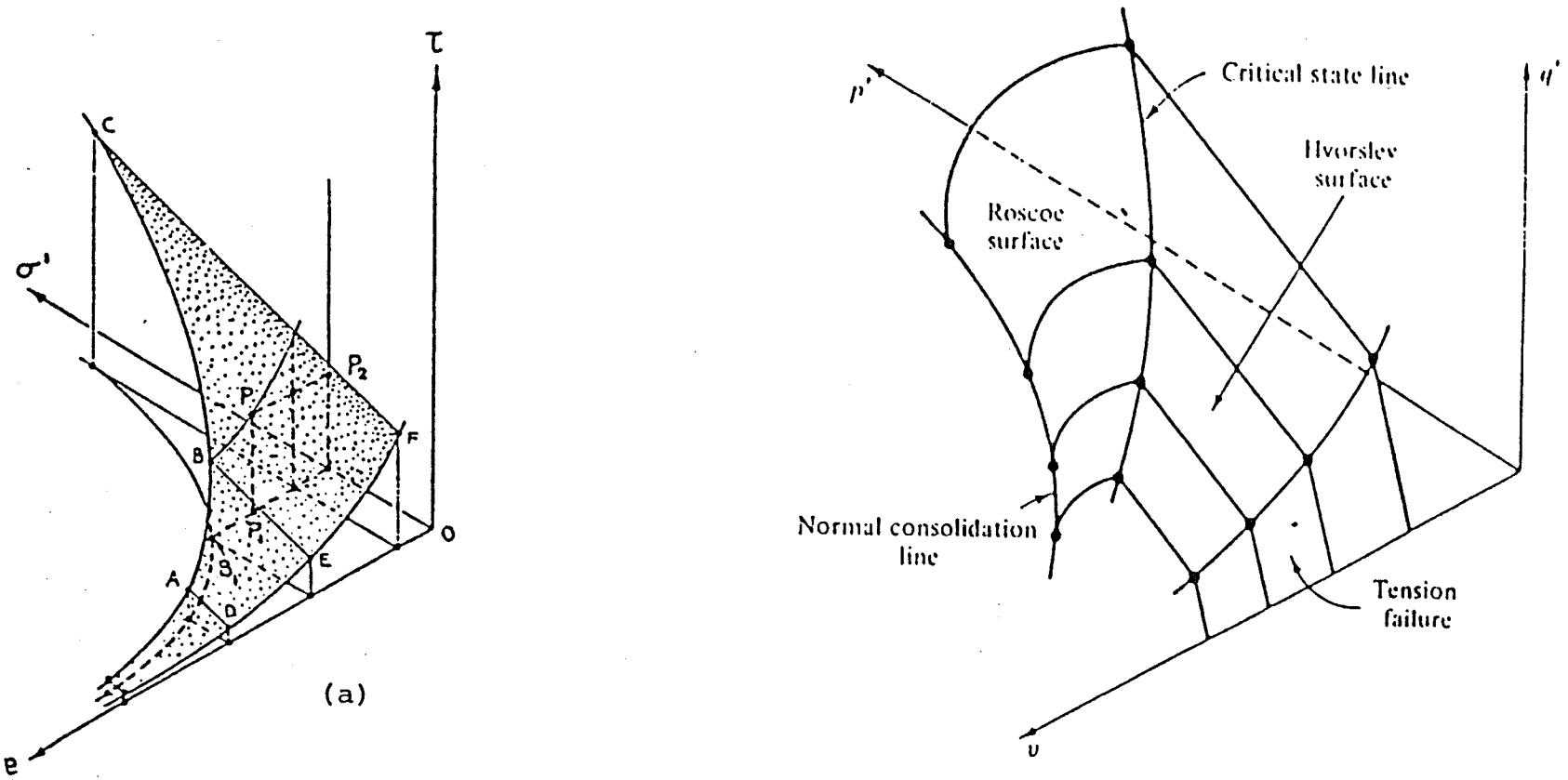

FIG 2.1 - THREE-DIMENSIONAL REPRESENTATION OF THE CRITICAL STATE MODEL.
(a) AFTER ROSCOE, SCHOFIELD AND WROTH (1958),
(b) AFTER ATKINSON AND BRANSBY (1978).

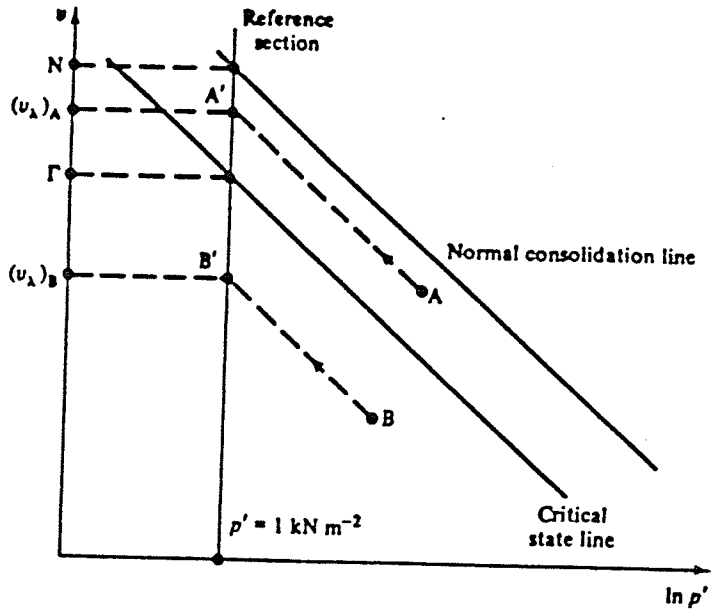

FIG 2.2 - THE NORMAL CONSOLIDATION LINE (NCL), CRITICAL STATE LINE (CSL) AND THE "REFERENCE SECTION" AFTER ATKINSON AND BRANSBY (1978)

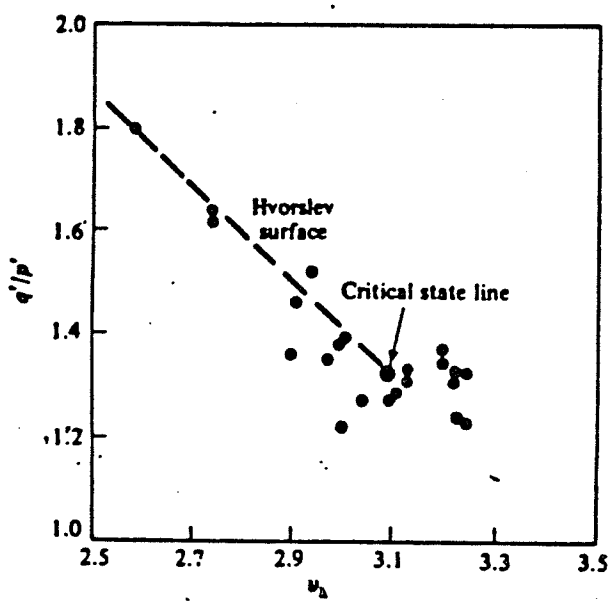

FIG 2.3 - NORMALIZED PLOT OF THE CRITICAL STATE MODEL FOR SAND, AFTER ATKINSON AND BRANSBY (1978)

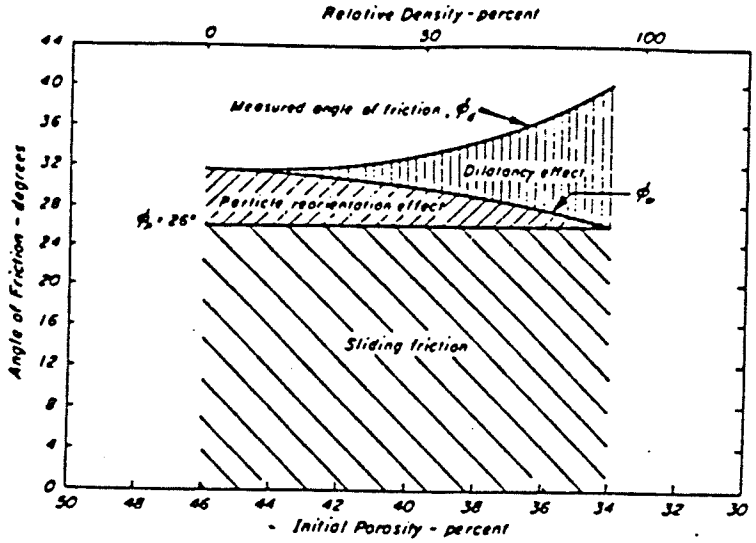

FIG 2.4 - COMPONENTS OF STRENGTH OF SAND, AFTER ROWE (1967).

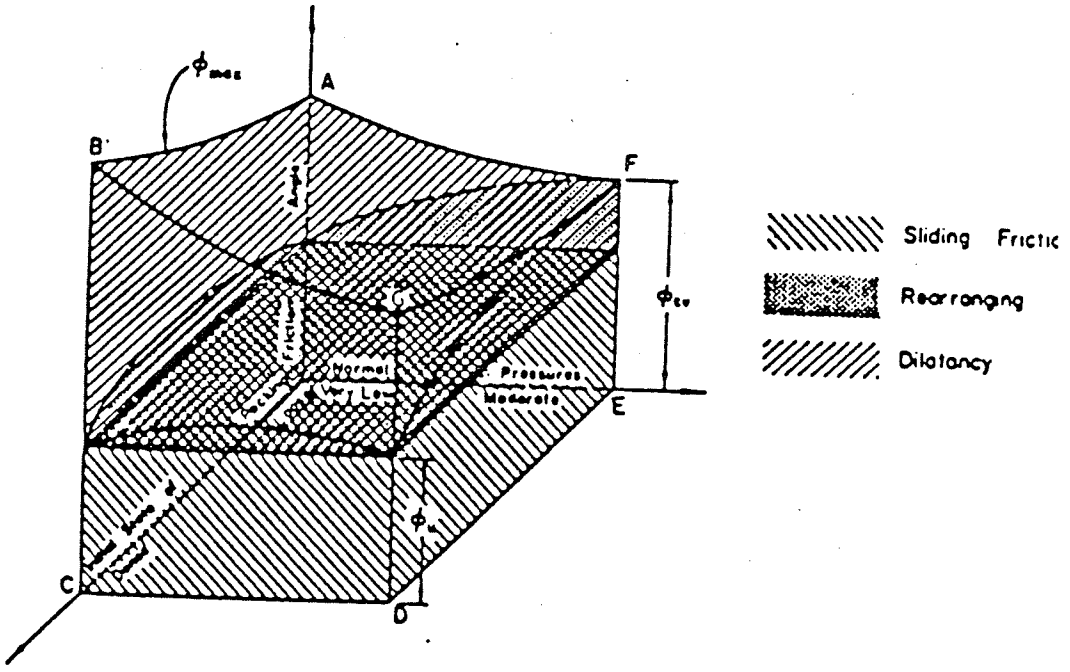

FIG 2.5 - THREE-DIMENSIONAL REPRESENTATION OF ANGLE OF SHEARING RESISTANCE, AFTER PONCE AND BELL (1971).

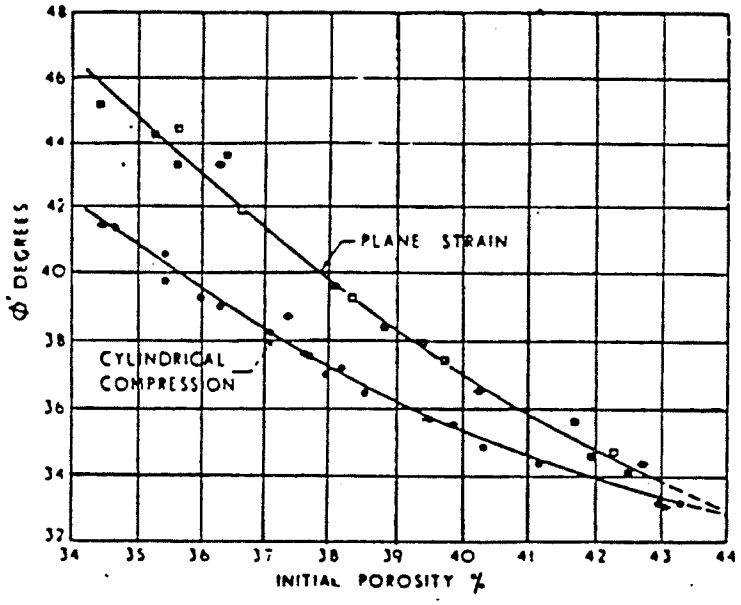

FIG 2.6 – COMPARISON OF RESULTS OF DRAINED PLANE STRAIN AND CYLINDRICAL COMPRESSION TESTS ON BRASTED SAND, AFTER CORNFORTH (1961), PRESENTED BY BISHOP (1966)

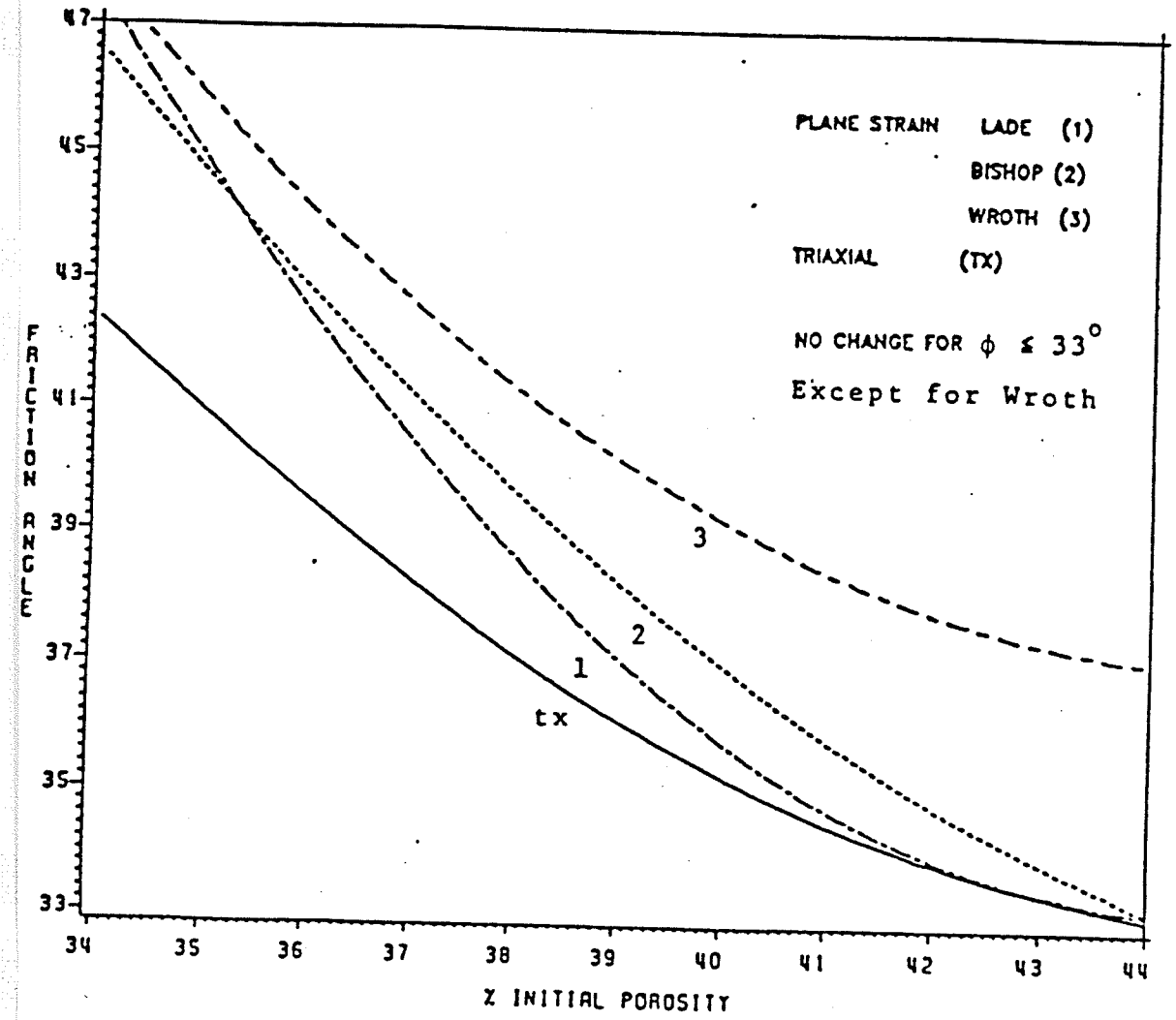

G 2.7 — COMPARISON OF VARIOUS PLANE STRAIN ϕ-ANGLES VERSUS TRIAXIAL ϕ-ANGLE RELATIONSHIPS

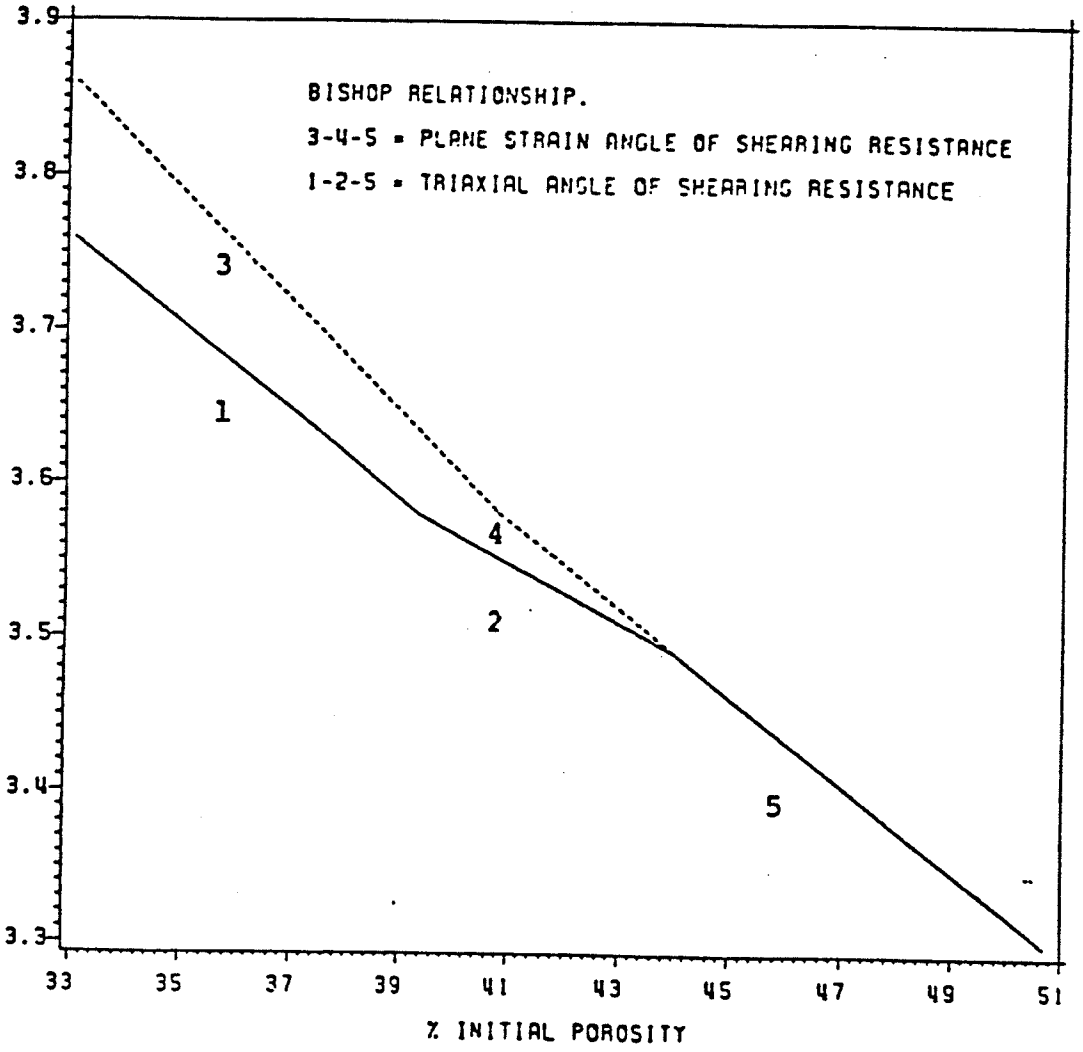

G 2.8 – THE BISHOP (1966) ϕ_{ps}—ϕ_{tx} RELATIONSHIP, LOG-LOG SCALES.

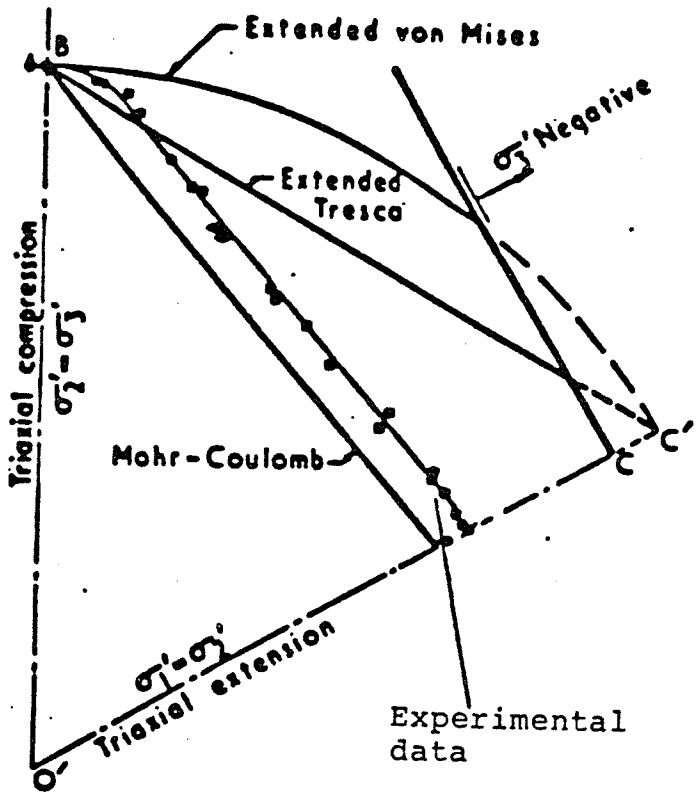

FIG 3.1 – COMPARISON OF VARIOUS YIELD CRITERIA,
After Green and Bishop (1969)

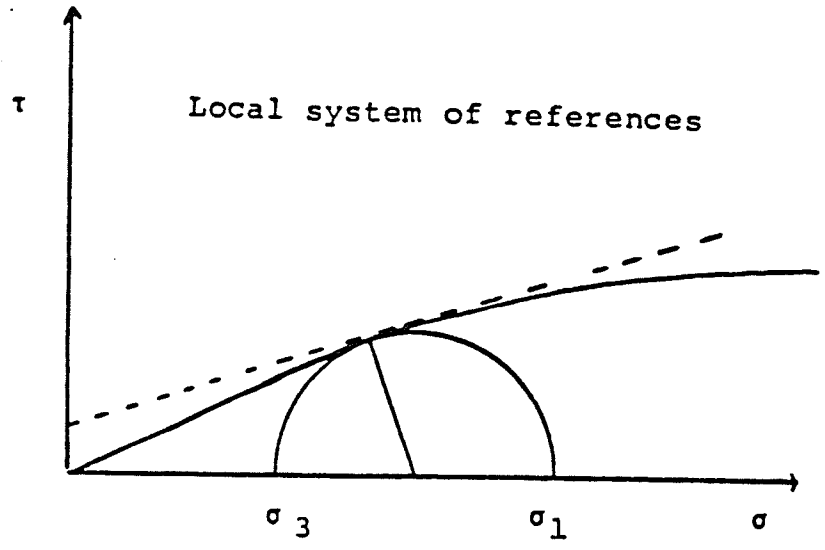

FIG 3.2 – LOCAL REFERENCE SYSTEM OF STRESS AND STRENGTH COORDINATES

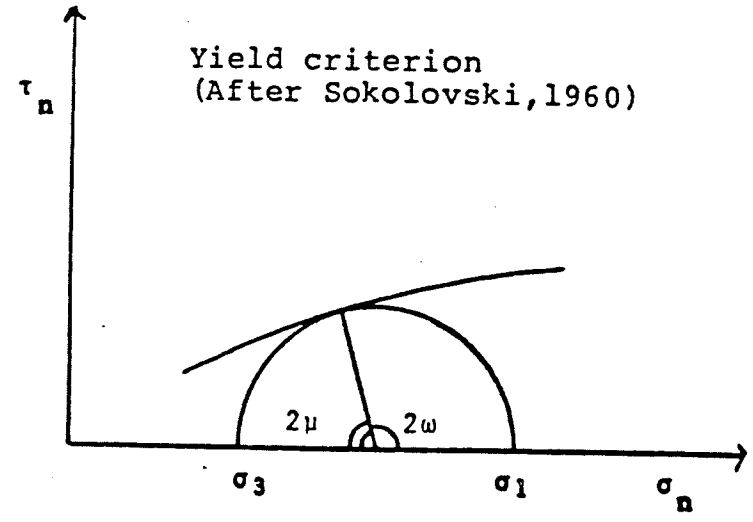

FIG 3.3 – YIELD CRITERION, AFTER SOKOLOVSKI (1960)

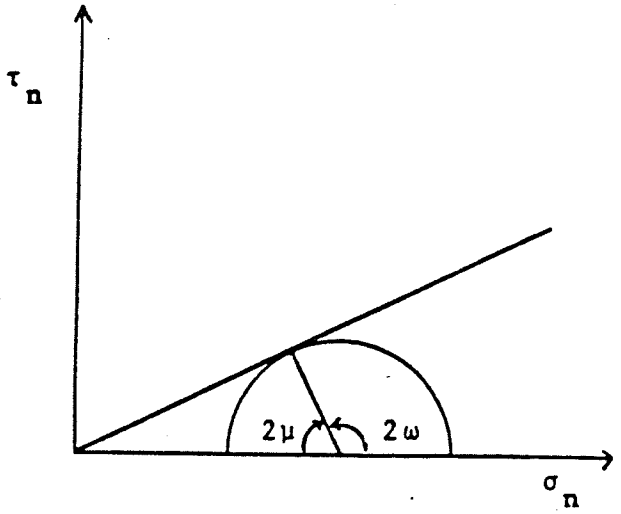

FIG 3.4 — GENERAL RELATIONSHIP BETWEEN μ AND ω

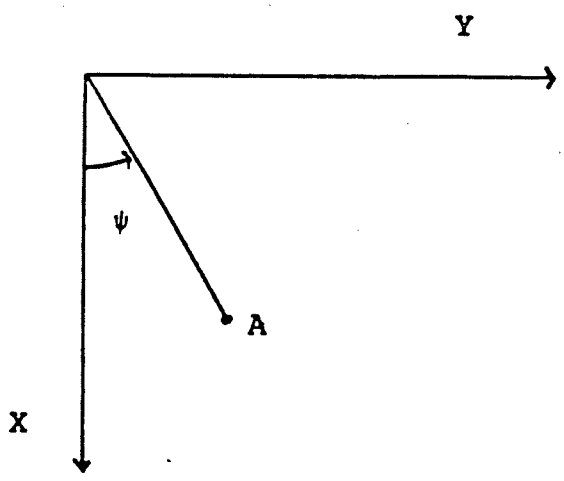

IG 3.5 — GENERAL SYSTEM OF COORDINATES

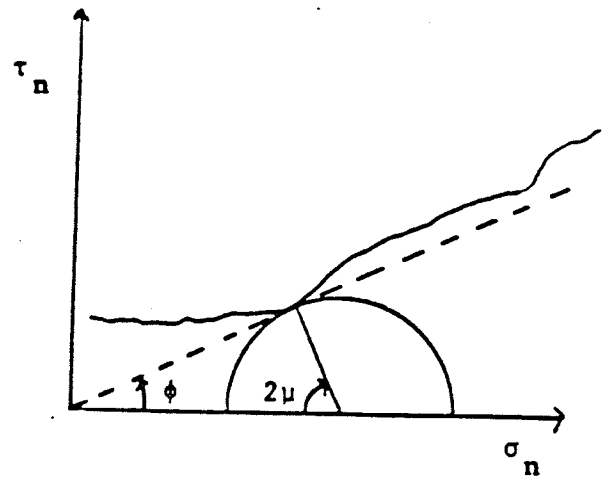

FIG 3.6 - DEFINITION OF ϕ

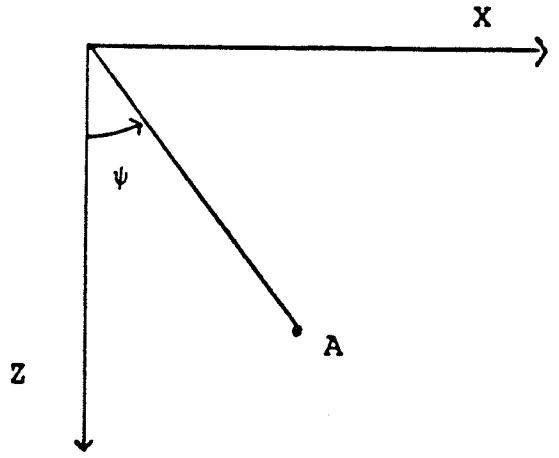

FIG 3.7 - AUTHOR'S SYSTEM OF COORDINATES

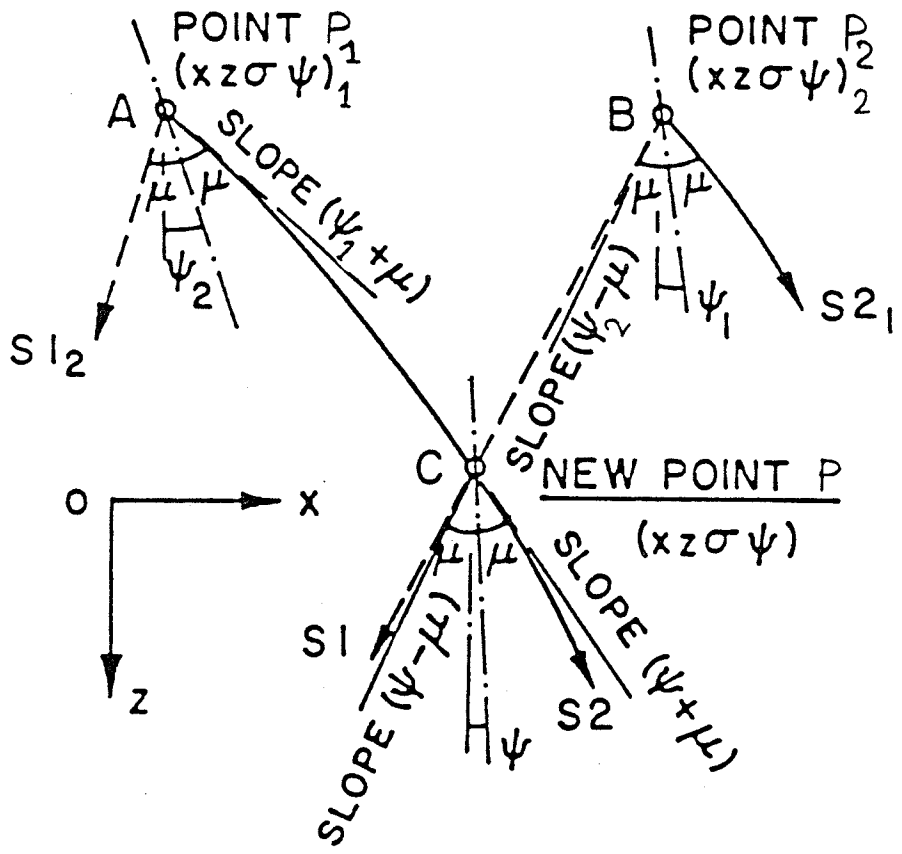

FIG 3.8 - COMPUTATION OF NEW POINT P FROM KNOWN POINTS P_1, P_2, (AFTER GRAHAM, 1968)

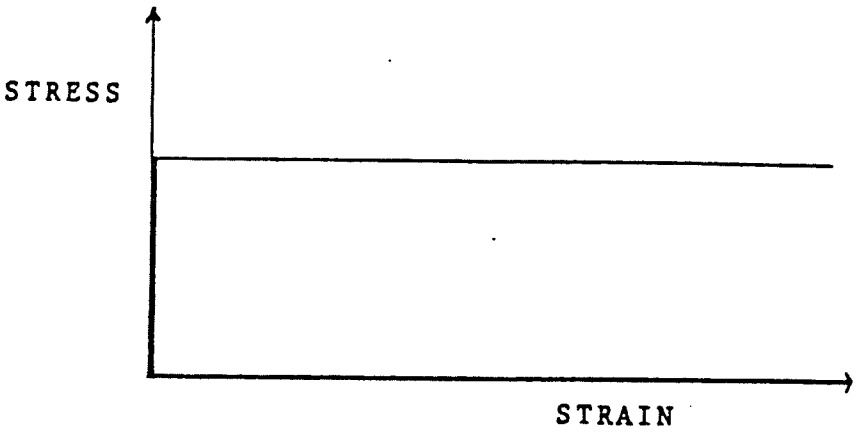

FIG 3.9 – THE RIGID-PLASTIC SOIL MODEL

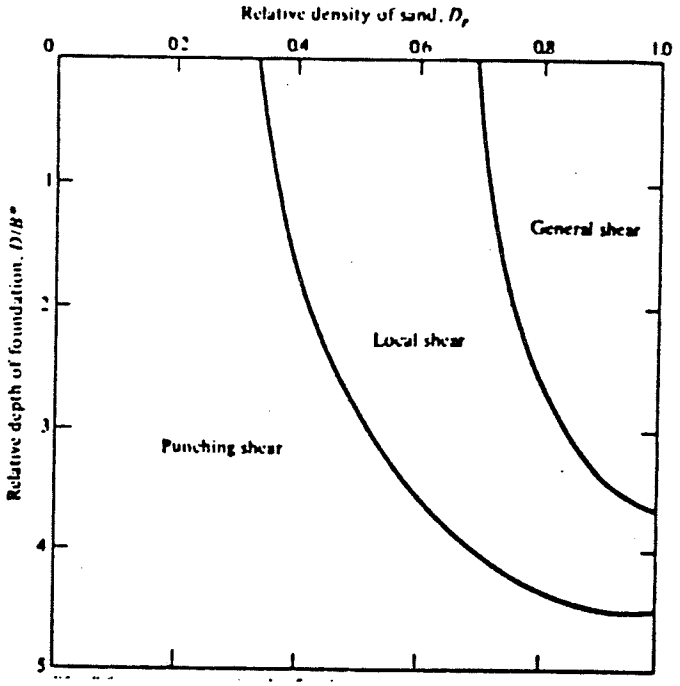

FIG 3.10- MODES OF FAILURE OF MODEL FOOTINGS IN SAND, AFTER VESIC (1963), AS MODIFIED BY DE BEER (1970)

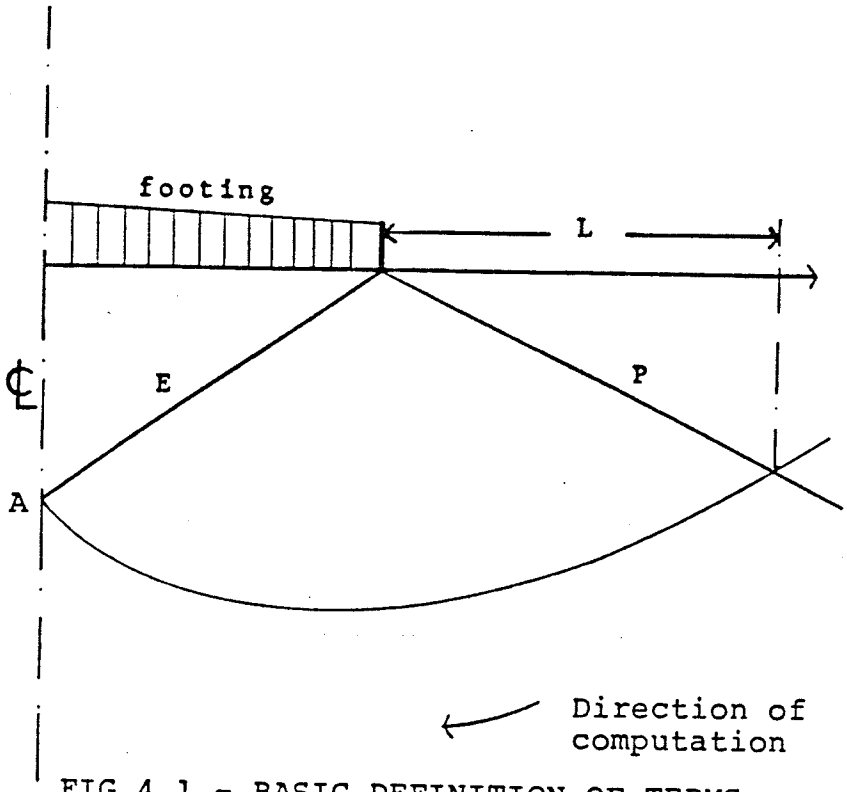

FIG 4.1 - BASIC DEFINITION OF TERMS, THE FOOTING PROBLEM

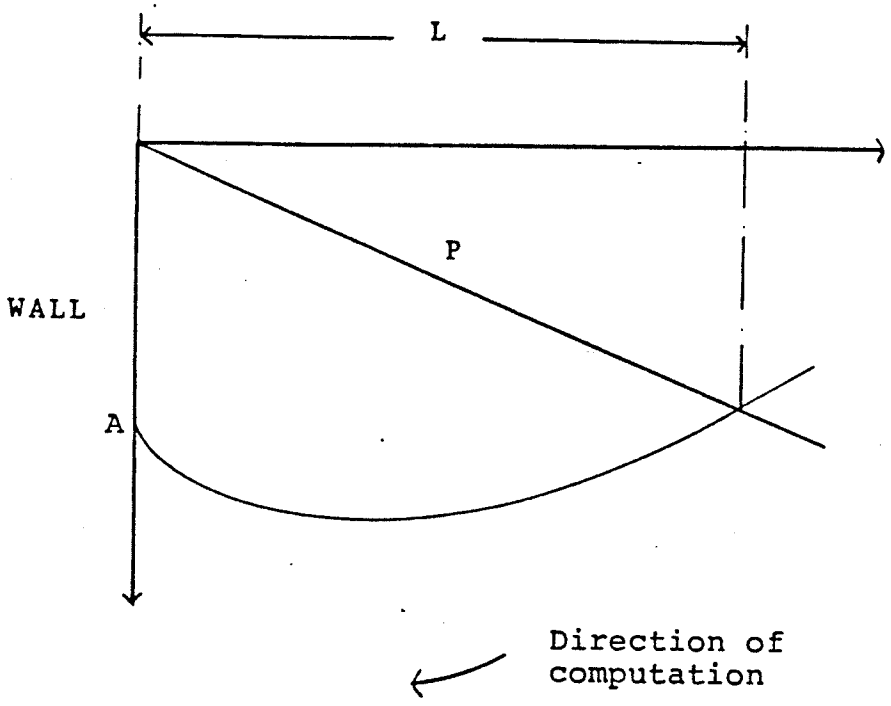

FIG 4.2 - BASIC DEFINITION OF TERMS, THE PASSIVE WALL PROBLEM

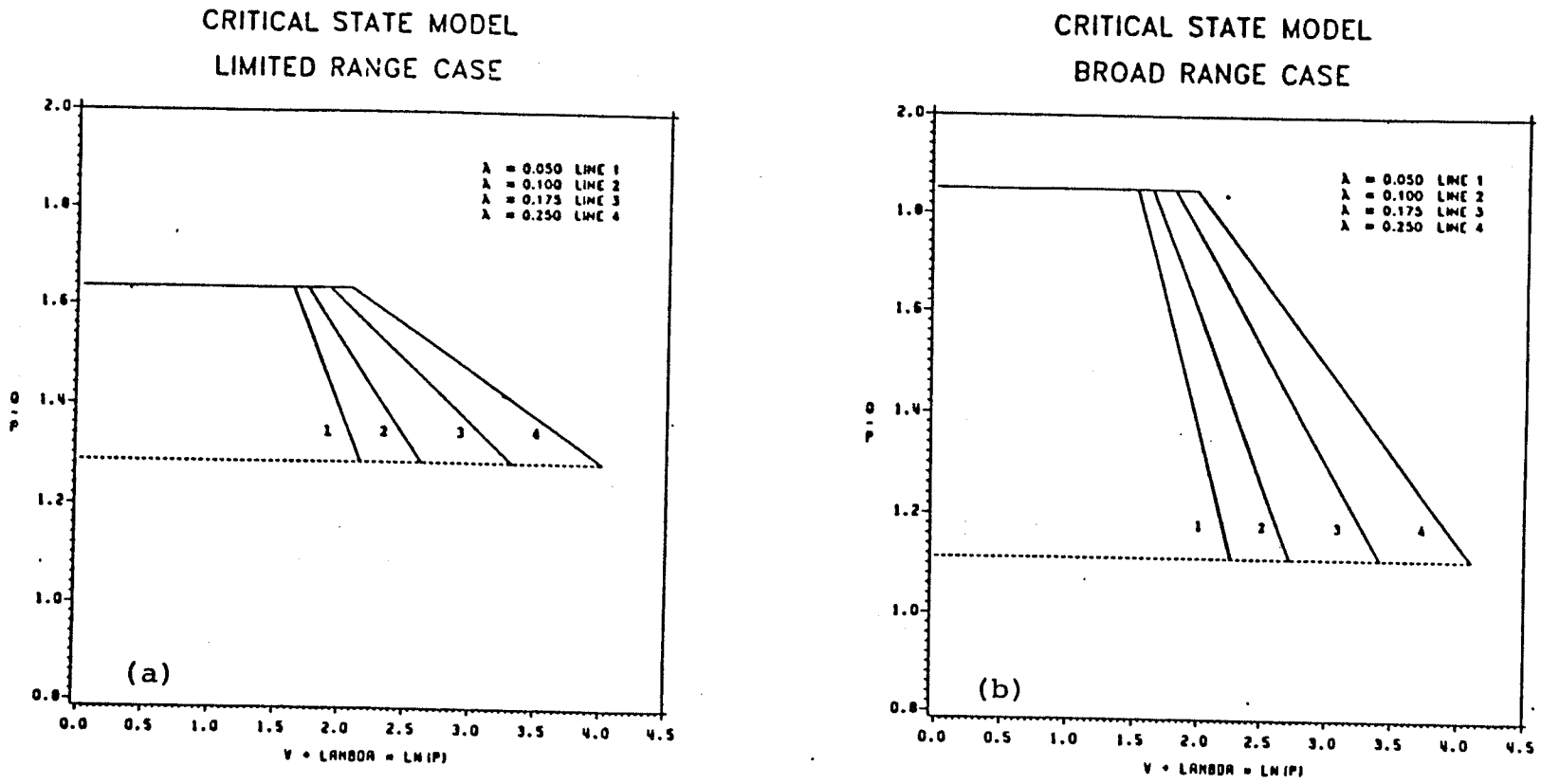

FIG 4.3 - PARAMETRIC DEFINITION OF THE ADOPTED CRITICAL CRITICAL STATE MODEL. (a) LIMITED RANGE CASE, (b) BROAD RANGE CASE.

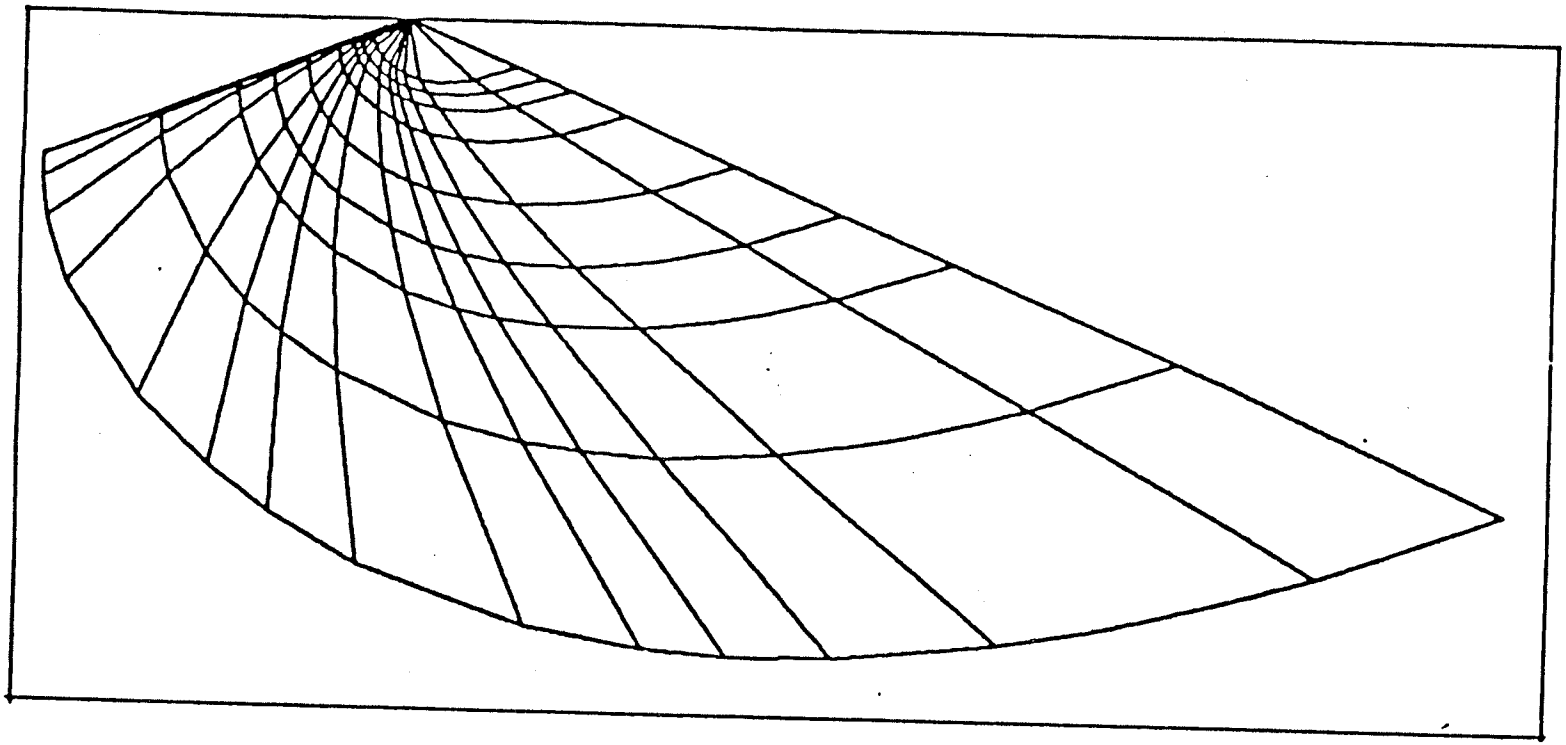

FIG 5.1 - SLIP-LINE FIELD (STRESS-CHARACTERISTICS)
BENEATH SURFACE FOOTING

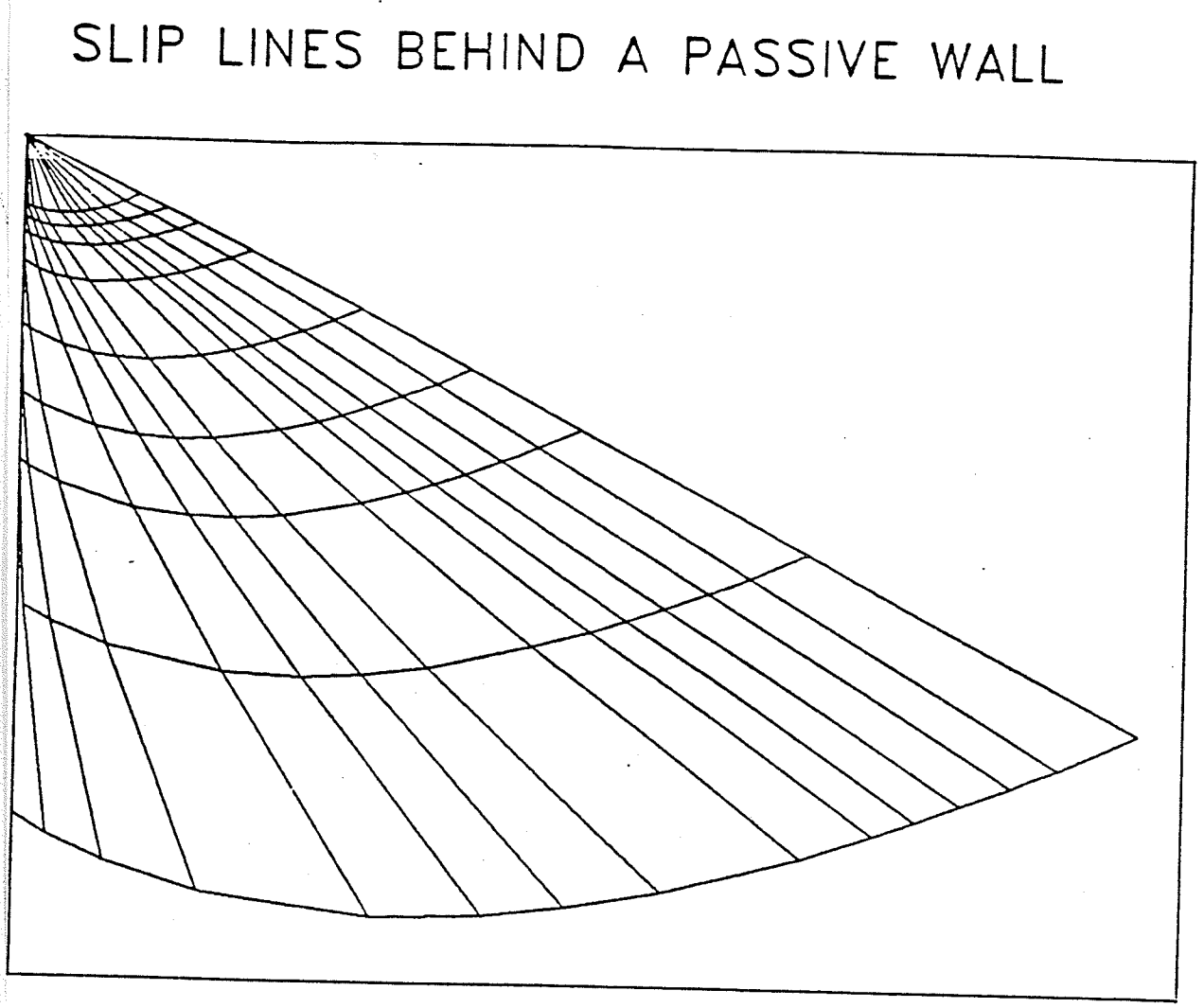

IG 5.2 — SLIP-LINE FIELD (STRESS-CHARACTERISTICS) BEHIND PASSIVE WALL

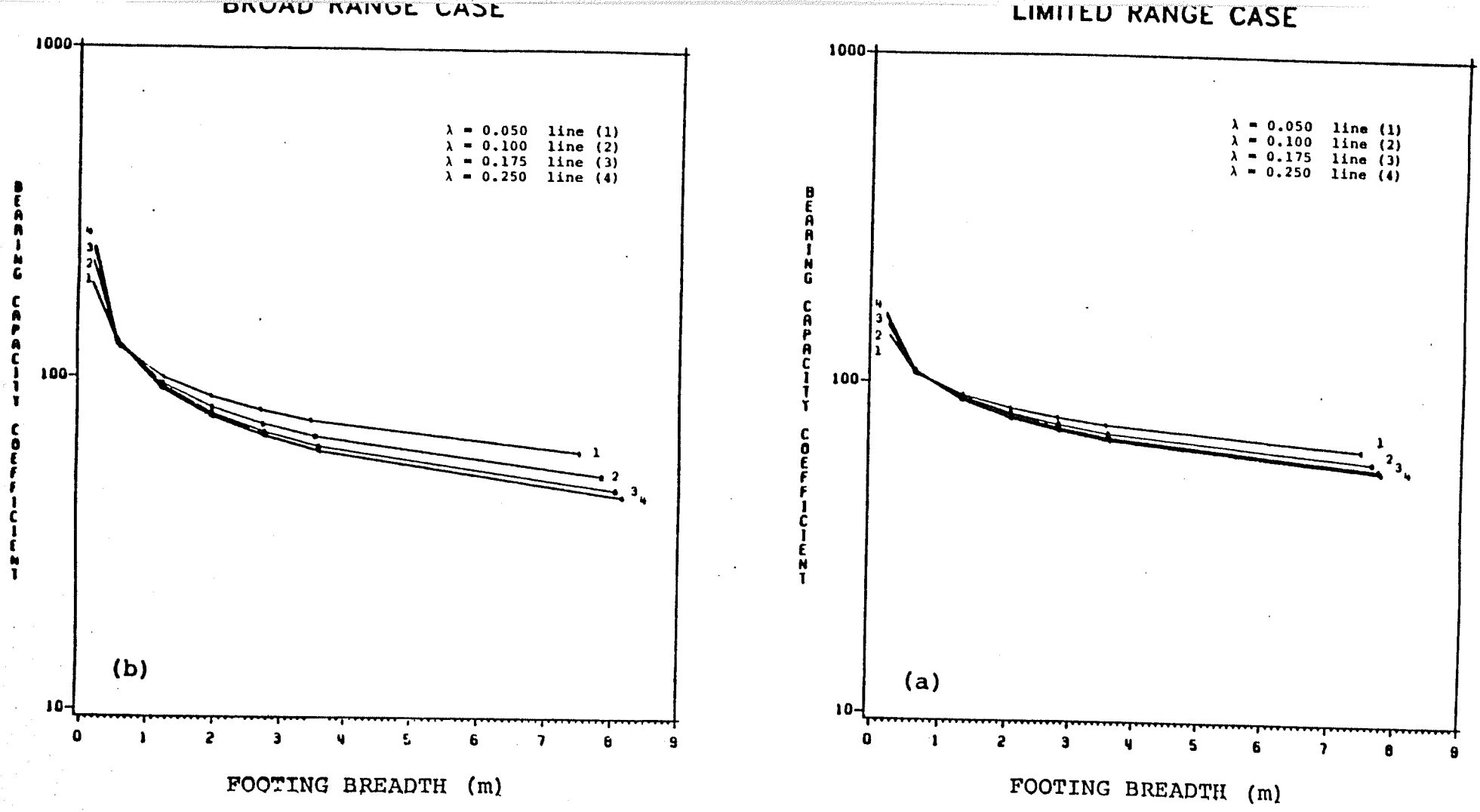

FIG 5.3 — BEARING CAPACITY COEFFICIENTS , (a) LIMITED RANGE, (b) BROAD RANGE (SEMI LOG SCALE)

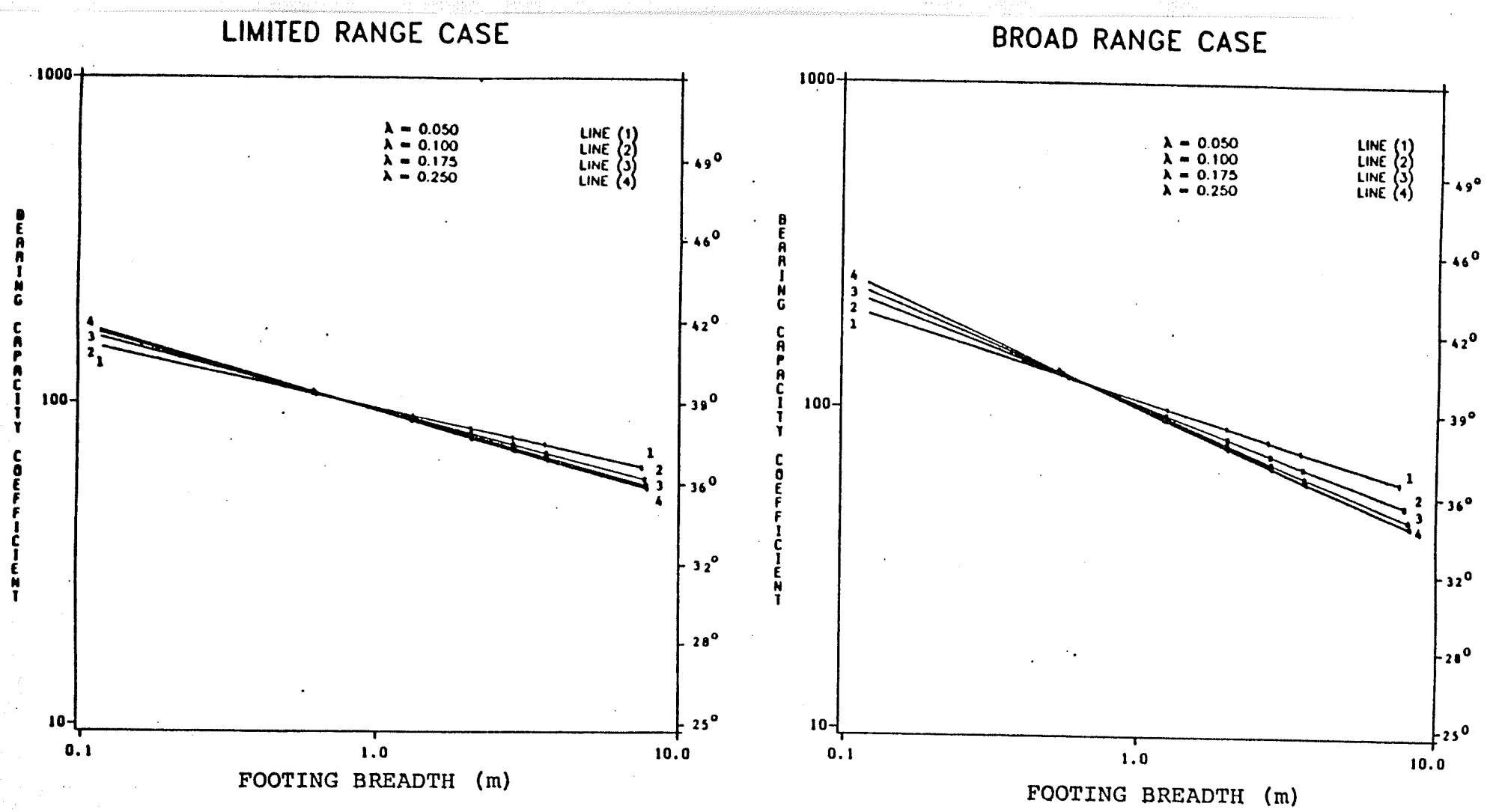

FIG 5.4 — BEARING CAPACITY COEFFICIENTS , (a) LIMITED RANGE, (b) BROAD RANGE (LOG-LOG SCALES)

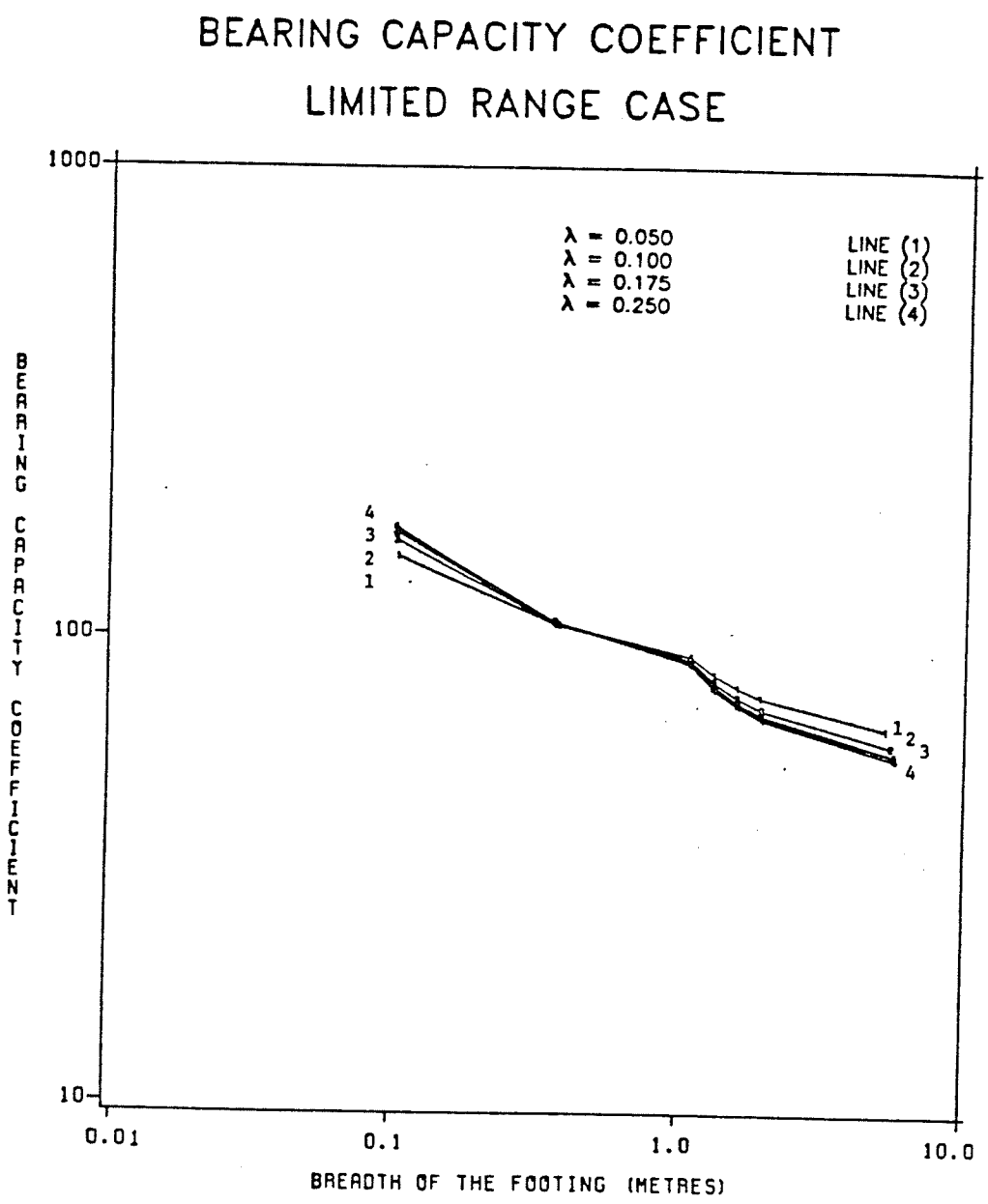

FIG 5.5a - BEARING CAPACITY COEFFICIENTS,
(a) LIMITED RANGE

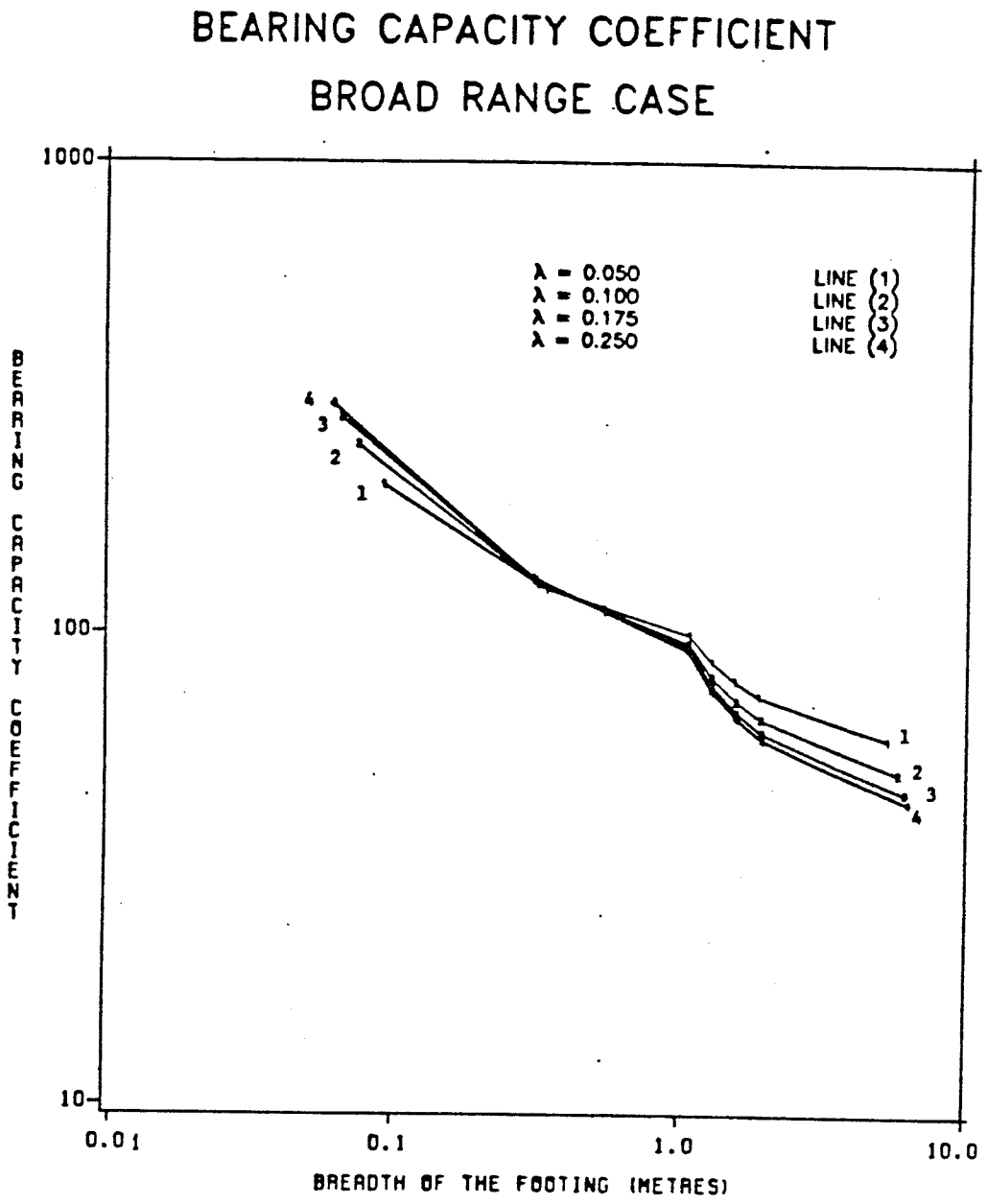

FIG 5.5b - BEARING CAPACITY COEFFICIENTS,
(b) BROAD RANGE

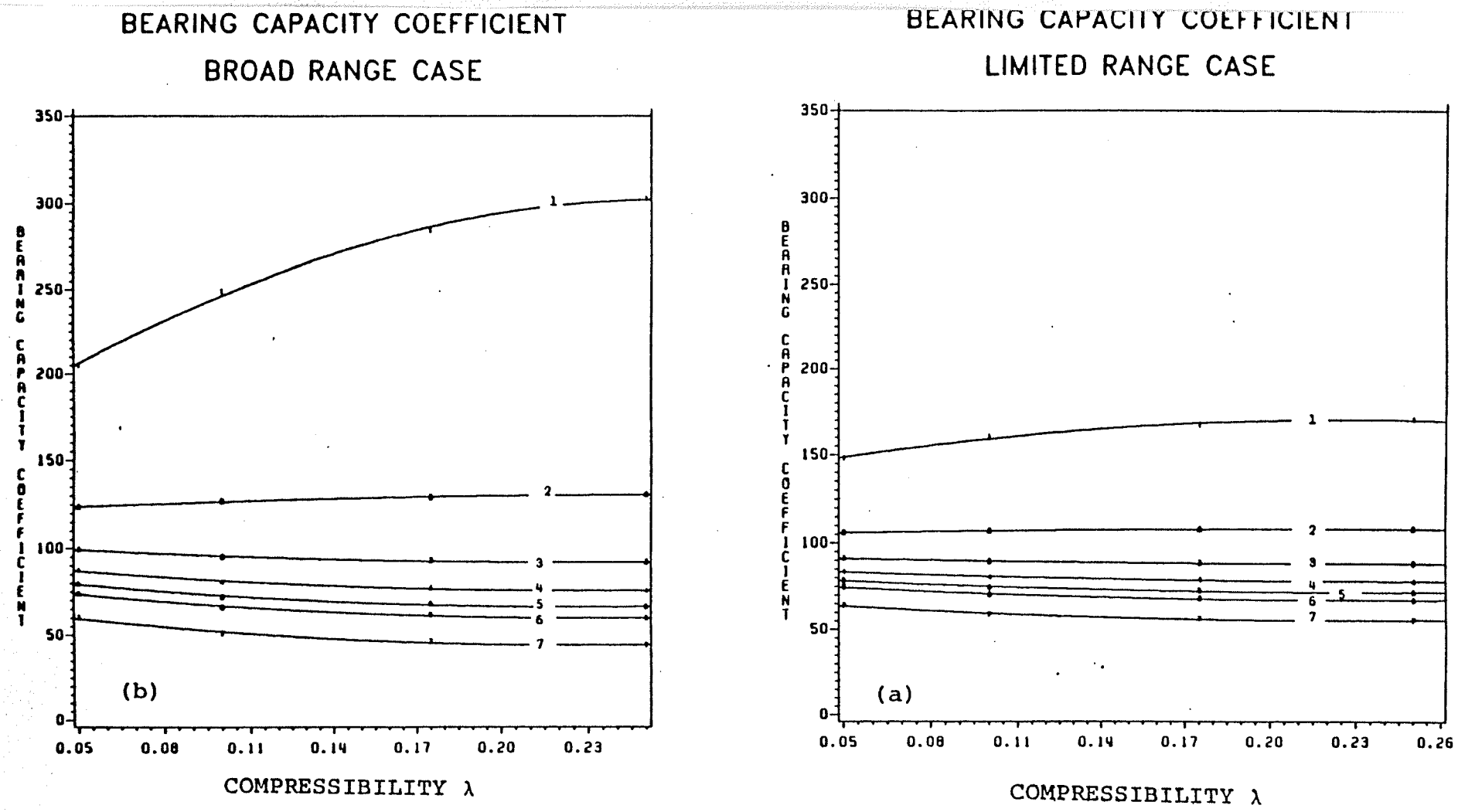

Line number : 1 2 3 4 5 6 7

Footing breadth : 0.10 0.55 1.25 1.95 2.80 3.60 8.10

FIG 5.6 - RELATIONSHIPS BETWEEN BEARING CAPACITY COEFFICIENTS AND COMPRESSIBILITY, (a) LIMITED RANGE, (b) BROAD RANGE.

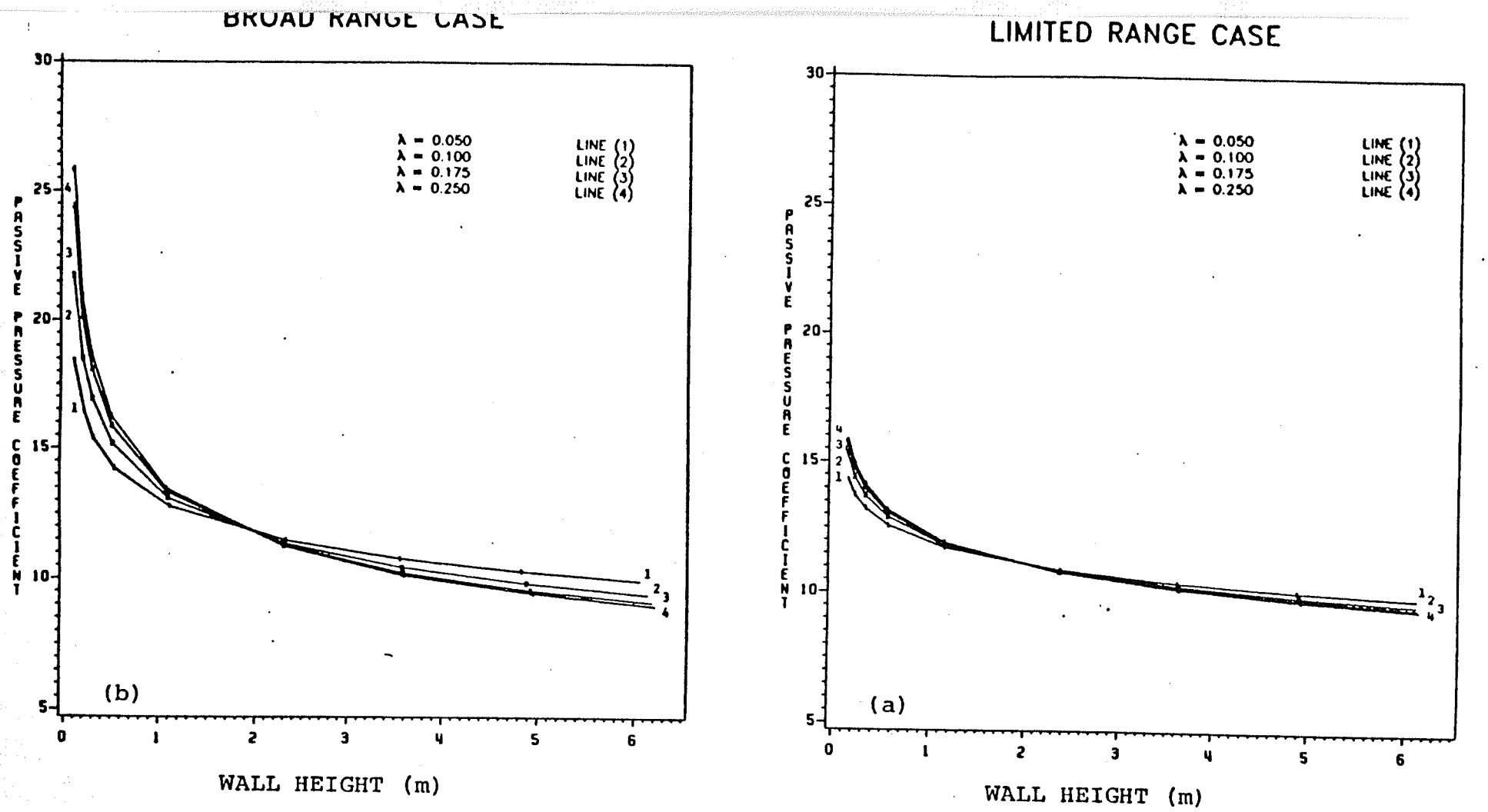

FIG 5.7 – PASSIVE PRESSURE COEFFICIENTS, (a) LIMITED RANGE, (b) BROAD RANGE (SEMI LOG SCALE)

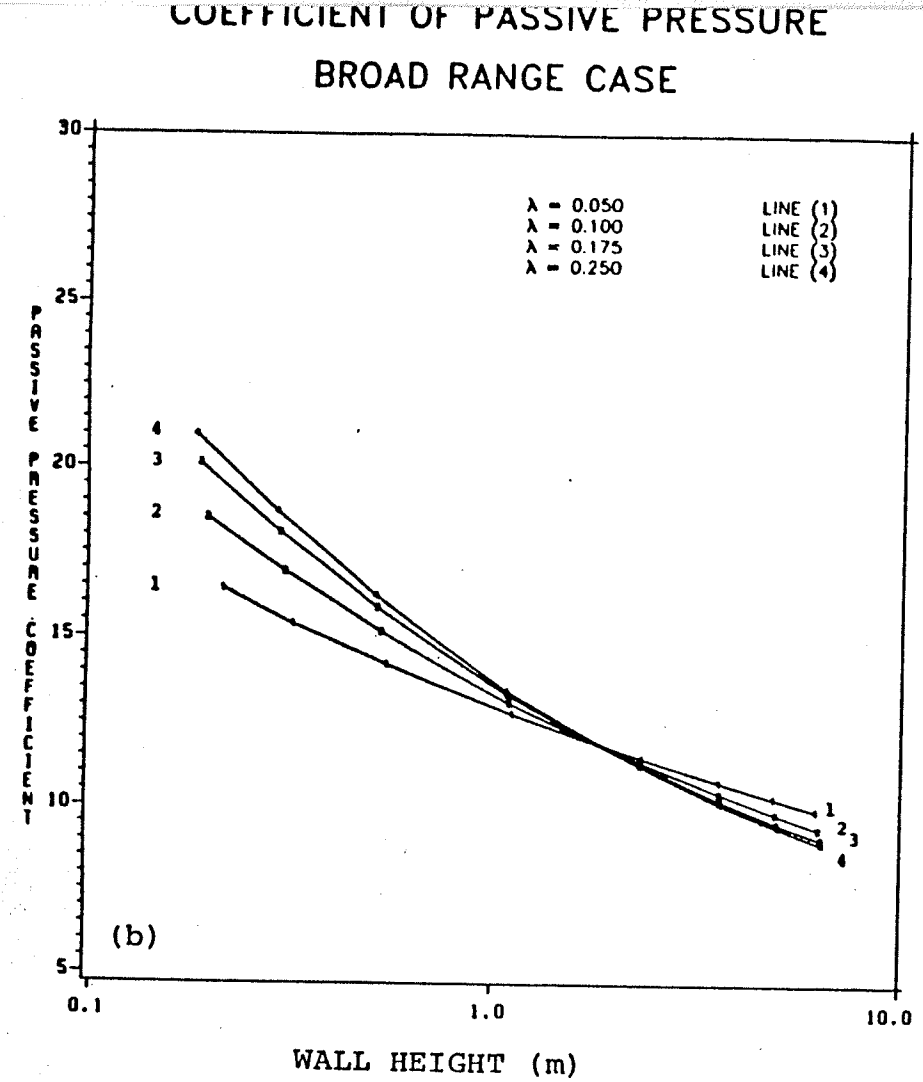

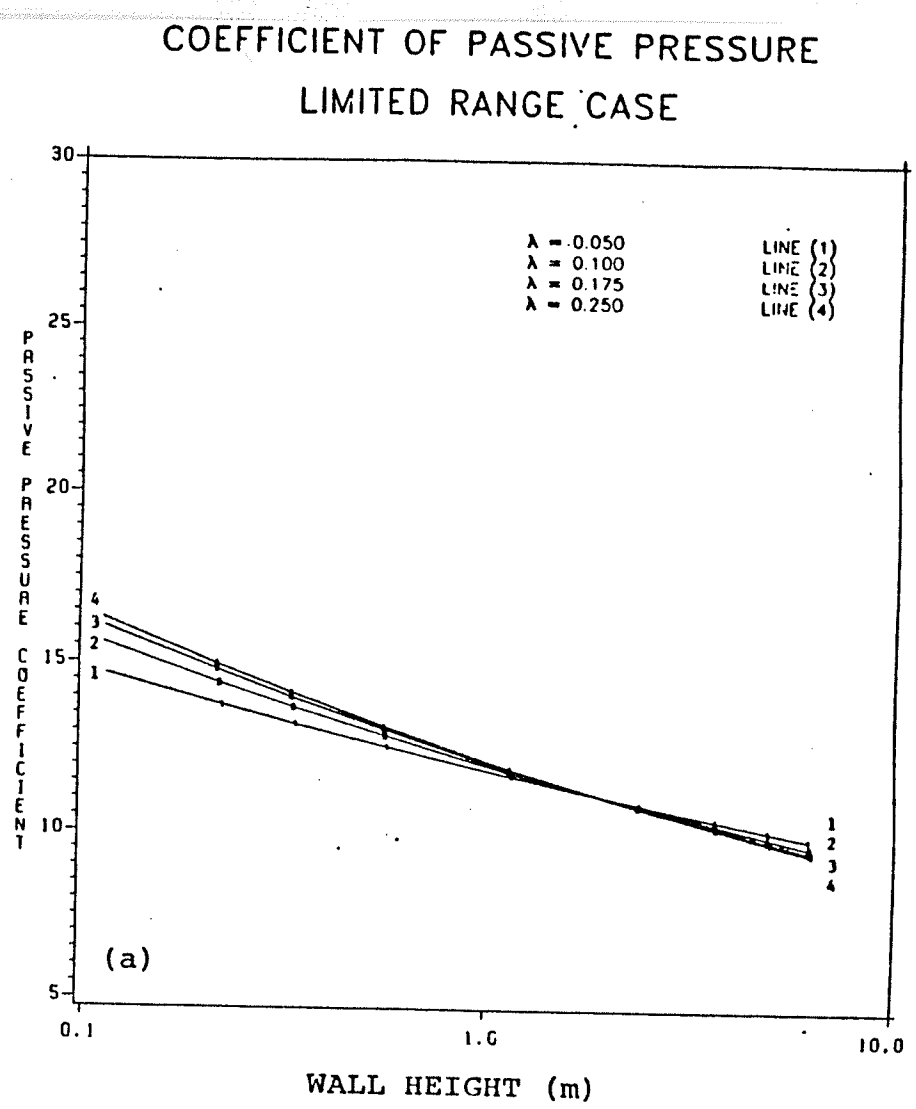

FIG 5.8 – PASSIVE PRESSURE COEFFICIENTS, (a) LIMITED RANGE, (b) BROAD RANGE (LOG-LOG SCALES)

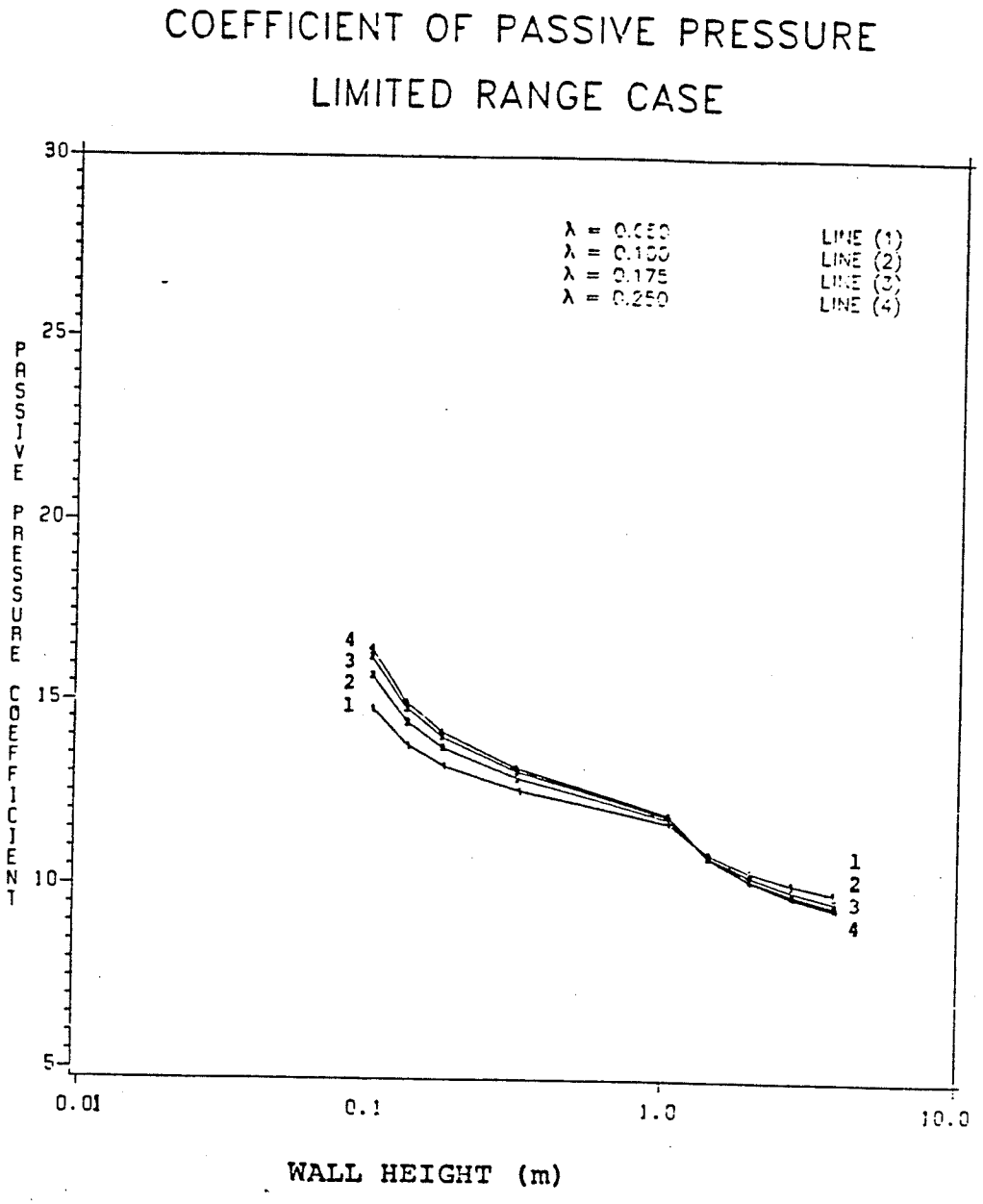

FIG 5.9a - PASSIVE PRESSURE COEFFICIENTS, LIMITED RANGE.

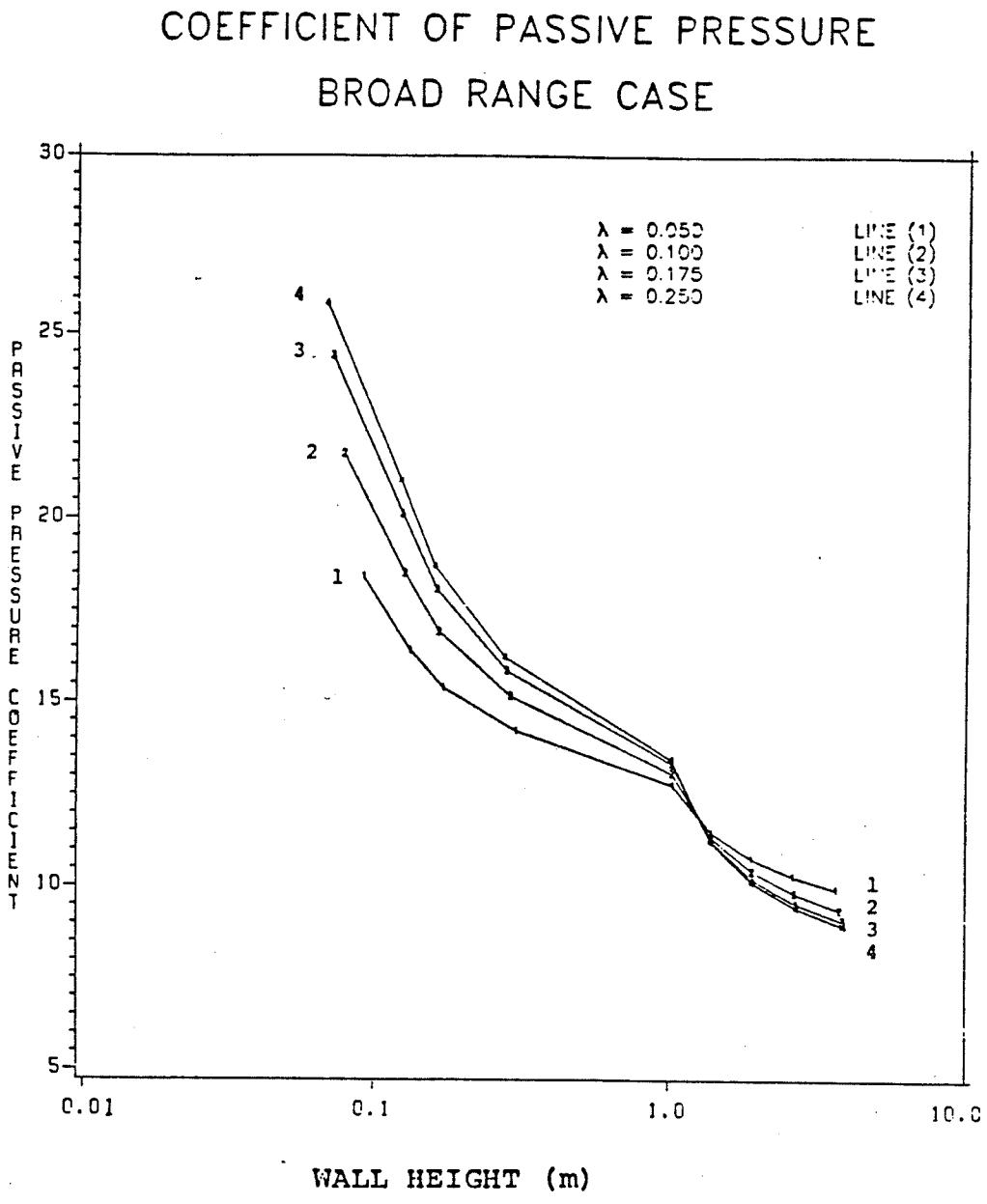

FIG 5.9b - PASSIVE PRESSURE COEFFICIENTS, BROAD RANGE.

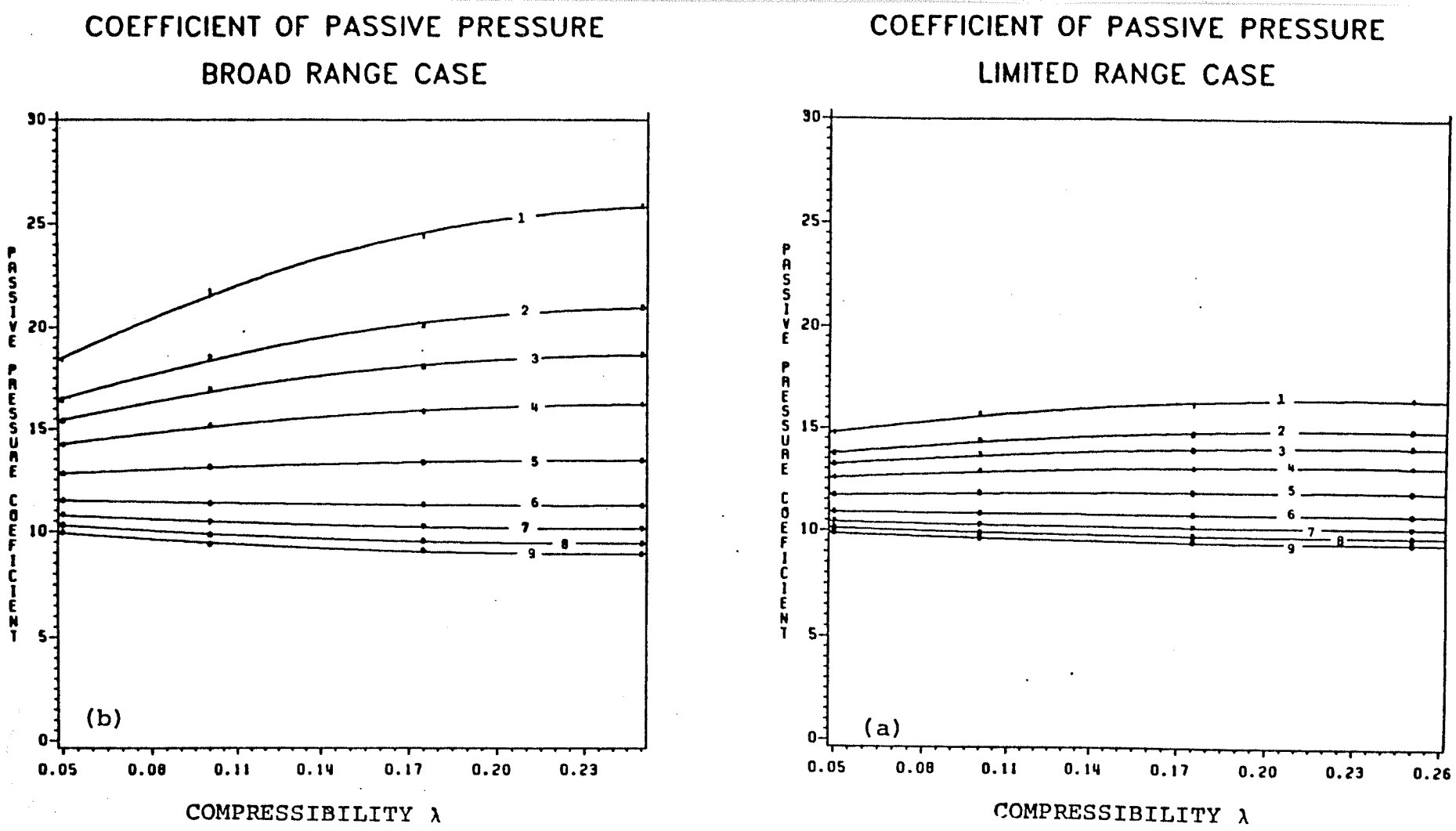

Line number	: 1	2	3	4	5	6	7	8	9
Wall height (m)	: 0.10	0.18	0.28	0.50	1.10	2.30	3.60	4.90	6.40

FIG 5.10 - RELATIONSHIPS BETWEEN PASSIVE PRESSURE COEFFICIENTS AND COMPRESSIBILITY, (a) LIMITED RANGE, (b) BROAD RANGE.

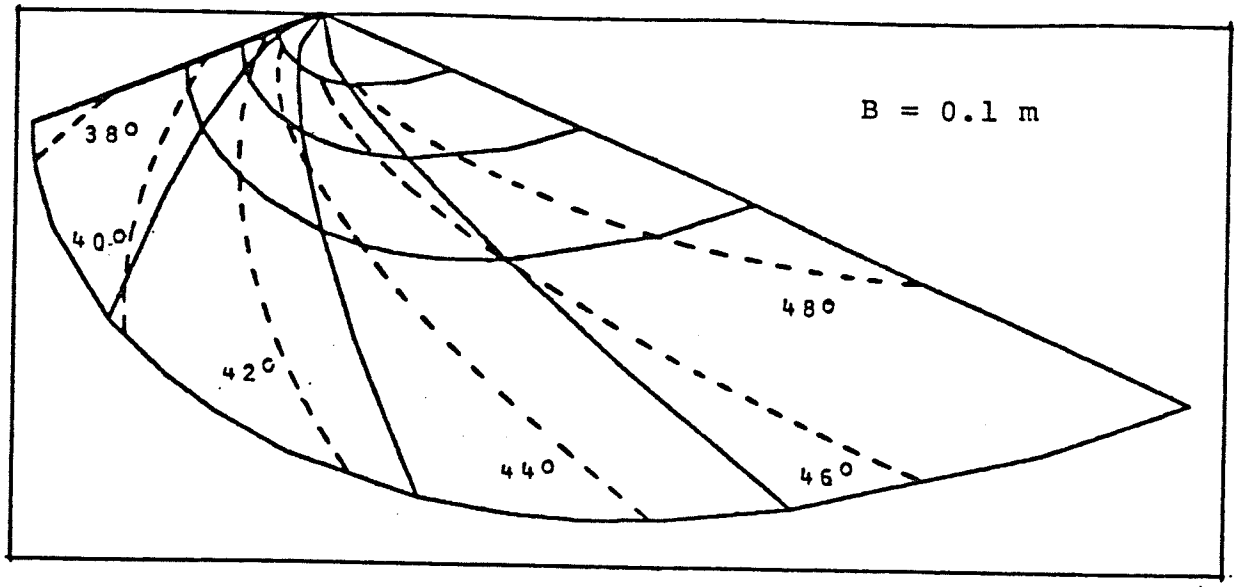

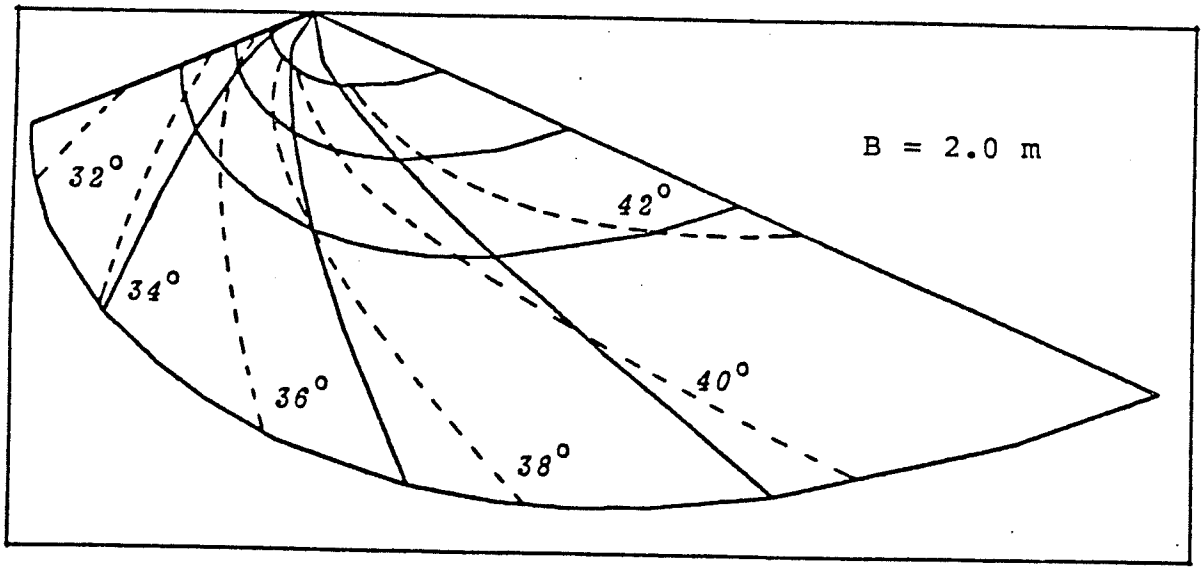

6.1 – CONTOURS OF MOBILIZED ANGLE OF SHEARING RESISTANCE (ISOPHIS) BENEATH SURFACE FOOTING

CONTOURS OF THE ANGLE OF SHEARING RESISTANCE

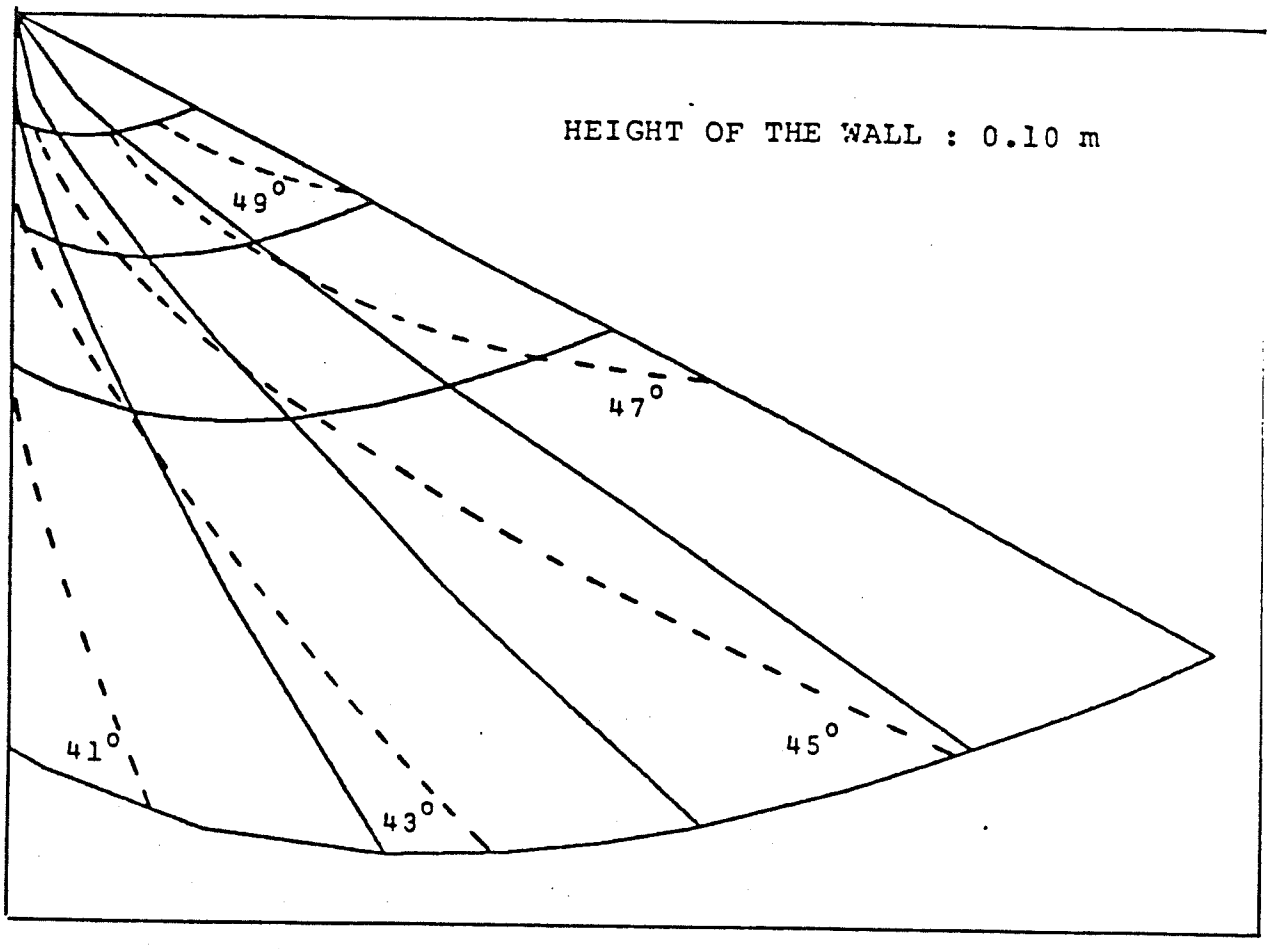

FIG 6.2a : CONTOURS OF MOBILIZED ANGLE OF SHEARING RESISTANCE BEHIND PASSIVE WALL

CONTOURS OF THE ANGLE OF SHEARING RESISTANCE

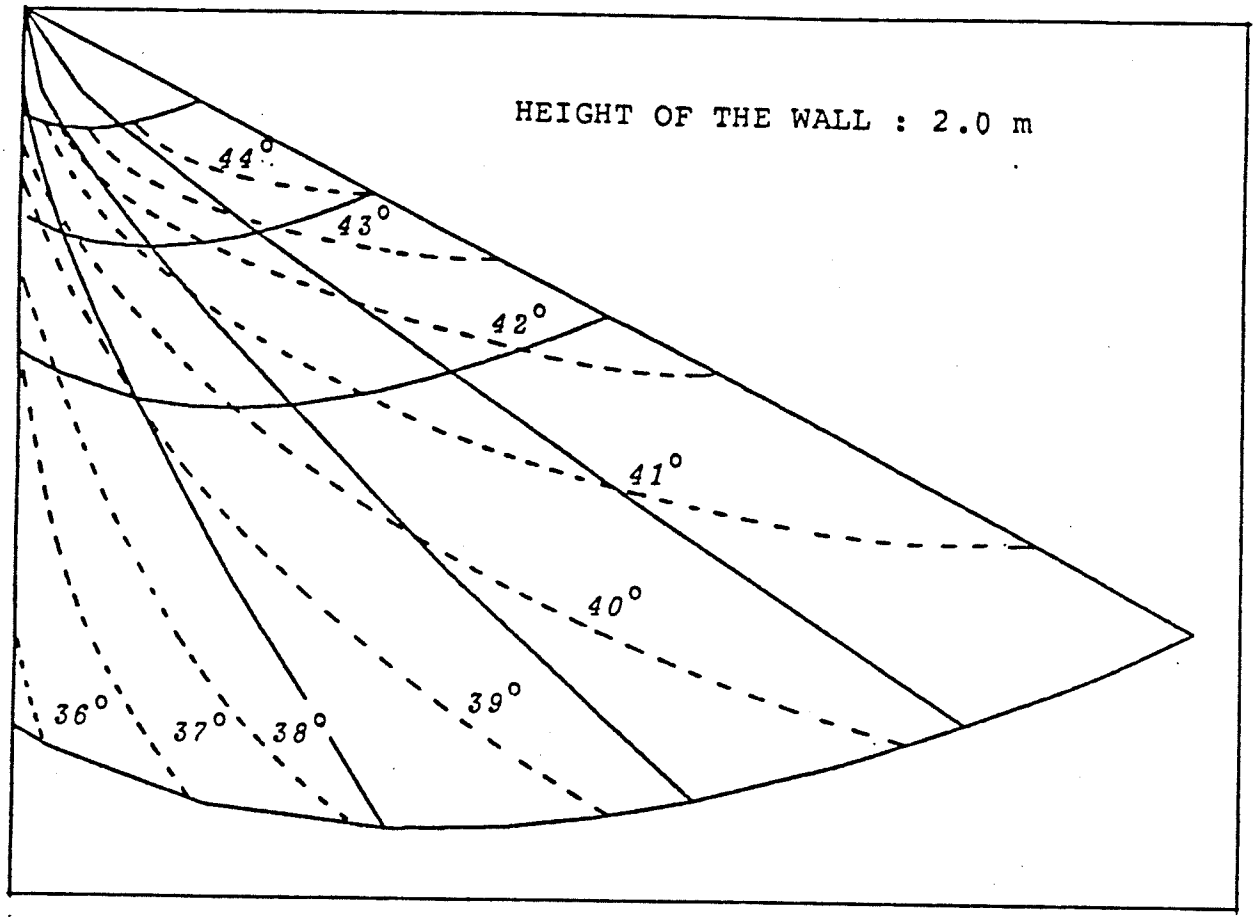

FIG 6.2b : CONTOURS OF MOBILIZED ANGLE OF SHEARING RESISTANCE BEHIND PASSIVE WALL

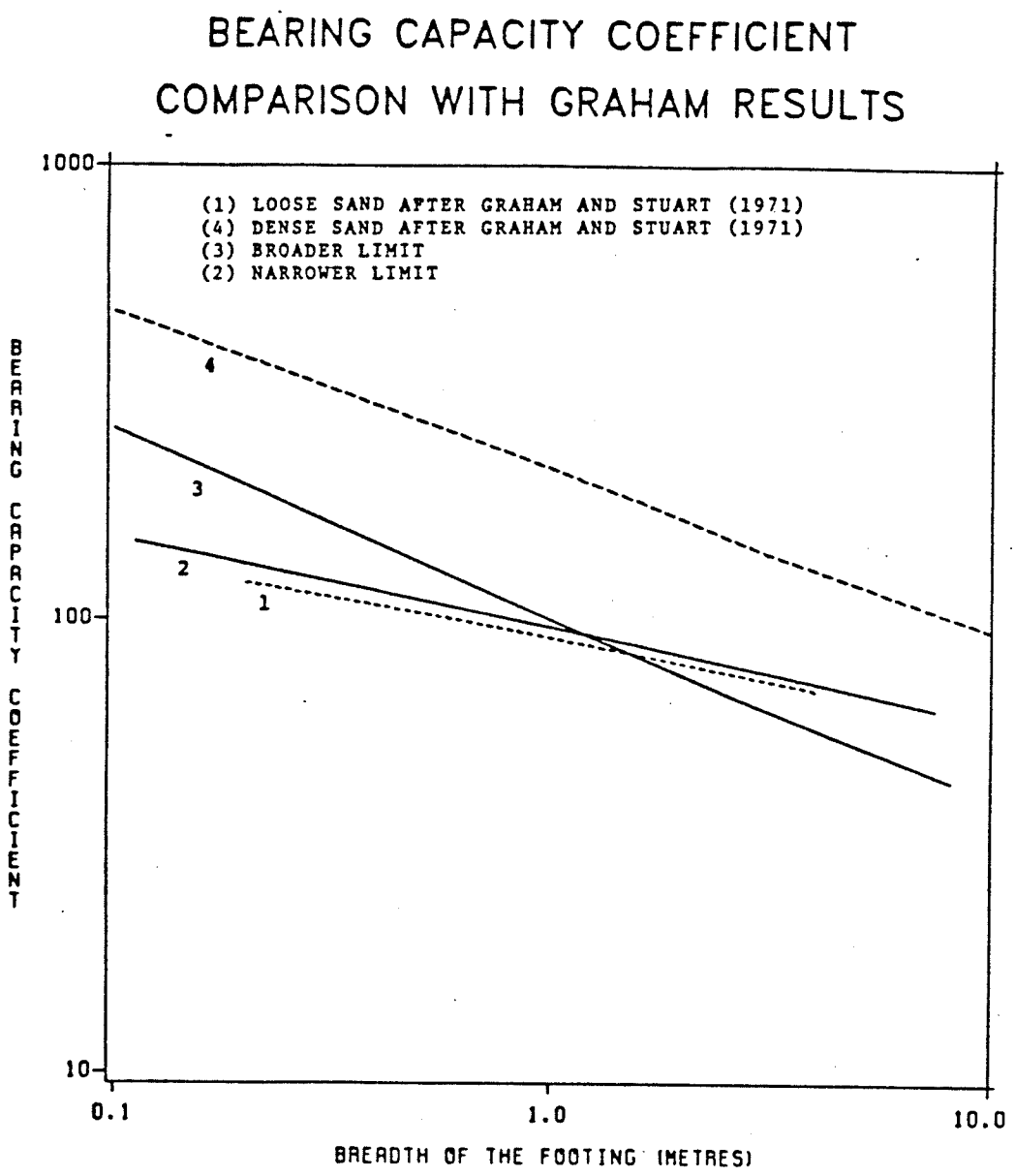

FIG 6.3 - VARIATION OF N_γ WITH FOOTING BREADTH, COMPARISON WITH THEORETICAL RESULTS FROM GRAHAM AND STUART (1971).

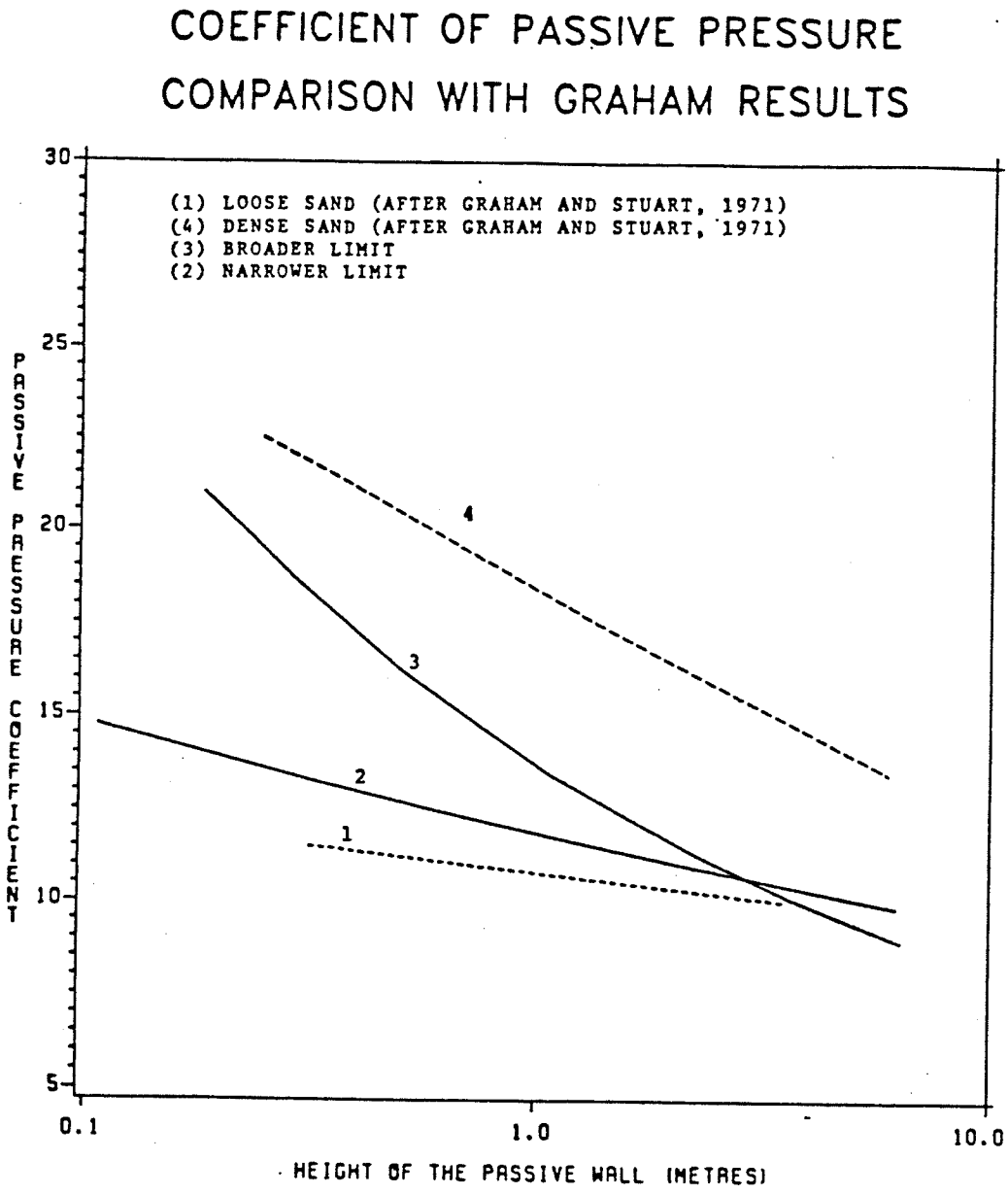

FIG 6.4 - VARIATION OF K_p WITH WALL HEIGHT, COMPARISON WITH THEORETICAL RESULTS FROM GRAHAM AND STUART (1971).

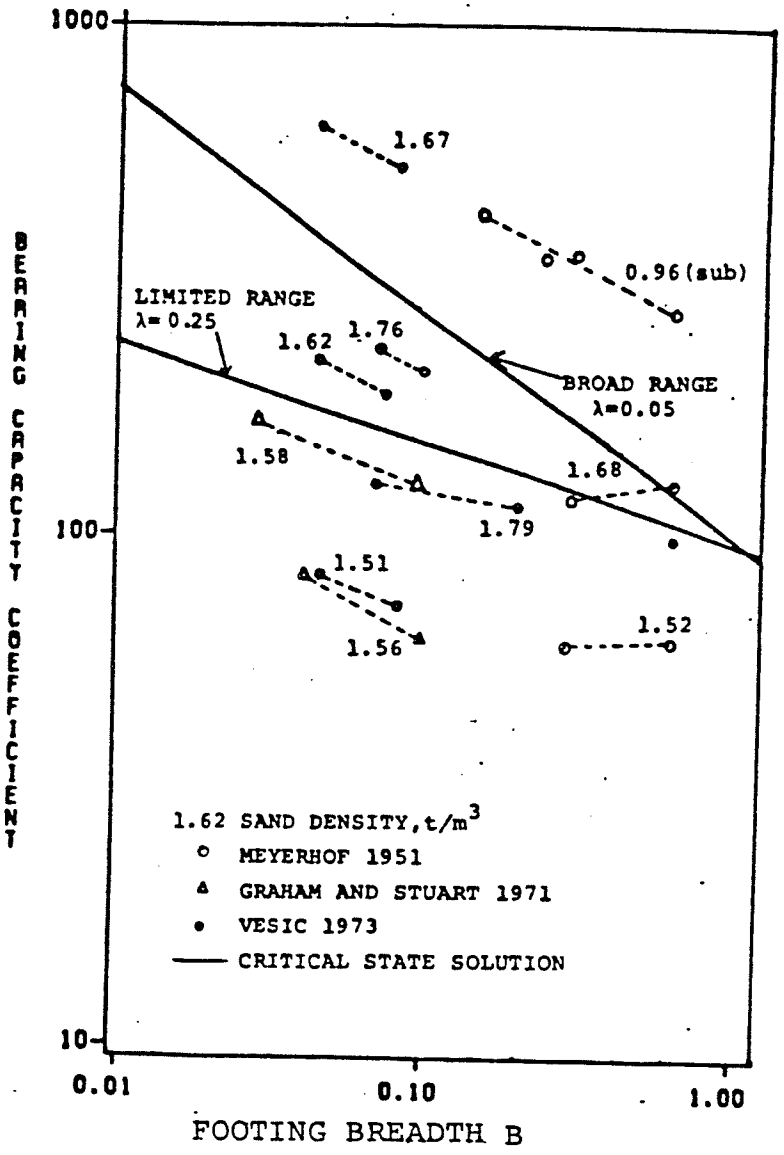

FIG 6.5 : VARIATION OF N WITH FOOTING BREADTH B, COMPARISON WITH EXPERIMENTAL RESULTS.

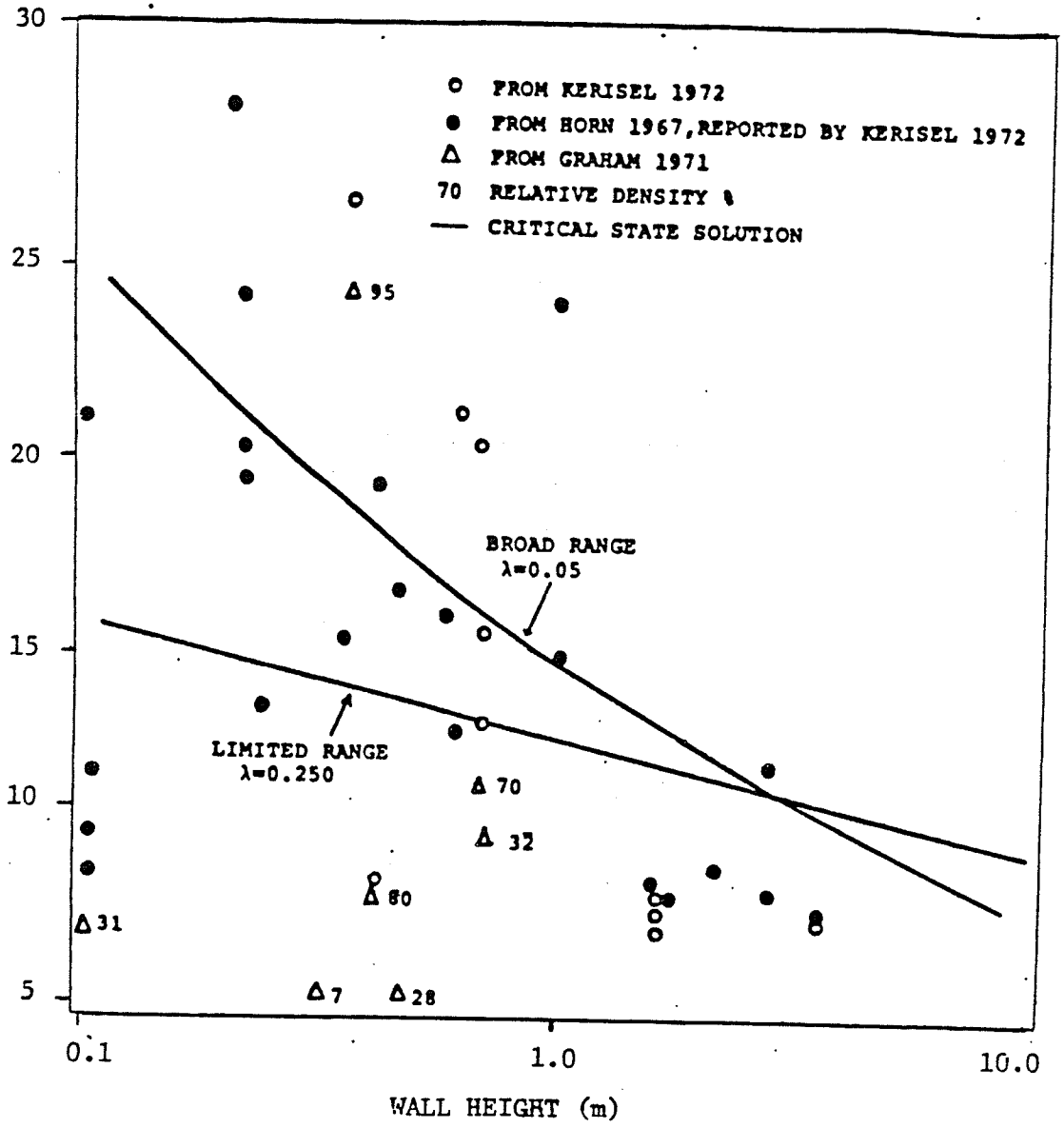

G 6.6 — VARIATION OF K_p WITH WALL HEIGHT H, COMPARISON WITH EXPERIMENTAL RESULTS.

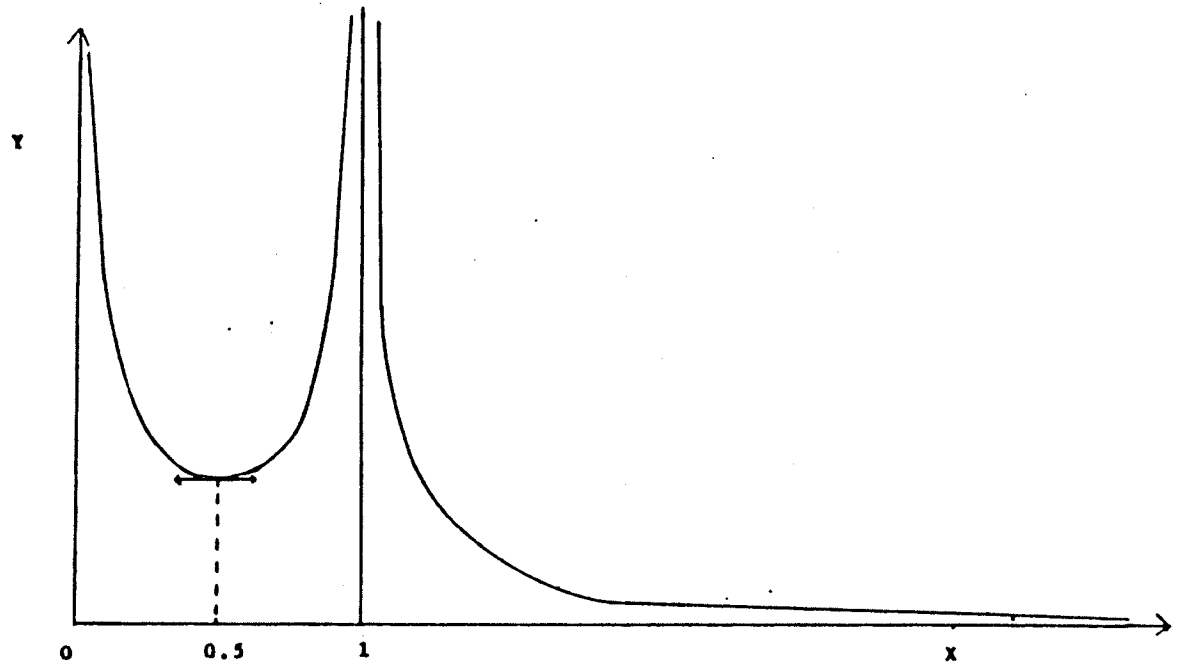

FIG 6.7 – PLOT OF THE FUNCTION Y=1/|X(X-1)|

Appendix A

FACTORS INFLUENCING THE CHOICE OF PARAMETERS FOR COMPUTATION

Bearing in mind that the computer program has been developed for a sand failing in a rigid-plastic mode, it is relatively easy to make use of the program to analyse practical applications. This appendix summarizes the necessary input parameters and proposes guidelines for their estimation.

A.1 NECESSARY INPUT PARAMETERS

The input is fed into the computer in the following order :

1. e_{min}, e_{max} : minimum, maximum void ratio
2. p'_{min}, p'_{max} : minimum, maximum pressure
3. ϕ'_{min}, ϕ'_{max} : minimum, maximum angle of shearing resistance
4. λ : compressibility ($\lambda = Cc/2.3$)
5. l : scale parameter
6. n : number of spiral lines
7. m : number of radial lines
8. x(n) : abscissa of the intersections of the spirals and of the edge of the passive zone

A.2 PRACTICAL ESTIMATION

A.2.1 Void ratio

Table A.1 indicates for various soils the :

1. maximum void ratio
2. minimum void ratio

The initial condition of a sand can be described by its relative density $I_D = (e_{max} - e)/(e_{max} - e_{min})$. The medium dense range of behaviour can be taken to be cases where the I_D is greater than 35 and less than than 85 (Lambe and Whitman,1969).

A.2.2 Pressures

Minimum as well as maximum pressures can be estimated as the unloaded state of the sand and from the anticipated maximum stress intensity under the footing or behind a passive wall. Typical values are respectively 10 kPa and 10^4 kPa.

A.2.3 Angle of shearing resistance

Usually, the engineer who calculates the size of a footing or that of a wall has also the task of estimating the angle of shearing resistance of the soil. The choice lies in the results of laboratory tests combined with experience. Minimum and maximum angles of shearing resistance can be taken as the extreme values that the engineer considers can be mobilized in the sand by the pressure levels in the problem. The values are affected by the density, mineralogy, and by the particle size distribution, particle shape of the sand.

A.2.4 Compressibility λ

Since $\lambda = Cc/2.304$, the determination of λ is related to that of of the compression index. Compression tests into the normally consolidated (linear V,logp') range can supply such information. Such tests are rare. In the absence of reliable data, a typical value of λ is 0.1 (Atkinson and Bransby,1978).

A.2.5 Scale parameter

Note that this is not equal to the height of the wall or the footing breadth and the structure size results from this choice. Any figure can be taken as scale parameter. Confusion might appear for the user who is not familiar with the computer program. The choice of the horizontal length of the edge of the passive zone is recommended. This figure corresponds to the abcissa of the intersection on the extreme spiral and of the edge of the passive zone (Figs 4.1 and 4.2).

A.2.6 Radial and spiral lines

Augmenting the number of spiral and radials lines leads to greater accuracy. Nonetheless, the user should keep it mind that it will also increase the computing time. Ten spirals and twenty radials in the present work have been used.

A.2.7 Edge of the passive zone

If ten spirals are chosen, the horizontal length of the edge of the passive zone is divided in ten equal segments. A spiral line will depart from each of these ten points. The abscissa x(n) are the required input parameters. The dimensionless figures $n\pi/10$ are convenient (n = 1,10).

Appendix B

LISTING OF THE COMPUTER PROGRAM

PHI - ϕ

FIRPHI - First ϕ

PHILO - Local ϕ

XX,ZZ - Physical coordinates

SIMA, SIGMA1, SIGMA2 - σ

PSSI, PSI1,PSI2 - ψ

P - Pressure

E - voids ratio

L - Number of spirals

K - Number of radials

C - Control

LANDA - λ

GS - Specific gravity

GW - Water density

PP, QQ - Iteration counts

SUBSCRIPTS :

MIN - Minimun

MAX - Maximum

COMPUTER PROGRAM

```
      REAL FIRPHI
      COMMON FIRPHI, BETA, DELTA, TOL, CONVG,SIZE,GAMMA
      INTEGER L,K,C
      COMMON L,K,C
      REAL XX, ZZ, SIMA, PSSI, PHHI
      COMMON /TATA/ X1,X2,XX,Z1,Z2,ZZ,PHHI
      COMMON /TITI/ SIGMA1,SIGMA2,SIMA
      COMMON /TETE/ PSI1,PSI2,PSSI
      COMMON /TOTO/ PI ,SNPHI,CSPHI
      INTEGER PP,QQ ,CONTRO
      COMMON /OUI/ PP,QQ,CONTRO
      REAL MU
      COMMON /AH/ MU,PHILO,SIGLOC,PHI1,PHI2,PHILOP,PHILOT
      REAL
X(40,40),Z(40,40),SIGMA(40,40),PSI(40,40),PHI(40,40)
      COMMON /LALA/ X,Z,SIGMA,PSI
      COMMON /ALO/ PHI
      INTEGER P(40),Q(40)
      COMMON /LOLO/ P,Q
      REAL EO,LANDA
      COMMON                                          /CRIT/
EO,LANDA,PMIN,PMAX,PHIMIN,PHIMAX,PHII,EMIN,EMAX
      INTEGER SPI,RAD,W,H,H1,KS,L1,LK,I,J,RAD1
      REAL DIF,DI,TNPHI
      REAL KP,NY,FIRSIG,GS,GW
C
C
C
      PI= ARCOS(-1.)
      READ,FIRPHI,DELTA,BETA,TOL,CONVG,SIZE,GS,GW
      READ,CONTRO
      IF(CONTRO .EQ. 1) THEN DO
      PRINT 43
   43
FORMAT('1',/////////20X,'**********************************',
     1                                              /20X,'*
*',
     2                        /20X,'*        CONTROL=      1
*',
     3                                              /20X,'*
*',
     4                   /20X,'*   PARTIAL  RESULTS PRINTOUT
*',
     5                                              /20X,'*
*',
```



```
     6
/20X,'**********************************')
      ELSE
      GO TO 44
      ENDIF
   44 CONTINUE
      READ,L,K
      READ,EMIN,EMAX,LANDA,PMIN,PMAX,PHIMIN,PHIMAX
      EO=(EMIN+EMAX)/2.
      GAMMA=(GW * GS)/(1. + EO)
      PHIMIN=PHIMIN * PI /180.
      PHIMAX=PHIMAX * PI /180.
      IF (ABS(BETA) .LE. 0.0001) BETA =0.0001
C     INITIALISATION
      CALL HEADIN
      PRINT 825
  825 FORMAT('1',///////////////20X)
      PRINT,'
**************************************************'
      PRINT,'                                                *
*'
      PRINT,'          *   THE PROGRAM  COMPUTES  THE  FAILURE
LINES OF      *'
      PRINT,'                                                *
*'
      PRINT,'          *   A SAND  HAVING A  PLASTI CBEHAVIOUR.
THIS IS       *'
      PRINT,'                                                *
*'
      PRINT,'          *  THE CASE OF A WALL (ROUGH OR SMOOTH),
OR            *'
      PRINT,'                                                *
*'
      PRINT,'          *  A FOOTING. THE COMPUTATION PRESENTS A
FEATURE   *'
      PRINT,'                                                *
*'
      PRINT,'          *   WHICH  CONSISTS   OF  TRAPPING  THE
FAILURE LINES    *'
      PRINT,'                                                *
*'
      PRINT,'          *  AROUND A POLE BY IMPLEMENTING VARIOUS
SCALE     *'
      PRINT,'                                                *
*'
      PRINT,'          *   REDUCTIONS   WITH  A   DIMINISHING
SURCHARGE EFFECT.*'
      PRINT,'                                                *
*'
      PRINT,'
**************************************************'
      L1=40
      LK=40
      DO 1 I=1,L1
```

```
      DO 2 J=1,LK
         X(I,J)=0.
         Z(I,J)=0.
         SIGMA(I,J)=0.
         PSI(I,J)=0.
         PHI(I,J)=0.
    2 CONTINUE
    1 CONTINUE C C
      DO 3 I=1,L1
         P(I)=0
         Q(I)=0
    3 CONTINUE
      BETA= BETA * PI/180.
      DELTA= DELTA * PI/180.
      FIRPHI=FIRPHI/57.2957795
      CSPHI= COS(FIRPHI)
      SNPHI= SIN(FIRPHI)
      TNPHI= TAN(FIRPHI)
      X(1,1)=0.0
      Z(1,1)=0.0
   21 CONTINUE
      FIRSIG = 1.0/(1 - SIN(FIRPHI))
      GAMMA=GAMMA * 6.369
      SIZE= SIZE * 3.2808
      SIGLO C= FIRSIG * SIZE * GAMMA
      GAMMA=GAMMA/6.369
      SIZE=SIZE/3.2808
      CALL PHILOC
      DI=(FIRPHI-PHILO)/PHILO
      IF(ABS(DI) .GT. 0.001) THEN
      FIRPHI=PHILO
      GO TO 21
      ELSE
      GO TO 24
      ENDIF
   24 CONTINUE
      SIGMA(1,1)=SIGLOC/(SIZE*GAMMA*3.2808*6.369)
      PSI(1,1)=0.5*3.1415927
      PHI(1,1)=PHILO
      PHI(1,1)=PHI(1,1)*180./PI
      PRINT,PHI(1,1)
      PHI(1,1)=PHI(1,1)*PI/180.
      DO 5 I=2,L
         READ, X(I,1)
    5 CONTINUE
      C=0
      CALL EDGEPA
      PRINT 12
   12 FORMAT('1',//////12X,'    EDGE  OF RECTILINEAR PASSIVE
ZONE')
      PRINT 19
   19 FORMAT(//17X,'X',13X,'Z',12X,'SIGMA',12X,'PSI',
     1          15X,'P',4X,'Q',8X,'PHI'/)
      DO 15 I=1,L
```

- iii -

```
         CALL RESOUT(I,1)
   15 CONTINUE
      C=1
      CALL POLCOM
      SPI=L-1
C     FIRST TIME COMPUTATION
      C=0
  450 C=C+1
      PRINT 22,C
   22 FORMAT('1',////25X,'*********************************',
     1                /25X,'*                               *',
     2                /25X,'*     SCALE  ITERATION   C=',I3,'
*',
     3                /25X,'*                               *',
     4                /25X,'*   REGULAR DOMAIN              *',
     5                /25X,'*                               *',
     6                /25X,'*********************************')
      IF( C.EQ.1 ) THEN DO
           RAD= K+1
             W=0
      ELSE DO
           RAD= K+ SPI
             W= SPI-1
      ENDIF
      DO 100 J=1,RAD
        IF(CONTRO .EQ. 1) GO TO 53
        PRINT,' '
        PRINT,' '
        PRINT,' '
      PRINT 37,J
      PRINT 39
   39 FORMAT(10X,' *****')
   37 FORMAT(10X,' J=',I3)
      PRINT 19
   53 CONTINUE
      IF(J .EQ. 1) GO TO 50
      DO 75 I= 3,L
         X1= X(I-1,J)
         Z1= Z(I-1,J)
         SIGMA1= SIGMA(I-1,J)
         PSI1= PSI(I-1,J)
         X2= X(I,J-1)
         Z2= Z(I,J-1)
         SIGMA2= SIGMA(I,J-1)
         PSI2= PSI(I,J-1)
         PHI1=PHI(I-1,J)
         PHI2=PHI(I,J-1)
         CALL NUPT C
         X(I,J)= XX
         Z(I,J)= ZZ
         SIGMA(I,J)= SIMA
         PSI(I,J)= PSSI
         P(I)= PP
         Q(I)= QQ
```

- iv -

```
          PHI(I,J)=PHHI
   75 CONTINUE
   50 GO TO 51
   51 IF(CONTRO .EQ. 1) GO TO 100
      IF(J.EQ.1) THEN
      PRINT 19
            DO 80 I=2,L
               CALL RESOUT(I,1)
   80       CONTINUE
          ELSE
            GO TO 100
      ENDIF
  100 CONTINUE
C     END OF RADIAL ZONE COMPUTATION
      IF(CONTRO .EQ. 1) GO TO 67
      PRINT,' '
      PRINT,' '
      PRINT,' '
      PRINT 25
   25 FORMAT( 11X,'RADIAL ZONE COMPUTATION COMPLETED')
      PRINT 26
   26 FORMAT( 11X,'**********************************')
      PRINT 678
  678 FORMAT('1',////25X,' COMPUTATION OF THE EXTRA DOMAIN',
     1           //25X,' **********************************')
   67 CONTINUE
      H=2
      J=RAD
  300 H= H+1
      J= J+1
      H1=H+1
      IF(CONTRO .EQ. 1) GO TO 68
      PRINT,' '
      PRINT,' '
      PRINT,' '
      PRINT,' '
      PRINT 47,J,H
   47 FORMAT(10X,'J=',I3,5X,'FIRST SPIRAL=',I3)
      PRINT 59
   59 FORMAT(10X,'*****',5X,'*****************')
      PRINT 19
   68 CONTINUE
      X1= X(H-1,J-1)
      Z1= Z(H-1,J-1)
      SIGMA1= SIGMA(H-1,J-1)
      PSI1= PSI(H-1,J-1)
      X2= X(H,J-1)
      Z2= Z(H,J-1)
      SIGMA2= SIGMA(H,J-1)
      PSI2= PSI(H,J-1)
      PHI1=PHI(H-1,J-1)
      PHI2=PHI(H,J-1)
      CALL ENDPT
      X(H,J)= XX
```



```
      Z(H,J)= ZZ
      SIGMA(H,J)= SIMA
      PSI(H,J)= PSSI
      PHI(H,J)=PHHI
      IF(H1 .GT. L) GO TO 117
      DO 250 I=H1,L
         X1= X(I-1,J)
         Z1= Z(I-1,J)
         SIGMA1= SIGMA(I-1,J)
         PSI1= PSI(I-1,J)
         X2= X(I,J-1)
         Z2= Z(I,J-1)
         SIGMA2= SIGMA(I,J-1)
         PSI2= PSI(I,J-1)
         PHI1=PHI(I-1,J)
         PHI2=PHI(I,J-1)
         CALL NUPT
         X(I,J)= XX
         Z(I,J)= ZZ
         SIGMA(I,J)= SIMA
         PSI(I,J)= PSSI
         P(I)= PP
         Q(I)= QQ
         PHI(I,J)=PHHI
  250    CONTINUE
  117    IF(H .LT. L) GO TO 300
         RAD1=RAD+L-2
         PRINT,RAD1
         IF(ABS(BETA) .GE. 0.1) THEN
         CALL NGAMA(RAD)
         ELSE
         CALL KAPE(RAD)
         ENDIF
         DIF=(SIGMA(L,RAD1)-10*SIGMA(2,RAD))
         DIF=DIF/SIGMA(L,RAD1)
         DIF= ABS(DIF)
         PRINT 200, SIGMA(L,RAD1) ,SIGMA(2,RAD),DIF,CONVG
  200
FORMAT(////////20X,'**********************************',
     1                                          //20X,'*
SIGMA(L,RAD+L-2)=',F12.6,'*',
     2                  //20X,'*    SIGMA(2,  RAD)=',F12.6,'
*',
     3                        //20X,'*          DIF=',F8.5,'
*',
     4                        //20X,'*         CONVG=',F8.5,'
*',
     5
//20X,'**********************************')
         IF(DIF .GT. CONVG) THEN
         DO 500 I=2,L
            SIGMA(I,1)= (Z(I,1)-Z(2,1))/(1.0-SNPHI)
            SIGMA(I,1)= SIGMA(I,1) + (SIGMA(L,1)/10.0)
  500    CONTINUE
```

```
          KS=K+SPI
          DO 510 J= 2, KS
             X(2,J)= (X(L,W+J))/10.0
             Z(2,J)= (Z(L,W+J))/10.0
             SIGMA(2,J)= (SIGMA(L,W+J))/10.0
             PSI(2,J)= PSI(L,W+J)
             PHI(2,J)=PHI(L,W+J)
  510     CONTINUE
          PRINT 22,C
          PRINT
27,X(2,RAD),Z(2,RAD),SIGMA(2,RAD),PSI(2,RAD),PHI(2,RAD)
   27     FORMAT(////10X,'X(2,RAD)=',F5.2,
     1    //10X           ,'Z(2,RAD)=',F5.2,
     2    //10X           ,'SIGMA(2,RAD)=',F12.8,
     3    //10X           ,'PSI(2,RAD)=',F12.8,
     4    //10X           ,'PHI(2,RAD)=',F12.8//)
          PRINT 30,C
   30      FORMAT('1',//////14X,'RESULTS   OF  FIRST   SPIRAL
AFTER',I3,
     1   '  SCALE REDUCTION')
          PRINT 19
          DO 415 J=1,RAD
             CALL RESOUT(2,J)
  415     CONTINUE
          GO TO 450
          ELSE
          GO TO 222
          ENDIF
  222     PRINT 333
  333
FORMAT('1',//////20X,'**********************************',
     1                                                  /20X,'*
*',
     2                    /20X,'*   END OF  FINAL COMPUTATION
*',
     3                                                  /20X,'*
*',
     4                      /20X,'*   ZERO   SURCHARGE   CASE
*',
     5                                                  /20X,'*
*',
     6                    /20X,'*  FIRST: REGULAR RADIAL ZONE
*',
     7                                                  /20X,'*
*',
     8
/20X,'**********************************'//)
          DO 555 J=2,RAD
             PRINT 890,J
             PRINT 891
  890        FORMAT(////10X,'J=',I3)
  891        FORMAT(10X,'*****')
             PRINT 19
             DO 666 I=1,L
```



```
                CALL RESOUT(I,J)
  666        CONTINUE
  555     CONTINUE
          DO 557 I=1,L
             PRINT 893,I
             PRINT 896
  893        FORMAT('1',////10X,'I=',I3)
  896        FORMAT(10X,'*****')
             PRINT 19
             DO 669 J=2,RAD
                CALL RESOUT(I,J)
  669        CONTINUE
  557     CONTINUE
          DO 92 I=1,L
          DO 93 J=1,RAD
            CALL OUTPUT(I,J,RAD)
   93     CONTINUE
   92     CONTINUE
  103      PRINT 104
  104      FORMAT( 20X,'*************')
             PRINT 756
  756
FORMAT('1',////45X,'**********************************',
     1                                                  /45X,'*
*',
     2                    /45X,'*    EXTRA DOMAIN CREATED BY
*',
     3                                                  /45X,'*
*',
     4                      /45X,'*       SCALE   REDUCTIONS
*',
     5                                                  /45X,'*
*',
     6
/45X,'**********************************'//)
             KP=0.0
          DO 777 H=3,L
             J=RAD+H-2
             PRINT 890,J
             PRINT 891
             PRINT 19
             DO 888 I=H,L
                CALL RESOUT(I,J)
                CALL OUTPUT(I,J,RAD)
  888        CONTINUE
             KP=(1+SIN(PHI(H,J)))/(1-SIN(PHI(H,J)))+KP
  777     CONTINUE
          KP=KP/(L-2)
          PRINT 112,KP
C234567
  112     FORMAT('1',////////20X,'KP=',F9.4) C
          PRINT 104
          STOP
          END
```

```
C
C*****************************************************************
C
      SUBROUTINE HEADIN
      REAL FIRPHI
      COMMON FIRPHI, BETA, DELTA,TOL, CONVG,SIZE,GAMMA
      INTEGER L,K,C
      COMMON L,K,C
      REAL XX, ZZ, SIMA, PSSI,PHHI
      COMMON /TATA/ X1,X2,XX,Z1,Z2,ZZ,PHHI
      COMMON /TITI/ SIGMA1,SIGMA2,SIMA
      COMMON /TETE/ PSI1,PSI2,PSSI
      COMMON /TOTO/ PI ,SNPHI,CSPHI
      INTEGER PP, QQ , CONTRO
      COMMON /OUI/ PP,QQ,CONTRO
      REAL MU
      COMMON /AH/ MU,PHILO,SIGLOC,PHI1,PHI2,PHILOP,PHILOT
      REAL
X(40,40),Z(40,40),SIGMA(40,40),PSI(40,40),PHI(40,40)
      COMMON /LALA/ X,Z,SIGMA,PSI
      COMMON /ALO/ PHI
      INTEGER P(40),Q(40)
      COMMON /LOLO/ P,Q
      REAL EO,LANDA
     COMMON                                                /CRIT/
EO,LANDA,PMIN,PMAX,PHIMIN,PHIMAX,PHII,EMIN,EMAX
C
      PRINT 10,FIRPHI,BETA,DELTA,TOL,CONVG,SIZE,GAMMA
   10    FORMAT('1',////////////10X,'   FIRPHI=',F5.1,
     1   //10X        ,'   BETA=',F5.1,
     2   //10X        ,'   DELTA=',F5.1,
     3   //10X        ,'   TOL=',F7.5,
     4   //10X        ,'   CONVG=',F7.5,
     5   ////////10X ,'   SIZE=',F6.3,
     6   //10X        ,'   GAMMA=',F6.3)
      PHIMIN=PHIMIN*180./PI
      PHIMAX=PHIMAX*180./PI
      PRINT                    11,                          L,
K,EO,LANDA,EMIN,EMAX,PMIN,PMAX,PHIMIN,PHIMAX
   11    FORMAT(////10X,'   NUMBER OF SPIRAL LINES=',I3,
     1   //10X        ,'   NUMBER OF RADIAL LINES=',I3,
     2   //10X        ,'   VOID RATIO EO =',F6.3,
     3   //10X        ,'   SLOPE LANDA=',F6.3,
     4   //10X        ,'   E-MINIMUM=',F6.3,
     5   //10X        ,'   E-MAXIMUM=',F6.3,
     6   //10X        ,'   P-MINIMUM=',F7.1,
     7   //10X        ,'   P-MAXIMUM=',F7.1,
     8   //10X        ,'   PHI-MIN=',F5.2,
     9   //10X        ,'   PHI-MAX=',F5.2)
      PHIMIN=PHIMIN*PI/180.
      PHIMAX=PHIMAX*PI/180.
      RETURN
      END
C
```

```
C*****************************************************************
C
      SUBROUTINE RESOUT(A,B)
      REAL FIRPHI
      COMMON FIRPHI,BETA,DELTA,TOL,CONVG,SIZE,GAMMA
      INTEGER L,K,C
      COMMON L,K,C
      REAL XX,ZZ,SIMA,PSSI,PHHI
      COMMON /TATA/ X1,X2,XX,Z1,Z2,ZZ,PHHI
      COMMON /TITI/ SIGMA1,SIGMA2,SIMA
      COMMON /TETE/ PSI1,PSI2,PSSI
      COMMON /TOTO/ PI ,SNPHI,CSPHI
      INTEGER PP,QQ,CONTRO
      COMMON /OUI/ PP,QQ,CONTRO
      REAL MU
      COMMON /AH/ MU,PHILO,SIGLOC,PHI1,PHI2,PHILOP,PHILOT
      REAL
X(40,40),Z(40,40),SIGMA(40,40),PSI(40,40),PHI(40,40)
      COMMON /LALA/ X,Z,SIGMA,PSI
      COMMON /ALO/ PHI
      INTEGER P(40),Q(40)
      COMMON /LOLO/ P,Q
      REAL EO,LANDA
     COMMON                                                /CRIT/
EO,LANDA,PMIN,PMAX,PHIMIN,PHIMAX,PHII,EMIN,EMAX
      INTEGER A,B
C
      PHI(A,B)=PHI(A,B)*180./PI
      PRINT
20,X(A,B),Z(A,B),SIGMA(A,B),PSI(A,B),P(A),Q(A),
     1PHI(A,B)
   20
FORMAT(11X,F12.6,3X,F12.6,E15.5,3X,F12.6,8X,I4,1X,I4,6X,
     1F6.3)
      PHI(A,B)=PHI(A,B)*PI/180.
      RETURN
      END
C
C
C
C*****************************************************************
      SUBROUTINE OUTPUT(A,B,RAD)
      REAL FIRPHI
      COMMON FIRPHI,BETA,DELTA,TOL,CONVG,SIZE,GAMMA
      INTEGER L,K,C
      COMMON L,K,C
      REAL XX,ZZ,SIMA,PSSI,PHHI
      COMMON /TATA/ X1,X2,XX,Z1,Z2,ZZ,PHHI
      COMMON /TITI/ SIGMA1,SIGMA2,SIMA
      COMMON /TETE/ PSI1,PSI2,PSSI
      COMMON /TOTO/ PI ,SNPHI,CSPHI
      INTEGER PP,QQ,CONTRO
      COMMON /OUI/ PP,QQ,CONTRO
      REAL MU
```

```
      COMMON /AH/ MU,PHILO,SIGLOC,PHI1,PHI2,PHILOP,PHILOT
      REAL
X(40,40),Z(40,40),SIGMA(40,40),PSI(40,40),PHI(40,40)
      COMMON /LALA/ X,Z,SIGMA,PSI
      COMMON /ALO/ PHI
      INTEGER P(40),Q(40)
      COMMON /LOLO/ P,Q
      REAL EO,LANDA
     COMMON                                          /CRIT/
EO,LANDA,PMIN,PMAX,PHIMIN,PHIMAX,PHI1,EMIN,EMAX
      INTEGER A,B,THI(40,40),AN,BN,LHI(40,40),MI,RAD1,RAD
      REAL T,R,XP(40,40),XN(40,40),TN,RN,MN,M C
      RAD1=RAD*L 2 C
      MN=(B 1)/2.
      MI=INT(MN)
      MC=MN   MI
      IF(M C.GT. 0.001) THEN
      GO TO 44
      ELSE
      GO TO 33
      ENDIF
   33   PHI(A,B)=PHI(A,B)*1800./PI
       THI(A,B)=INT(PHI(A,B))
        PHI(A,B)=PHI(A,B)*PI/1800.
      WRITE(8,20) X(A,B),Z(A,B),A,B,THI(A,B)
   20   FORMAT(F8.4,3X,F8.4,8X,I8,8X,I8,3X,I3)
   21   FORMAT(F8.4,3X,F8.4,3X,F9.0,3X,F9.0,3X,I3)
      T=A*100.
      R=B*100.
      IF(R .EQ. 500) GO TO 44
      IF(R .EQ. 700) GO TO 44
      IF(R .EQ. 900) GO TO 44
      IF(R .EQ. 1100) GO TO 44
        WRITE(8,21) X(A,B),Z(A,B),R,T,THI(A,B)
   44 CONTINUE
      RETURN
      END
C
C
C*********************************************************************
C
C345678
      SUBROUTINE POLCOM
      REAL FIRPHI
      COMMON FIRPHI, BETA, DELTA, TOL, CONVG,SIZE,GAMMA
      INTEGER L,K,C
      COMMON L,K,C
      REAL XX, ZZ, SIMA, PSSI,PHHI
      COMMON /TATA/ X1,X2,XX,Z1,Z2,ZZ,PHHI
      COMMON /TITI/ SIGMA1,SIGMA2,SIMA
      COMMON /TETE/ PSI1,PSI2,PSSI
      COMMON /TOTO/ PI  ,SNPHI,CSPHI
      INTEGER PP, QQ,CONTRO
      COMMON /OUI/ PP,QQ,CONTRO
```

```
      REAL MU
      COMMON /AH/ MU,PHILO,SIGLOC,PHI1,PHI2,PHILOP,PHILOT
      REAL
X(40,40),Z(40,40),SIGMA(40,40),PSI(40,40),PHI(40,40)
      COMMON /LALA/ X,Z,SIGMA,PSI
      COMMON /ALO/ PHI
      INTEGER P(40),Q(40)
      COMMON /LOLO/ P,Q
      REAL EO,LANDA
     COMMON                                          /CRIT/
EO,LANDA,PMIN,PMAX,PHIMIN,PHIMAX,PHI1,EMIN,EMAX
      INTEGER KK, K1, I, J
      REAL PSI1,PSIF,INT,FIRSIG,FINSIG,TNPHI,FINPHI
C
      PSI1= 3.1415927 / 2.
      FINPHI=39./57.2957795
      MU=PI/4.-FINPHI/2.
  400 PSIF=MU+ BETA
  405 INT= (PSI1-PSIF)/ K
      KK=K-1
      PRINT,' '
      PRINT,'*****************************************************
     1*********************************************'
      PRINT,' '
      PRINT,'              POLE   COMPT     <   >    FIRST
SPIRAL:(1,J) '
      PRINT,' '
      PRINT,' '
      PRINT 14
      PRINT,' '
      DO 350 J=2,K
         X(1,J)=X(1,1)
         Z(1,J)=Z(1,1)
         FIRPHI=PHI(1,J-1)
   34    TNPHI=TAN(FIRPHI)
         FIRSIG=EXP(ALOG(SIGMA(1,J-1))+INT*2*TNPHI)
         SIGLOC=FIRSIG*SIZE*GAMMA*3.2808*6.369
         CALL PHILOC
         DI=(PHILO-FIRPHI)/PHILO
         IF(ABS(DI) .GT. 0.001) THEN
         FIRPHI=PHILO
         GO TO 34
         ELSE
         GO TO 37
         ENDIF
   37    SIGMA(1,J)=FIRSIG
         PHI(1,J)=PHILO
         PSI(1,J)= PSI(1,J-1) - INT
         PRINT 12,X(1,J),Z(1,J),SIGMA(1,J),PSI(1,J)
   12  FORMAT(11X,F8.5,3X,F8.5,3X,E15.5,3X,F8.5)
  350  CONTINUE
      PRINT,'
      PRINT,'*****************************************************
     1*********************************************'
```

```
      IF(CONTRO .EQ. 1) GO TO 64
      PRINT,' '
      PRINT,'              SECOND SPIRAL '
      PRINT,' '
      PRINT 19
   19 FORMAT(////17X,'X',13X,'Z',12X,'SIGMA',12X,'PSI',
     1              15X,'P',4X,'Q',8X,'PHI'/)
      PRINT,' '
   64 CONTINUE
      PRINT,' '
      DO 355 J=2,K
      X1= X(1,J)
      Z1= Z(1,J)
      SIGMA1= SIGMA(1,J)
      PSI1= PSI(1,J)
      X2= X(2,J-1)
      Z2= Z(2,J-1)
      SIGMA2= SIGMA(2,J-1)
      PSI2= PSI(2,J-1)
      PHI1=PHI(1,J)
      PHI2=PHI(2,J-1)
      CALL NUPT
      X(2,J)= XX
      Z(2,J)= ZZ
      SIGMA(2,J)= SIMA
      PSI(2,J)= PSSI
      P(J)=PP
      Q(J)= QQ
      PHI(2,J)=PHHI
  355 CONTINUE
C      CALCULATION OF A WALL POINT
      X1= X(1,K)
      Z1= Z(1,K)
      SIGMA1= SIGMA(1,K)
      PSI1= PSI(1,K)
      X2= X(2,K)
      Z2= Z(2,K)
      SIGMA2= SIGMA(2,K)
      PSI2= PSI(2,K)
      PHI1=PHI(1,K)
      PHI2=PHI(2,K)
C
      CALL ENDPT
      K1=K+1
      X(2,K1)=XX
      Z(2,K1)=ZZ
      SIGMA(2,K1)=SIMA
      PSI(2,K1)=PSSI
      P(K1)=PP
      Q(K1)=QQ
      PHI(2,K1)=PHHI
      PRINT,' '
      PRINT,'*************************************************************
     1*********************************************'
```

```
      PRINT,' '
      PRINT,' '
      PRINT,' '
      PRINT,'            FINAL  2-ND SPIRAL LINE  WITH THE
LAST POINT:
     1 (2,K+1)'
      PRINT,' '
      PRINT,' '
      PRINT 11
 C2345678
   11
FORMAT(14X,'X',10X,'Z',10X,'SIGMA',9X,'PSI',15X,'P',4X,'Q',
     18X,'PHI')
   14 FORMAT(14X,'X',10X,'Z',10X,'SIGMA',10X,'PSI')
      PRINT,' '
      PRINT,' '
      DO 65 J=1,K1
      PHI(2,J)=PHI(2,J)*180./PI
      PRINT
16,X(2,J),Z(2,J),SIGMA(2,J),PSI(2,J),P(J),Q(J),
    1PHI(2,J)
   16
FORMAT(11X,F8.5,3X,F8.5,E15.5,3X,F8.5,9X,I4,1X,I4,7X,F6.3)
      PHI(2,J)=PHI(2,J)*PI/180.
   65 CONTINUE
      RETURN
      END
 C
 C
 C*****************************************************************
 C
 C
      SUBROUTINE NUPT
      REAL FIRPHI
      COMMON FIRPHI, BETA, DELTA, TOL, CONVG,SIZE,GAMMA
      INTEGER L,K,C
      COMMON L,K,C
      REAL XX, ZZ, SIMA, PSSI,PHHI
      COMMON /TATA/ X1,X2,XX,Z1,Z2,ZZ,PHHI
      COMMON /TITI/ SIGMA1,SIGMA2,SIMA
      COMMON /TETE/ PSI1,PSI2,PSSI
      COMMON /TOTO/ PI ,SNPHI,CSPHI
      INTEGER PP, QQ,CONTRO
      COMMON /OUI/ PP,QQ,CONTRO
      REAL MU
      COMMON /AH/ MU,PHILO,SIGLOC,PHI1,PHI2,PHILOP,PHILOT
      REAL
X(40,40),Z(40,40),SIGMA(40,40),PSI(40,40),PHI(40,40)
      COMMON /LALA/ X,Z,SIGMA,PSI
      COMMON /ALO/ PHI
      INTEGER P(40),Q(40)
      COMMON /LOLO/ P,Q
      REAL EO,LANDA
 C2345678
```

```
      COMMON                                                    /CRIT/
     EO,LANDA,PMIN,PMAX,PHIMIN,PHIMAX,PHI1,EMIN,EMAX
              REAL ZIGMA1,ZIGMA2,PZI1,PZI2,SUM1,SUM2
              REAL DIFF1,DIFF2,CSDIF1,CSSUM2
              REAL A,B,ETA,XI,F,G,U,V
              INTEGER I,J
              REAL TNPHI,PHHHI
     C
     C
     C
              SIMA= (SIGMA1+SIGMA2)/2.
              PSSI= (PSI1+PSI2)/2.
              PP=1
              QQ=1
     C23456789
              PHII=(PHI1+PHI2)/2.0
              PHILOP=PHII
      201     PHII=PHILOP
              CALL RPLANE
              CALL CRITIC
              MU=PI/4.-PHILOP/2.
              ZIGMA1=(SIMA+SIGMA1)/2.
              ZIGMA2=(SIMA+SIGMA2)/2.
              PZI1= (PSSI+PSI1)/2.
              PZI2= (PSSI+PSI2)/2.
              SUM1= SIN(PZI1+MU)
              SUM2= SIN(PZI2+MU)
              DIFF1= SIN(PZI1-MU)
              DIFF2= SIN(PZI2-MU)
              CSDIF1= COS(PZI1-MU)
              CSSUM2= COS(PZI2+MU)
              A=SUM1/(2*ZIGMA1*SNPHI*CSDIF1)
              B=-1. * (DIFF2)/(2.*ZIGMA2*SNPHI*CSSUM2)
              ZZ=Z1*DIFF1/CSDIF1-Z2*SUM2/CSSUM2-X1+X2
              ZZ=ZZ/(DIFF1/CSDIF1-SUM2/CSSUM2)
              TNPHI=TAN(PHILOP)
              ETA=ALOG(SIGMA1) / (2.*TNPHI)-PSI1 + A*(ZZ Z1)
              XI=ALOG(SIGMA2) / (2.*TNPHI) + PSI2 +B*(ZZ-Z2)
              F= EXP((XI+ETA)*TNPHI)
              G= (XI-ETA)/2.
              U= ABS((F-SIMA)/F)
              V= ABS((G-PSSI)/G)

     C
              IF(V.GT.U) GO TO 202
              IF(U.LE.TOL) GO TO 203
              SIMA = F
              PP = PP+1
              IF(PP-100) 201,201,203
     C2345678
      202     IF(V.LE.TOL) GO TO 203
              PSSI=G
              QQ=QQ+1
              IF(QQ-100) 201,201,203
```



```
      203     XX=X1+(ZZ-Z1)*DIFF1/CSDIF1
              XX=(XX+X2+(ZZ-Z2)*SUM2/CSSUM2)/2.
              PHHI=PHILOP
              PHHHI=PHHI*180./PI
     C
              IF(CONTRO .EQ. 1) GO TO 16
              PRINT 13,  XX,ZZ,SIMA,PSSI,PP,QQ,PHHHI
       13
    FORMAT(11X,F12.8,3X,F12.8,E15.5,3X,F12.8,8X,I4,1X,I4,
          16X,F6.3)
       16     CONTINUE
              RETURN
              END
     C
     C**********************************************************************
     C
              SUBROUTINE ENDPT
              REAL FIRPHI
              COMMON FIRPHI, BETA, DELTA, TOL, CONVG,SIZE,GAMMA
              INTEGER L,K,C
              COMMON L,K,C
              REAL XX, ZZ, SIMA, PSSI, PHHI
              COMMON /TATA/ X1,X2,XX,Z1,Z2,ZZ,PHHI
              COMMON /TITI/ SIGMA1,SIGMA2,SIMA
              COMMON /TETE/ PSI1,PSI2,PSSI
              COMMON /TOTO/ PI  ,SNPHI,CSPHI
              INTEGER PP, QQ,CONTRO
              COMMON /OUI/ PP,QQ,CONTRO
              REAL MU
              COMMON /AH/ MU,PHILO,SIGLOC,PHI1,PHI2,PHILOP,PHILOT
              REAL
    X(40,40),Z(40,40),SIGMA(40,40),PSI(40,40),PHI(40,40)
              COMMON /LALA/ X,Z,SIGMA,PSI
              COMMON /ALO/ PHI
              INTEGER P(40),Q(40)
              COMMON /LOLO/ P,Q
              REAL EO,LANDA
     C2345678
          COMMON                                                /CRIT/
    EO,LANDA,PMIN,PMAX,PHIMIN,PHIMAX,PHI1,EMIN,EMAX
              REAL ENDPSI
              REAL ZIGMA2,PZI2,SUM2,DIFF2,CSSUM2
              REAL B,XI,F,U,PHHHI
              INTEGER I,J
     C
     C
              PP=1
              QQ=1
              SIMA=(SIGMA1+SIGMA2)/2.
              PHII=(PHI1+PHI2)/2.0
              PHILOP=PHII
      302     PHII=PHILOP
              CALL RPLANE
              CALL CRITIC
```

```
      MU=PI/4.-PHILOP/2.
      DELTA=PHILOP
      IF(BETA .LE. 0.001) THEN
      GO TO 301
      ELSE
      GO TO 309
      ENDIF
C2345678
 301  ENDPSI=MU+BETA
      GO TO 305
 309  ENDPSI=MU   (1.732   DELTA)
 305  PSSI=ENDPSI
      ZIGMA2= (SIMA+SIGMA2)/2.
      PZI2=(PSSI+PSI2)/2.
      SUM2=SIN(PZI2+MU)
      DIFF2=SIN(PZI2-MU)
      CSSUM2= COS(PZI2+MU)
      B=-1.*(DIFF2)/(2.*ZIGMA2*SNPHI*CSSUM2)
      IF(ABS(BETA) .LE. 0.0001) THEN
      BETA=0.0001
      ELSE
      BETA=-1.*(1.732-DELTA)
      ENDIF
      ZZ=Z1*TAN(BETA)-X1-Z2*SUM2/CSSUM2+X2
      ZZ=ZZ/(TAN(BETA)-(SUM2/CSSUM2))
      XI=ALOG(SIGMA2)/(2.*TAN(PHILOP))+PSI2+B*(ZZ-Z2)
      F=EXP(2.*TAN(PHILOP)*(XI-PSSI))
      U=ABS((F-SIMA)/F)
      IF(U .LE. TOL) GO TO 303
      SIMA=F
      PP=PP+1
      IF(PP-100) 302,302,303
C2345678
 303  XX=X1+(ZZ-Z1)*TAN(BETA)
      PHHI=PHILOP
      PHHHI=PHHI*180./PI
      IF (CONTRO .EQ. 1) GO TO 26
      PRINT 13,   XX,ZZ,SIMA,PSSI,PP,QQ,PHHHI
  13
FORMAT(11X,F12.8,3X,F12.8,E15.5,3X,F12.8,8X,I4,1X,I4,
     16X,F6.3)
      PRINT 306
 306  FORMAT('1','
     1
     2  BOUNDARY')
  26  CONTINUE
      RETURN
      END
C
C
C*****************************************************************
C
      SUBROUTINE EDGEPA
      REAL FIRPHI
```



```
      COMMON FIRPHI,BETA,DELTA,TOL,CONVG,SIZE,GAMMA
      INTEGER L,K,C
      COMMON L,K,C
      REAL XX, ZZ, SIMA, PSSI,PHHI
      COMMON /TATA/ X1,X2,XX,Z1,Z2,ZZ,PHHI
      COMMON /TITI/ SIGMA1,SIGMA2,SIMA
      COMMON /TETE/ PSI1,PSI2,PSSI
      COMMON /TOTO/ P1,SNPHI,CSPHI
      INTEGER PP,QQ,CONTRO
      COMMON /OUI/ PP,QQ,CONTRO
      REAL MU
      COMMON /AH/ MU,PHILO,SIGLOC,PHI1,PHI2,PHILOP,PHILOT
      REAL
X(40,40),Z(40,40),SIGMA(40,40),PSI(40,40),PHI(40,40)
      COMMON /LALA/ X,Z,SIGMA,PSI
      COMMON /ALO/ PHI
      INTEGER P(40),Q(40)
      COMMON /LOLO/ P,Q
      REAL EO,LANDA
C2345678
      COMMON                                        /CRIT/
EO,LANDA,PMIN,PMAX,PHIMIN,PHIMAX,PHI1,EMIN,EMAX
      INTEGER CC,I,J
      REAL DI,NUZ,NSIMA
C
C
      IF( C.EQ. 0) THEN
      CC=2
      C=1
      ELSE
      CC=3
      ENDIF
      DO 23 I=CC,L
      FIRPHI=PHI(I-1,1)
      MU=PI/4.0-FIRPHI/2.0
      PHILOP=FIRPHI
      CALL RPLANE
      PHI1=PHILOT
      MU=PI/4.-PHI1/2.
      Z(I,1)=X(I,1)*TAN(MU)
      SIMA=(1.0+Z(I,1))/(1.0-SIN(PHI1))
      CALL CRITIC
      MU=PI/4.0-PHILOP/2.0
      NUZ=X(I,1)*TAN(MU)
      NSIMA=(1.0+NUZ)/(1.0-SIN(PHILOP))
      SIMA=NSIMA
C234567
      Z(I,1)=NUZ
      PHI(I,1)=PHILOP
      SIGMA(I,1)=NSIMA
      PSI(I,1)=3.1415927/2.0
  23  CONTINUE
      RETURN
      END
```

```
C*****************************************************************
C
C
C
      SUBROUTINE PHILOC
      REAL FIRPHI
      COMMON FIRPHI,BETA,DELTA,TOL,CONVG,SIZE,GAMMA
      INTEGER L,K,C
      COMMON L,K, C
      REAL XX,ZZ,SIMA,PSSI,PHHI
      COMMON /TATA/ X1,X2,XX,Z1,Z2,ZZ,PHHI
      COMMON /TITI/ SIGMA1,SIGMA2,SIMA
      COMMON /TETE/ PSI1,PSI2,PSSI
      COMMON /TOTO/ PI,SNPHI,CSPHI
      INTEGER PP,QQ,CONTRO
      COMMON /OUI/ PP,QQ,CONTRO
      REAL MU
      COMMON /AH/ MU,PHILO,SIGLOC,PHI1,PHI2,PHILOP,PHILOT
      REAL
X(40,40),Z(40,40),SIGMA(40,40),PSI(40,40),PHI(40,40)
      COMMON /LALA/ X,Z,SIGMA,PSI
      COMMON /ALO/ PHI
      INTEGER P(40),Q(40)
      COMMON /LOLO/ P,Q
      REAL EO,LANDA
      COMMON                                        /CRIT/
EO,LANDA,PMIN,PMAX,PHIMIN,PHIMAX,PHII,EMIN,EMAX
      REAL TT
      INTEGER DD
C
C*** SIGLO CIS DIMENSIONAL ****
C
      DD=2
      IF(DD .EQ. 1) THEN
      GO TO 10
      ELSE
      GO TO 11
      ENDIF
   11 IF(ABS(SIGLOC) .LT. 1000.0) THEN
C234567
      PHILO=(47.8-4.7*(ALOG(SIGLOC)-2.30258)/4.60517)/57.295779
      ELSE
      IF(ABS(SIGLOC) .LT. 200000.0) THEN
      PHILO=(43.2-11.2*(ALOG(SIGLOC)-6.90776)/5.29832)/57.295779
      ELSE
      PHILO=32.0/57.2957795
      ENDIF
      ENDIF
      GO TO 30
C234567
   10 IF(ABS(SIGLOC) .LT. 100.0) THEN
      PHILO=(47.8-4.7*(ALOG(SIGLOC)-2.30258)/4.60517)/57.295779
      ELSE
```



```
      TT=(47.8-4.7*(ALOG(100.0)-2.30258)/4.60517)/(100.0
**0.5)
      PHILO=(TT*(SIGLOC**0.5))/57.295779
      ENDIF
   30 SNPHI=SIN(PHILO)
      CSPHI=COS(PHILO)
      RETURN
      END
C
C
C*****************************************************************
C2345678
      SUBROUTINE CRITIC
      REAL FIRPHI
      COMMON FIRPHI,BETA,DELTA,TOL,CONVG,SIZE,GAMMA
      INTEGER L,K,C
      COMMON L,K,C
      REAL XX,ZZ,SIMA,PSSI,PHHI
      COMMON /TATA/ X1,X2,XX,Z1,Z2,ZZ,PHHI
      COMMON /TITI/ SIGMA1,SIGMA2,SIMA
      COMMON /TETE/ PSI1,PSI2,PSSI
      COMMON /TOTO/ PI,SNPHI,CSPHI
      INTEGER PP,QQ,CONTRO
      COMMON /OUI/ PP,QQ,CONTRO
      REAL MU
      COMMON /AH/ MU,PHILO,SIGLOC,PHI1,PHI2,PHILOP,PHILOT
      REAL
X(40,40),Z(40,40),SIGMA(40,40),PSI(40,40),PHI(40,40)
      COMMON /LALA/ X,Z,SIGMA,PSI
      COMMON /ALO/ PHI
      INTEGER P(40),Q(40)
      COMMON /LOLO/ P,Q
      REAL EO,LANDA
      COMMON                                        /CRIT/
EO,LANDA,PMIN,PMAX,PHIMIN,PHIMAX,PHII,EMIN,EMAX
      REAL V,VLANDA,KK,PHIC1,QOP,DI,PPR,M
      REAL MMAX,MMIN,VLAMAX,VLAMIN,AA,BB
C
      V=1.0+EO
      PHII=PHILOT
    5 KK=(1.0+SIN(PHII))/(1.0-SIN(PHII))
      SIMA=SIMA*GAMMA*SIZE
      PPR=(2*(1.0+2*KK)*SIMA)/(3*(1+KK))
      SIMA=SIMA/(SIZE*GAMMA)
      VLANDA=V + LANDA*ALOG(PPR)
      VLAMAX=(1.+EMAX) + LANDA*ALOG(PMAX)
      VLAMIN=(1.+EMIN) + LANDA*ALOG(PMIN)
      IF(VLANDA .GT. VLAMAX) THEN
      VLANDA=VLAMAX
      PHIC1=PHIMIN
      GO TO 2
      ELSE
      GO TO 7
      ENDIF
```

```
     7  IF(VLANDA .LT. VLAMIN) THEN
        VLANDA=VLAMIN
        PHIC1=PHIMAX
        GO TO 2
        ELSE
        GO TO 3
        ENDIF
     3  MMAX=(6.*SIN(PHIMIN))/(3-SIN(PHIMIN))
        MMIN=(6.*SIN(PHIMAX))/(3-SIN(PHIMAX))
        AA=(MMAX-MMIN)/(VLAMAX-VLAMIN)
        BB=MMAX   AA*VLAMAX
        QOP=AA*VLANDA + BB
        M=QOP
        TT=(3*M)/(6+M)
        PHIC1=ARSIN(TT)
     2  PHILOT=PHIC1
        DI=(PHILOT-PHI1)/PHILOT
        IF(ABS(DI).GT.0.11) THEN
        PHI1=PHILOT
        GO TO 5
        ELSE
        GO TO 9
        ENDIF
     9  CALL PPLANE
        PHI1=PHILOP
        SNPHI=SIN(PHILOP)
        CSPHI=COS(PHILOP)
        RETURN
        END
C*****************************************************************
        SUBROUTINE PPLANE
        REAL FIRPHI
        COMMON FIRPHI,BETA,DELTA,TOL,CONVG,SIZE,GAMMA
        INTEGER L,K,C
        COMMON L,K,C
        REAL XX,ZZ,SIMA,PSSI,PHHI
        COMMON /TATA/ X1,X2,XX,Z1,Z2,ZZ,PHHI
        COMMON /TITI/ SIGMA1,SIGMA2,SIMA
        COMMON /TETE/ PSI1,PSI2,PSSI
        COMMON /TOTO/ PI,SNPHI,CSPHI
        INTEGER PP,QQ,CONTRO
        COMMON /OUI/ PP,QQ,CONTRO
        REAL MU
        COMMON /AH/ MU,PHILO,SIGLOC,PHI1,PHI2,PHILOP,PHILOT
        REAL
X(40,40),Z(40,40),SIGMA(40,40),PSI(40,40),PHI(40,40)
        COMMON /LALA/ X,Z,SIGMA,PSI
        COMMON /ALO/ PHI
        INTEGER P(40),Q(40)
        COMMON /LOLO/ P,Q
        REAL EO,LANDA
C234567
```



```
      COMMON                                          /CRIT/
EO,LANDA,PMIN,PMAX,PHIMIN,PHIMAX,PHI1,EMIN,EMAX
        REAL PHIPL1,PHIPL2
C
C
C
        PHIPL1=32.8328*PI/180.
        PHIPL2=36.*PI/180.
        IF(PHILOT .LT. PHIPL1) GO TO 10
        IF(PHILOT .GT. PHIPL2) GO TO 20
        PHILOT=PHILOT*180./PI
        PHILOP=1.6667*ALOG(PHILOT) - 2.3362
        PHILOP=EXP(PHILOP)
        PHILOP=PHILOP*PI/180.
        GO TO 35 C
C234567
   10   PHILOP=PHILOT
        GO TO 35
   20   PHILOT=PHILOT*180./PI
        PHILOP=1.2944*ALOG(PHILOT)-1.002
        PHILOP=EXP(PHILOP)
        PHILOP=PHILOP*PI/180.
        GO TO 35
   35   RETURN
        END
C
C*****************************************************************
        SUBROUTINE RPLANE
        REAL FIRPHI
        COMMON FIRPHI,BETA,DELTA,TOL,CONVG,SIZE,GAMMA
        INTEGER L,K,C
        COMMON L,K,C
        REAL XX,ZZ,SIMA,PSSI,PHHI
        COMMON /TATA/ X1,X2,XX,Z1,Z2,ZZ,PHHI
        COMMON /TITI/ SIGMA1,SIGMA2,SIMA
        COMMON /TETE/ PSI1,PSI2,PSSI
        COMMON /TOTO/ PI,SNPHI,CSPHI
        INTEGER PP,QQ,CONTRO
        COMMON /OUI/ PP,QQ,CONTRO
        REAL MU
        COMMON /AH/ MU,PHILO,SIGLOC,PHI1,PHI2,PHILOP,PHILOT
        REAL
X(40,40),Z(40,40),SIGMA(40,40),PSI(40,40),PHI(40,40)
        COMMON /LALA/ X,Z,SIGMA,PSI
        COMMON /ALO/ PHI
        INTEGER P(40),Q(40)
        COMMON /LOLO/ P,Q
        REAL EO,LANDA
C234567
      COMMON                                          /CRIT/
EO,LANDA,PMIN,PMAX,PHIMIN,PHIMAX,PHI1,EMIN,EMAX
        REAL PHIPL1,PHIPL2
C
C
```

```
      PHIPL1=32.8328*PI/180.
      PHIPL2=37.9569*PI/180.
      IF(PHILOP .LT. PHIPL1) GO TO 10
      IF(PHILOP .GT. PHIPL2) GO TO 20
      PHILOP=PHILOP*180./PI
      PHILOT=(ALOG(PHILOP)+2.3362)/1.6667
      PHILOT=EXP(PHILOT)
      PHILOT=PHILOT*PI/180.
      GO TO 35
C234567
   10 PHILOT=PHILOP
      GO TO 35
   20 PHILOP=PHILOP*180./PI
      PHILOT=(ALOG(PHILOP)+1.002)/1.2944
      PHILOT=EXP(PHILOT)
      PHILOT=PHILOT*PI/180.
      GO TO 35
   35 RETURN
      END
C
C*****************************************************************
C
      SUBROUTINE NGAMA(RAD)
      REAL FIRPHI
      COMMON FIRPHI,BETA,DELTA,TOL,CONVG,SIZE,GAMMA
      INTEGER L,K,C
     COMMON L,K,C
     REAL XX,ZZ,SIMA,PSSI,PHHI
     COMMON /TATA/ X1,X2,XX,Z1,Z2,ZZ,PHHI
     COMMON /TITI/ SIGMA1,SIGMA2,SIMA
     COMMON /TETE/ PSI1,PSI2,PSSI
     COMMON /TOTO/ PI,SNPHI,CSPHI
     INTEGER PP,QQ,CONTRO
     COMMON /OUI/ PP,QQ,CONTRO
     REAL MU
     COMMON /AH/ MU,PHILO,SIGLOC,PHI1,PHI2,PHILOP,PHILOT
     REAL
X(40,40),Z(40,40),SIGMA(40,40),PSI(40,40),PHI(40,40)
     COMMON /LALA/ X,Z,SIGMA,PSI
     COMMON /ALO/ PHI
     INTEGER P(40),Q(40)
     COMMON /LOLO/ P,Q
     REAL EO,LANDA
C2345678
     COMMON                                          /CRIT/
EO,LANDA,PMIN,PMAX,PHIMIN,PHIMAX,PHI1,EMIN,EMAX
     REAL COSPSI,SIMAV(30),NGAMMA,F,E,SOMME,RATIO,CENTRE
     REAL*8 B
     INTEGER L1,RAD,I,J,H,RAD1,RAD3
C
     RAD1=RAD+L-2
     RAD3=RAD+L-3
      I=0
      H=0
```

```
      J=RAD-2
   4  H=H+1
      J=J+1
C2345678
      I=I+1
      SINPHI=SIN(PHI(H,J))
      PSI(H,J)=2.*PSI(H,J)
      COSPSI=COS(PSI(H,J))
      PSI(H,J)=PSI(H,J)/2.
      SIMAV(I)=SIGMA(H,J)*(1+SINPHI*COSPSI)
      IF(H .LT. L) GO TO 4
      I=2
      H=2
      J=RAD
      NGAMMA=0.0
      SOMME=0.0
   6  I=I+1
      H=H+1
      J=J+1
      SOMME=(SIMAV(I-1)+SIMAV(I))/2.
      SOMME=SOMME*(X(H,J)-X(H-1,J-1))
      NGAMMA=NGAMMA + SOMME
      L1=L
      IF(I .LT. L1) GO TO 6
C234567
      NGAMMA=-2.*(NGAMMA)
      PRINT 10,NGAMMA
      B=X(L,RAD1)*2.
      RATIO= 1./B**2
      NGAMMA=NGAMMA*RATIO*2.
      PRINT 10,NGAMMA
  10  FORMAT('1',////////20X,'NGAMMA=',F9.4)
      B=B*SIZE/1.732
      PRINT 12,B
  12  FORMAT(/////20X,'BREADTH=',F9.4)
      B=B*1.732/SIZE
     B=(1./B)*(10.**(1-C))
      PRINT 11,B
  11  FORMAT(////////20X,'D/B=',F9.4)
      RETURN
      END
C*****************************************************************
C
      SUBROUTINE KAPE(RAD)
      REAL FIRPHI
      COMMON FIRPHI,BETA,DELTA,TOL,CONVG,SIZE,GAMMA
      INTEGER L,K,C
     COMMON L,K,C
     REAL XX,ZZ,SIMA,PSSI,PHHI
     COMMON /TATA/ X1,X2,XX,Z1,Z2,ZZ,PHHI
     COMMON /TITI/ SIGMA1,SIGMA2,SIMA
     COMMON /TETE/ PSI1,PSI2,PSSI
     COMMON /TOTO/ PI,SNPHI,CSPHI
     INTEGER PP,QQ,CONTRO
```

```
      COMMON /OUI/ PP,QQ,CONTRO
      REAL MU
      COMMON /AH/ MU,PHILO,SIGLOC,PHI1,PHI2,PHILOP,PHILOT
      REAL
X(40,40),Z(40,40),SIGMA(40,40),PSI(40,40),PHI(40,40)
      COMMON /LALA/ X,Z,SIGMA,PSI
      COMMON /ALO/ PHI
      INTEGER P(40),Q(40)
      COMMON /LOLO/ P,Q
      REAL EO,LANDA
C234567
     COMMON                                          /CRIT/
EO,LANDA,PMIN,PMAX,PHIMIN,PHIMAX,PHI1,EMIN,EMAX
      REAL COSPSI,SIMAH(30),KP,F,E,SOMME,B,RATIO,CENTRE
      INTEGER L1,RAD,I,J,H,RAD1,RAD3
C
       RAD1=RAD+L-2
       I=0
       H=0
       J=RAD-2
       RAD3=RAD+L-3
   4   H=H+1
       J=J+1
C2345678
       I=I+1
       SINPHI=SIN(PHI(H,J))
       PSI(H,J)=2.*PSI(H,J)
       COSPSI=COS(PSI(H,J))
       PSI(H,J)=PSI(H,J)/2.
       SIMAH(I)=SIGMA(H,J)*(1-SINPHI*COSPSI)
       IF(H .LT. L) GO TO 4
C
       I=1
       H=1
       J=RAD-1
       KP=0.0
       SOMME=0.0
   6   I=I+1
       H=H+1
       J=J+1
       SOMME=(SIMAH(I-1)+SIMAH(I))/2.
       SOMME=SOMME*(Z(H,J)-Z(H-1,J-1))
       KP=KP + SOMME
       L1=L
       IF(I .LT. L1) GO TO 6
C234567
       KP=KP
       PRINT 10,KP
       B=Z(L,RAD1)
       B=B*SIZE/1.732
       PRINT 14,B
  14   FORMAT(///////20X,'HEIGHT=',F9.4)
       B=B*1.732/SIZE
       RATIO=1./B**2
```



```
       KP=KP*RATIO*2.
C
       PRINT 10,KP
  10   FORMAT(/////////20X,'KP=',F9.4)
       RETURN
       END
C*************************************************************
C
C      L'ORGANISATION DE L'ENTREE DES DONNEES
C      EST LA SUIVANTE:
C
C   FIRPHI,DELTA,BETA,TOL,CONVG,SIZE,GS,GW
C   CONTROL
C   L,K
C   EMIN,EMAX,LANDA,PMIN,PMAX,PHIMIN,PHIMAX
C   X(I,1)
C
C*************************************************************
C
C
ENTRY
  30.0    30.0   -30.0 0.0001  0.001     0.2    2.65    9.81
  2
   10     20
 0.40   0.80 0.175     10 10000     28     45
0.1732
0.215
0.260
0.346
0.519
0.693
0.866
1.216
1.732
$STOP
//FT08F001 DD DSN=HOVAN.SAS.OUTPU2,DISP=OLD
/*
```

The following pages (115-117) show a sample of the computer print-out. Each point is characterized by :

- X, Z, Physical coordinates
- SIGMA, Stress
- PSI, Direction of the major principal stress
- P,Q, Iteration counts
- PHI, Angle of shearing resistance

The radial number is J. For each radial, the print-out shows the characteristics (X,Z,SIGMA,PSI,P,Q,PHI) of the intersections of the spirals with the radial.

COMPUTATION OF THE EXTRA DOMAIN

J= 30 FIRST SPIRAL= 3

X	Z	SIGMA	PSI	P	Q	PHI	
0.00001288	0.12878980	0.25534E 01	0.45423710	5	1	37.960	BOUNDARY
0.00047608	0.15258320	0.27553E 01	0.49788420	4	3	37.895	
0.00401488	0.20177190	0.31138E 01	0.55628030	4	3	37.274	
0.02040788	0.30987840	0.37430E 01	0.66847570	4	3	36.645	
0.04783745	0.42561180	0.43071E 01	0.73838130	4	3	36.167	
0.08400065	0.54478360	0.48148E 01	0.79455700	4	3	35.791	
0.17771180	0.78511840	0.57533E 01	0.87837630	4	3	35.181	
0.35387220	1.17343100	0.69785E 01	0.98158120	4	3	34.548	

J= 31 FIRST SPIRAL= 4

X	Z	SIGMA	PSI	P	Q	PHI	
0.00001522	0.15224380	0.29283E 01	0.45835840	4	1	37.487	BOUNDARY
0.00150884	0.20019380	0.33010E 01	0.52765750	3	3	37.074	
0.01333430	0.30621200	0.39574E 01	0.62904450	3	3	36.455	
0.03593770	0.42084350	0.45443E 01	0.70306010	3	3	35.986	
0.08696808	0.53913190	0.50711E 01	0.75923530	3	3	35.615	
0.15031390	0.78871870	0.60430E 01	0.84482040	3	3	35.027	
0.31143700	1.16745100	0.73085E 01	0.93018770	4	3	34.393	

J= 32 FIRST SPIRAL= 5

X	Z	SIGMA	PSI	P	Q	PHI	
0.00001992	0.19918340	0.36282E 01	0.48477110	4	1	36.753	BOUNDARY
0.00478881	0.30150620	0.43269E 01	0.58783390	3	3	36.150	
0.01860883	0.41347970	0.49549E 01	0.64348880	3	3	35.694	
0.04262328	0.52888910	0.55147E 01	0.70112080	3	2	35.333	
0.10928480	0.77728800	0.65437E 01	0.78834620	3	3	34.761	
0.24575180	1.15554900	0.78781E 01	0.87802170	4	3	34.144	

J= 33 FIRST SPIRAL= 8

X	Z	SIGMA	PSI	P	Q	PHI	
0.00002884	0.28842800	0.49843E 01	0.67400680	4	1	35.694	BOUNDARY
0.00378835	0.40491920	0.56440E 01	0.55184050	3	2	35.256	
0.01510309	0.51711880	0.62583E 01	0.61124460	3	3	34.810	
0.05899202	0.75884580	0.73820E 01	0.70304010	4	2	34.380	
0.15617370	1.13334500	0.88287E 01	0.78619840	4	3	33.787	

J= 34 FIRST SPIRAL= 7

X	Z	SIGMA	PSI	P	Q	PHI	
0.00004025	0.40250870	0.62318E 01	0.68072880	4	1	34.824	BOUNDARY
0.00301403	0.51034300	0.68813E 01	0.64152290	3	2	34.586	
0.02670457	0.74556500	0.80928E 01	0.63586250	3	3	34.055	
0.08785414	1.11443600	0.98322E 01	0.73188870	3	3	33.461	

J= 35 FIRST SPIRAL= 8

X	Z	SIGMA	PSI	P	Q	PHI	
0.00005084	0.50843820	0.74360E 01	0.68588450	4	1	34.335	BOUNDARY
0.00888252	0.73703140	0.87031E 01	0.58159830	3	3	33.815	
0.05943602	1.09854900	0.10321E 02	0.67887550	3	3	33.254	

J= 36 FIRST SPIRAL= 9

X	Z	SIGMA	PSI	P	Q	PHI	
0.00007311	0.73109820	0.97745E 01	0.69374380	4	1	33.433	BOUNDARY
0.01613783	1.07843400	0.11525E 02	0.59513710	3	3	32.893	

J= 37 FIRST SPIRAL= 10

X	Z	SIGMA	PSI	P	Q	PHI	
0.00010702	1.07018200	0.13041E 02	0.69932180	4	1	32.793	BOUNDARY

37

HEIGHT= 4.9430

KP= 0.4483

```
**********************************
*   SIGMA(L,RAD+L-2)=   13.040830*
*   SIGMA(2, RAD)=     1.305003   *
*   DIF= 0.00070                  *
*   CONVG= 0.00100                *
**********************************
```

Appendix C

SAMPLE OF A PLOTTING COMPUTER PROGRAM

```
1          S A S   L O G    OS SAS 82.4          VS2/MVS JOB PRINT     STEP GO        PROC                          14:05 SATURDAY, NOVEMBER 17, 1984

NOTE: THE JOB PRINT HAS BEEN RUN UNDER RELEASE 82.4 OF SAS AT THE UNIVERSITY OF MANITOBA (02248001).

NOTE: CPUID    VERSION = 01  SERIAL = 000103  MODEL = 0580 .

NOTE: SAS OPTIONS SPECIFIED ARE:
      SORT=4

1           GOPTIONS DEVICE=VERSATIC;
2           DATA OYO;
3           INFILE SASDATA;                                                    6.
4           INPUT X    Z    A    B   PHI;                                     7.
                                                                               8.
                                                                               9.
NOTE: INFILE SASDATA IS:
      DSNAME=HOVAN.SAS.OUPUTW,
      UNIT=DISK,VOL=SER=USER06,DISP=SHR,
      DCB=(BLKSIZE=8080,LRECL=80,RECFM=FB)

NOTE: 282 LINES WERE READ FROM INFILE SASDATA.
NOTE: DATA SET WORK.OYO HAS 282 OBSERVATIONS AND 5 VARIABLES. 433 OBS/TRK.
NOTE: THE DATA STATEMENT USED 0.06 SECONDS AND 356K.

5           PROC PRINT;
                                                                               10.
NOTE: THE PROCEDURE PRINT USED 0.18 SECONDS AND 380K AND PRINTED PAGES 1 TO 6.

6           PROC GPLOT DATA=OYO UNIFORM;
7           LABEL Z=HEIGHT OF THE PASSIVE WALL                                 11.
8                 X=HORIZONTAL;                                                12.
9            TITLE .H=2 .F=DUPLEX SLIP LINES BEHIND A PASSIVE WALL;            13.
10          FOOTNOTE3 .H=1 .F=DUPLEX  POUR RIRE;                               14.
11          PLOT Z*X=A / NOLEGEND VREVERSE VAXIS=0 TO 1.8 BY 0.2               15.
12          HAXIS=0 TO 1.8 BY 0.2 VREF=1.8 HREF=1.8;                           16.
13          SYMBOL1  V=NONE L=1 I=JOIN;                                        16.1
14          SYMBOL2  V=NONE L=1 I=JOIN;                                        17.
15          SYMBOL3  V=NONE L=1 I=JOIN;                                        18.
16          SYMBOL4  V=NONE L=1 I=JOIN;                                        19.
17          SYMBOL5  V=NONE L=1 I=JOIN;                                        20.
18          SYMBOL6  V=NONE L=1 I=JOIN;                                        21.
19          SYMBOL7  V=NONE L=1 I=JOIN;                                        22.
20          SYMBOL8  V=NONE L=1 I=JOIN;                                        23.
21          SYMBOL9  V=NONE L=1 I=JOIN;                                        24.
22          SYMBOL10 V=NONE L=1 I=JOIN;                                        25.
23          SYMBOL11 V=NONE L=1 I=JOIN;                                        26.
24          SYMBOL12 V=NONE L=1 I=JOIN;                                        27.
25          SYMBOL13 V=NONE L=1 I=JOIN;                                        28.
26          SYMBOL14 V=NONE L=1 I=JOIN;                                        29.
27          SYMBOL15 V=NONE L=1 I=JOIN;                                        30.
28          SYMBOL16 V=NONE L=1 I=JOIN;                                        31.
29          SYMBOL17 V=NONE L=1 I=JOIN;                                        32.
30          SYMBOL18 V=NONE L=1 I=JOIN;                                        33.
31          SYMBOL19 V=NONE L=1 I=JOIN;                                        34.
32          SYMBOL20 V=NONE L=1 I=JOIN;                                        35.
33          SYMBOL21 V=NONE L=1 I=JOIN;                                        36.
34          SYMBOL22 V=NONE L=1 I=JOIN;                                        37.
35          SYMBOL23 V=NONE L=1 I=JOIN;                                        38.
36          SYMBOL24 V=NONE L=1 I=JOIN;                                        39.
37          SYMBOL25 V=NONE L=1 I=JOIN;                                        40.
                                                                               41.
38          SYMBOL26 V=NONE L=1 I=JOIN;
39          SYMBOL27 V=NONE L=1 I=JOIN;                                        42.
40          SYMBOL28 V=NONE L=1 I=JOIN;                                        43.
41          SYMBOL29 V=NONE L=1 I=JOIN;                                        44.
42          SYMBOL30 V=NONE L=1 I=JOIN;                                        45.
                                                                               46.
NOTE: THE PROCEDURE GPLOT USED 0.80 SECONDS AND 852K.
NOTE: SAS USED 852K MEMORY.

NOTE: SAS INSTITUTE INC.
      SAS CIRCLE
      PO BOX 8000
      CARY, N.C.  27511-8000
```